NOTICE

The quality of this microform is heavily dependent upon the quality of the original thesis submitted for microfilming. Every effort has been made to ensure the highest quality of reproduction possible.

If pages are missing, contact the university which granted the degree.

Some pages may have indistinct print especially if the original pages were typed with a poor typewriter ribbon or if the university sent us an inferior photocopy.

Reproduction in full or in part of this microform is governed by the Canadian Copyright Act, R.S.C. 1970, c. C-30, and subsequent amendments.

AVIS

La qualité de cette microforme dépend grandement de la qualité de la thèse soumise au microfilmage. Nous avons tout fait pour assurer une qualité supérieure de reproduction.

S'il manque des pages, veuillez communiquer avec l'université qui a conféré le grade.

La qualité d'impression de certaines pages peut laisser à désirer, surtout si les pages originales ont été dactylographiées à l'aide d'un ruban usé ou si l'université nous a fait parvenir une photocopie de qualité inférieure.

La reproduction, même partielle, de cette microforme est soumise à la Loi canadienne sur le droit d'auteur, SRC 1970, c. C-30, et ses amendements subséquents.

ISBN 0-315-56405-9

Canada

UNIVERSITÉ D'OTTAWA
UNIVERSITY OF OTTAWA

Abstract

During uniform heat generation within the wall of a cylinder placed in a cross flow, heat flows by conduction in the peripheral direction due to the asymmetric nature of the fluid flow around the perimeter of the cylinder. The variation of the surface temperature caused by peripheral wall conduction may affect the overall heat transfer rate significantly for geometrically similar surfaces.

In the present study, a non-dimensional conduction parameter, $K^* = K_L r_o / K_w b$ [1], is used to characterize the peripheral wall heat conduction. In the experimental investigation, the effects of flow velocity, degree of subcooling and system pressure were studied in both crossflow nucleate and film boiling. Two test sections having different values of K^* (0.0212 and 0.0384) were studied for crossflow nucleate boiling. For Freon-113 boiling outside horizontal tubes, the boiling curve is sensitive to crossflow velocity, degree of liquid subcooling and system pressure. The heat transfer rate increases with increasing flow velocity, degree of subcooling and system pressure. Increasing in flow velocity, degree of subcooling, system pressure and heat flux always causes an increasing in the variation of local heat transfer coefficient, especially in crossflow nucleate boiling. From the preliminary study, the effect of K* seems to disappear in crossflow nucleate boiling .

Acknowledgements

The author is deeply indebted to Dr. Yung Lee who initiated and supervised the present work. I am particularly grateful for his guidance, advice, encouragement, invaluable help and generous financial support during the course of this project.

Sincere thanks are also due to the technical staff of the Department of Mechanical Engineering, especially to Mr. George Spak, for the construction of the loop. The author wishes to thank Mr. Don Seaman and staff members of the Department of Mechanical Engineering.

Finally, the author wishes to extend his special gratitude to the author's wife for her understanding and encouragement.

Table of Contents

List of Tables

List of Figures

Nomenclature

A	heater area, m^2
b	wall thickness of the test tube, m
B	constant in Mikic-Rohsenow's correlation Eq. (2.2)
C	specific heat, $J/kg \cdot K$
C_{sf}	empirical constant in Rohsenow's correlation Eq. (2.1)
d	diameter, m
g	gravitational constant, 9.8 m/s^2
g_c	conversion factor, 1 $kg \cdot m/N \cdot s^2$
h	local heat transfer coefficient, $W/m^2 \cdot K$
h_{LV}	latent heat, J/kg
I	current flow, A
K	thermal conductivity, $W/m \cdot K$
K^*	dimensionless peripheral wall conduction parameter, $K_L r_o/K_w b$
L	power measurement length, m
Nu	Nusselt number, hd/K_L
P	pressure, Pa
q	heat flux, W/m^2
$\dot{q}$	heat generation per unit volume, W/m^3
Q	flow rate, m^3/s
r	radius of test tube, m
r^+	non-dimensional radius, r/r_o
Re	Reynolds number, ud/ν

T	temperature, K
T_w	outside wall temperature, K
ΔT	wall superheat, $\bar{T}_w - T_s$, K
ΔT_d	temperature difference across film, K
T^+	dimensionless temperature, $(T_w - T_s)/(\bar{T}_w - T_s)$
u, V	flow velocity, m/s
V	voltage drop within L, V

Greek Symbols

α	thermal diffusivity, m^2/s
δ	vapor film thickness, m
ϵ	emissivity of surface
ϵ'	eddy diffusivity, m^2/s
θ	angle in degree, *degree*
λ_c	critical wavelength, $2\pi[g_c\sigma/g(\rho_L - \rho_V)]^{1/2}$, m
μ	dynamic viscosity, $kg/m \cdot s$
ν	kinematic viscosity, m^2/s
ρ	density, kg/m^3
σ	surface tension, N/m
$\dot{\sigma}$	Stenfan-Boltzmann constant, $\dot{\sigma} = 5.67 \times 10^{-8} W/m^2 \cdot K^4$

Superscript

$-$	average

Subscript

b	bulk temperature of liquid
FC	forced convection
FB	film boiling
i	wall inside surface
L	liquid
PNB	pool nucleate boiling
o	wall outside surface
r	radiation
s	saturation
sub	subcooling
t	total effect
v	vapor
w	wall

Chapter 1

Introduction

Boiling is a complex phenomenon involving the interaction of fluid motion, heat and mass transfer, surface and interfacial phenomena. The design of water-tube boilers, refrigeration equipment, electronic power tubes, water-cooled nuclear reactors, evaporators, and many other major items of chemical and power plants are dependent on research and knowledge of processes occurring during boiling.

Pool nucleate and film boiling have been investigated for many years. The effects of thermal properties, surface finish, orientation of the heater, the container geometry and other parameters have been investigated. Most investigators seldom considered the effect of the circumferential heat conduction. Circumferential heat conduction is dependent on the thermal conductivity of the heater wall material, wall thickness, the heater diameter, the heat generation rate and other factors. In pool nucleate boiling, Zeng and Lee [2] were the first and only ones to study the circumferential heat conduction by introducing a non-dimensional parameter, $K^* = K_L r_o / K_W b$, which was deduced from the governing energy differential equation [1]. K^* has been used to characterize the peripheral wall heat conduction of the heater.

The knowledge of heat transfer in boiling from a tube or tube bundles in crossflow conditions is limited and most investigators seldom include circumferential heat conduction. For crossflow nucleate or film boiling, assumption of an isothermal test heater is not valid. Given uniform heat generation within a heater placed in a cross fluid flow boundary condition, heat flows by conduction within the wall of the heater and creates a non-uniform wall surface temperature distribution. The non-uniform temperature distribution within a heater may affect both the local and overall heat transfer rate since the type of the heating boundary has a strong effect on heat transfer rate. The non-uniform temperature distribution may be also dependent on crossflow velocity and degree of liquid subcooling. Therefore, a study on boiling heat transfer in a crossflow must recognize the effect of the peripheral wall conduction on the overall heat transfer rate at fixed crossflow velocity and degree of liquid subcooling. These considerations have led to the present study.

The present study investigated the effect of flow velocity, degree of liquid subcooling and system pressure on overall heat transfer rate for a fixed value of K^* in both crossflow nucleate and film boiling. The effects of flow velocity and degree of liquid subcooling on wall temperature distribution and on local heat transfer rate were also investigated. In crossflow nucleate boiling, the effect of K^*, which was varied by using different wall thicknesses for the same material, was studied for different flow velocities. Two test heaters made of 304 stainless steel with two different wall thicknesses (1.68 mm and 3.04 mm) were used. The non-dimensional parameter K^* for these two test heaters is 0.0384 and 0.0212, respectively. All the test heaters were directly electrically heated. The working fluid was 99% pure commercial grade Freon-113. The range of the flow velocity was from 0.11 to 0.84 m/s. The degree of liquid subcooling was varied from 18.1 to 38.7 $^\circ C$. The system pressure was varied from 0.157 to 0.258 MPa.

Chapter 2

Literature Survey

Almost no research on boiling heat transfer was conducted before 1934, when a landmark paper was published by Nukiyama [3] on boiling of water from an electrically heated platinum wire. The so-called "characteristic boiling curve" is typical of all boiling curves encountered in pool boiling heat transfer, and illustrates the dependence between the heat flux q and the temperature difference ΔT , called the wall superheater which is between the heating surface and the saturation temperature of the liquid. The shape of this curve should be determined by the heating surface/liquid combination, geometry, pressure, velocity, degree of subcooling, gravity and many other factors.

Figure 2.1 illustrates a characteristic boiling curve and regimes of boiling for pool boiling in the case of a temperature-controlled surface. In the region AB the heat transfer mechanism from the heating surface to the liquid is controlled by natural convection. In this region, there is no formation of bubbles when the heating surface T_w is only a few degrees above the saturation temperature T_s. At point B, the nucleate boiling BC begins and vapor bubbles are generated at favored

spots or nucleation sites on the heating surface. As ΔT is increased further, more nucleation sites are activated, bubbles coalesce and vapor jets and columns are formed close to the surface. With further increase in ΔT, point C is reached where the interaction of liquid and vapor streams causes a restriction of liquid supply to the heating surface. Point C is the upper limit of nucleate boiling and is called the peak heat flux or critical heat flux.

At point C, a decrease in the heat flux results as the wall temperature is raised because the heat transfer surface is blanketed by a partial vapor. This region CD is called the transition boiling regime and is characterized by an unstable vapor blanket which collapses and reforms rapidly under the action of circulation currents. As ΔT is increased, the vapor tends to cover a greater proportion of the surface by the vapor film. At point D the surface is entirely covered by a stable vapor film and therefore the liquid is separated from the heating surface. Point D is referred to as the minimum boiling heat flux. Region DE is called the film boiling regime. Heat transfer is accomplished principally by conduction through the vapor film, and radiation heat transfer becomes significant at higher ΔT's.

The preceding description is for the case of a temperature-controlled surface such in when the heat source is a condensing vapor. If the temperature of the heating surface is controlled by heat flux, such as nuclear reactors and electrically heated wires or tubes, the independent variable is the heat flux. Raising heat flux beyond a value corresponding to point C in Figure 2.1 would bring the nucleate boiling directly into film boiling with a large increase in ΔT (see the dotted path CC' in Figure 2.1). Because the boiling process can not remove heat as fast as it is generated, the temperature of the heater rises to some very high value; and for most systems this temperature is so high that the heater may melt or vaporize.

Boiling heat transfer can be classified in terms of the liquid temperature (saturated or subcooled boiling), the boiling mechanism (nucleate, transition, or film boiling), liquid circulation method (pool or crossflow boiling), and method of operation (steady state or transient boiling). In the following literature review, the focus will be on the steady state, pool or flow boiling of pure liquids on the outside of a single horizontal cylinder.

2.1 Pool Boiling from a Horizontal Cylinder

2.1.1 Nucleate Boiling

Today there is no completely satisfactory method of predicting nucleate boiling heat flux. It is almost impossible to correlate nucleate boiling heat transfer because it varies with different type of liquids and surface conditions (cleanliness and aging are impossible to put in a quantitative form).

Rohsenow's correlation [4] is widely used for nucleate pool boiling. He suggested the following equation by assuming a similarity between forced convection turbulent flow without boiling and nucleate pool boiling.

$$\frac{C_L \Delta T}{h_{LV}} = C_{sf}\left[\frac{\bar{q}}{\mu_L h_{LV}} \cdot \sqrt{\frac{g_c \sigma}{g(\rho_L - \rho_V)}}\right]^{1/3} \cdot Pr_L^s \tag{2.1}$$

The coefficient C_{sf} is dependent upon the way in which the liquid wets the heating surface. s is 1.0 for water and 1.7 for other liquids.

Mikic and Rohsenow [5] assumed that most important contributor to the heat transfer in nucleate boiling was transient conduction to the superheated liquid layer

in contact with the heating surface. They published another correlation.

$$\frac{\bar{q}\sqrt{\sigma g_c/g(\rho_L-\rho_v)}}{\mu_L h_{Lv}} = B(\phi\Delta T)^{m+1} \tag{2.2}$$

where

$$\phi^{(m+1)} = \frac{K_L^{1/2}\rho_L^{17/8}C_L^{19/8}h_{Lv}^{(m-23/8)}\rho_v^{(m-15/8)}}{\mu_L(\rho_L-\rho_v)^{9/8}\sigma^{(m-11/8)}T_s^{(m-15/8)}} \tag{2.3}$$

where m and B must be determined from experimental data.

Using the regression analysis, other correlations have been suggested by Stephan and Auracher [6] (for refrigerants) in a pressure range between $0.003 \leq P/P_k \leq 0.78$ given as:

$$\frac{hd}{K_L} = 207\left(\frac{\bar{q}d}{K_L T_s}\right)^{0.745}\left(\frac{\rho_v}{\rho_L}\right)^{0.581} Pr_L^{0.533} \tag{2.4}$$

and by McNelly [7].

$$\frac{hd}{K_L} = 0.225\left(\frac{\bar{q}d}{\mu_L h_{Lv}}\right)^{0.69}\left(\frac{Pd}{\sigma}\right)^{0.031}\left(\frac{\rho_L}{\rho_v-1}\right)^{0.31} Pr_L^{0.69} \tag{2.5}$$

Another common way to correlate nucleate pool boiling is in the form

$$\bar{q} = a(\Delta T)^b \tag{2.6}$$

Stephan and Abdelsalam [8] presented a correlation of nucleate boiling data for Freon-113 at 1 *atm*.

$$\bar{q} = 1.4523(\Delta T)^{3.92} \tag{2.7}$$

Yilmaz and Westwater [9] presented a correlation for Freon-113 at 1 *atm*.

$$\bar{q} = 0.532(\Delta T)^{3.72} \tag{2.8}$$

Zeng and Lee [10] presented correlations of pool nucleate boiling at different values of K^* for Freon-113 at 1 *atm*. The test heaters which they used is S.S 304. (1). For $K^* = 0.0206$

$$\bar{q} = 0.375(\Delta T)^{4.505} \tag{2.9}$$

(2). For $K^* = 0.0383$

$$\bar{q} = 0.556(\Delta T)^{4.215} \tag{2.10}$$

2.1.2 Film Boiling

In film boiling, heat transfer is accomplished by conduction through the vapor film and radiation from the heating surface. In the case of film boiling on cylinders, the vapor flows to the top of the cylinder where bubbles are formed. The vapor film thickens towards the top of the cylinder. An oscillating film is produced over the upper surface. Radiation becomes important only when the surface temperature is very high.

The stable film regime was studied experimentally and analytically by Bromley [11] for horizontal tubes. By balancing the buoyant and frictional forces on the vapor flowing in the film on the outside of a horizontal tube, Bromley suggested the following relation for calculation of heat-transfer coefficient in the stable film boiling region on the horizontal tube.

$$h_b = 0.62\left[\frac{K_v^3 \rho_v(\rho_L - \rho_v)g(h_{Lv} + 0.4C_v\Delta T)}{d\mu_v \Delta T}\right]^{1/4} \tag{2.11}$$

This heat-transfer coefficient considers only the conduction through the film and does not include the effects of radiation nor convection. The total heat-transfer coefficient may be calculated from the empirical relation.

$$h = h_b\left(\frac{h_b}{h}\right)^{1/3} + h_r \tag{2.12}$$

where h_r is the radiation heat-transfer coefficient and is calculated by assuming an emissivity of unity for the liquid. Thus

$$h_r = \frac{\dot{\sigma}\epsilon(T_w^4 - T_{sat}^4)}{\Delta T} \tag{2.13}$$

In 1962, Breen and Westwater [12] provided a empirical modification of Bromley's equation for wide region of cylinder diameter , given as:

$$h = \left[0.59 + 0.069\left(\frac{\lambda_c}{d}\right)\right]\left(\frac{F}{\lambda_c}\right)^{1/4} \tag{2.14}$$

where

$$F = \frac{K_v^3 \rho_v (\rho_L - \rho_v) g h'_{Lv}}{\mu_v \Delta T} \tag{2.15}$$

$$h'_{Lv} = h_{Lv}(1 + 0.34 C_v \Delta T / h_{Lv})^2 \tag{2.16}$$

In 1972, Bakhru and ˙˙enhard [13] presented an empirical equation for small cylinders given as:

$$\frac{Nu}{(Ra^*)^{1/4}} \simeq \frac{0.7}{(d')^{1/3}} \tag{2.17}$$

where

$$Ra^* = \frac{\rho_v (\rho_L - \rho_v) h'_{Lv} g d^3}{\mu_v K_v \Delta T} \tag{2.18}$$

$$d' = d\left[\frac{g(\rho_L - \rho_v)}{\sigma}\right]^{1/2} \tag{2.19}$$

$$h'_{Lv} = h_{Lv}(1 + 0.34 C_v \Delta T / h_{Lv})^2 \tag{2.20}$$

2.2 Crossflow Boiling

2.2.1 Single Phase Forced Convection

Fand [14] has investigated heat transfer by forced convection from a cylinder to water in terms of fluid properties evaluated at an arithmetic average film temperature. He recommended the relation

$$Nu = (0.35 + 0.56 Re_f^{0.52}) Pr_f^{0.30} \tag{2.21}$$

The relation is valid for $10^{-1} \leq Re_f \leq 10^5$.

Perkins and Leppert [15] have conducted an experimental investigation of crossflow heat transfer from a uniformly heated cylinder to water and ethylene glycol in crossflow for Reynolds numbers from 40 to 10^5 and Prandtl numbers from 1 to 300. Perkins and Leppert presented

$$Nu\left(\frac{\mu_{T_W}}{\mu_{T_L}}\right)^{0.25} = [0.30Re_b^{0.50} + 0.10Re_b^{0.67}]Pr_b^{0.40} \tag{2.22}$$

where subscript b refers to conditions at ambient temperature T_b.

2.2.2 Crossflow Nucleate Boiling

Experimental Studies

Vliet [16], McKee and Bell [17], Fand et. al. [18], Yilmaz and Westwater [9] [19] and Broussard and Westwater [27] are the main contributors in this field.

Vliet [16] studied the effect of flow velocity and the degree of liquid subcooling on crossflow nucleate boiling for water flowing vertically upward normal to an electrically heated stainless steel tube (type S.S. 304, 1/8 *in.* O.D., 8 *in.* long) at atmospheric pressure. He studied the effect of flow velocity (0.65 $ft/s \leq u \leq 11.0$ ft/s) on nucleate boiling at $50°F$ subcooling of water and the effect of degree of subcooling ($3°F \leq \Delta T_{sub} \leq 100°F$ at $u = 2.35$ ft/s). He observed that increasing either flow velocity or degree of subcooling always increased the heat transfer coefficient.

Boiling heat transfer from electrically heated cylinders at atmospheric pressure was studied both in a pool and in forced flow normal to the cylinder axis by McKee and Bell [17]. The cylinders (type S.S. 304) were 0.25 to 0.71 *in.* O.D. and were

mounted in a 3 $in.$ square cross-section channel. The working fluid was water. The flow velocities were 3.42 and 5.44 $ft/s.$ and the range of ΔT_{sub} was $3°F$ to $14°F$. The crossflow q versus ΔT curves are not strongly displaced from the corresponding pool boiling curves, except at low heat flux where the crossflow single-phase coefficient is greater than the pool boiling coefficient. They found that the surface temperature did not vary greatly with position around the periphery during nucleate boiling.

Fand et. al. [18] conducted an experimental study using an electrically heated horizontal cylinder of diameter approximately 12 mm in a water tunnel of diameter 86.6 mm with vertically upward flow. They investigated the effects of heat flux (166,000–335,000 W/m^2), flow velocity (0.024–0.122 m/s), degree of subcooling , surface material and pressure (2–4 atm). An empirical correlation equation was developed which allowed one to predict the performance of a cylindrical heater in crossflow boiling from the single phase crossflow heat transfer coefficient $\bar{h}_{FC}$ and pool nucleate boiling heat transfer coefficient $\bar{h}_{FNB}$.

The flow velocity effect on the entire boiling curve was discussed by Yilmaz and Westwater [9] [19]. They measured pool boiling and crossflow boiling heat transfer in Freon-113 from a horizontal cylinder at near atmospheric pressure. The cylinder was a steam-heated copper tube (0.25 $in.$ diameter and 5 $in.$ long). The upward flow velocities were relatively high; they were 2.4, 4.0 and 6.8 m/s. In nucleate boiling (except near the peak flux) a good estimate of the heat flux was given by simple addition of pool boiling heat flux and single phase crossflow heat flux (Rohsenow's method [20]). It was found that the entire boiling curve is sensitive to flow velocity. The boiling curves at different velocities did not intersect.

Correlations

A correlation suggested by Rohsenow [20] considers the combined effects of

crossflow and nucleate boiling in the transition region. The total heat flux is given simply by a superposition of the heat fluxes due to bubble motion and forced convection:

$$\bar{q} = \bar{q}_{PNB} + \bar{q}_{FC} \tag{2.23}$$

The crossflow term is the heat flux that is predicted by the applicable crossflow correlation at the local flow conditions. The effect of bubble motion is given by the correlation for saturated pool boiling for the particular fluid-surface combination. The boiling curve predicted by Equation (2.23) will merge with the crossflow curve at very low superheat and with the pool boiling curve at relatively high wall superheat.

The second approach to correlate crossflow nucleate boiling which was formulated by Kutateladze [21], is embodied in the following equation:

$$\frac{h}{h_{FC}} = \left[1 + \left(\frac{h_{PNB}}{h_{FC}}\right)^n\right]^{1/n} \tag{2.24}$$

Kutateladze found that, with n=2, Equation (2.24) correlated the results of several experimental studies of boiling water flowing inside tubes.

Fand et. al. [18] used Equation (2.24) to develop a correlation equation for simultaneous boiling and crossflow on the outside of a horizontal cylinder immersed in water. They defined $h_{PNB} = \bar{q}/(T_w - T_b)$ and correlated their data with n=5.5.

2.2.3 Crossflow Film Boiling

In 1953, Bromley et. al. [22] proposed two correlations for the heat transfer coefficient in crossflow film boiling for upward flow over a horizontal tube at very low and high flow velocities:

(1) For $u/\sqrt{gd} \leq 1.0$

$$h_{FB} = 0.62 \left[\frac{K_v^3 (\rho_L - \rho_v) \rho_v g h'_{LV}}{d \Delta T \mu_v} \right]^{1/4} \tag{2.25}$$

$$h_t = h_{FB} + (3/4) h_r \tag{2.26}$$

where h_r is given by Equation (2.13).

(2) For $u/\sqrt{gd} \geq 2.0$

$$h_{FB} = 2.7 \left[\frac{u K_v \rho_v h'_{LV}}{d \Delta T} \right]^{1/2} \tag{2.27}$$

$$h_t = h_{FB} + (7/8) h_r \tag{2.28}$$

where $h'_{LV} = h_{LV}(1 + 0.4 C_v \Delta T / h_{LV})^2$. Their experiments were carried out by flowing saturated liquids, i.e. ethyl alcohol, benzene, carbon tetrachloride and n-hexane, upward normal to electrically heated graphite tubes (9.53, 12.7 and 19.9 *mm* O.D. and 203.2 *mm* long). As the heat flux or the tube wall temperature was increased, a corresponding increase in the vapor film thickness was noted. As the flow velocity was increased, the vapor film thickness decreased. At high velocities, the bottom of the tube was about $45 - 90°C$ colder than the top half of the tube, indicating that the largest percentage of the heat was transferred on the lower half of the tube.

Motte and Bromley [23] obtained saturated crossflow film boiling data for subcooled benzene, carbon tetrachloride, ethyl alcohol and hexane. Three tubes (0.387, 0.496 and 0.638 *in.* O.D. and 8 *in.* long) were studied. The degree of subcooling was varied from 20 to $80°F$. They found that the heat transfer rate could be greatly improved by liquid subcooling and its value could be as high as that for nucleate boiling. The effect of thermal conduction is small to the subcooled liquid in forced convection film boiling. The eddy conduction was assumed as the dominant heat transfer mechanism in the liquid. They modified the high velocity correlation of Bromley et. al., Equation (2.27), by introducing an additional term that accounted

for the eddy conduction. They concluded that it was possible to use the dimensionless parameters

$$\frac{7.29}{h_{FB}}\left[\frac{uK_v\rho_v h'_{LV}}{d\Delta T}\right]^{1/2} - h_{FB}\left[\frac{d\Delta T}{uK_v\rho_v h'_{LV}}\right]^{1/2} \tag{2.29}$$

and

$$\Delta T_{sub}C_L\rho_L\left[\frac{\epsilon'}{\Delta T_d K_v\rho_v h'_{LV}}\right]^{1/2} \tag{2.30}$$

to correlate the data for the heat transfer in upward flow forced convection film boiling to subcooled liquids from a horizontal rod.

Yilmaz and Westwater [19] investigated the effect of flow velocity on complete boiling curves for Freon-113 boiling on a steam-heated copper cylinder at nearly atmospheric pressure. They observed that the heat flux increased with flow velocity. The forced convection film boiling heat transfer coefficient was found to be proportional to $u^{0.56}$.

2.3 Effect of Peripheral Wall Conduction

Like Rohsenow's correlation [4], most of the existing correlations do not contain the thermal properties of the heating surface, the wall thickness and the diameter of the heater. Due to the asymmetrical nature of the fluid flow around a horizontal heater, the surface temperature varies with the angle. A few studies on boiling heat transfer recognized that the variation of the surface temperature may affect on the surface heat transfer coefficient.

Bliss et. al. [24] conducted tests using electrically heated stainless steel for nucleate boiling. The tubes had been plated with thin layers of copper, zinc, tin, nickel, cadmium and chromium. They observed that the surface material strongly

influences the heat transfer coefficient during nucleate boiling of water from horizontal tubes. The effect can be either to increase or decrease the heat transfer coefficient.

Magrini and Nannei [25] investigated the influence of the thickness and thermal properties of heating wall under conditions of saturated pool nucleate boiling of water at atmospheric pressure. The heating walls, ranging in thickness from 5 to 250 μm, were obtained by plating copper, silver, zinc, nickel and tin on nonmetallic rods. They concluded that the heat transfer coefficient can be affected by the heating wall thickness. In particular, the smaller the thermal conductivity of the metal layer, the higher the influence of the thickness. A correlation was suggested.

$$\Delta T = (\bar{q})^n \cdot f(K_w b, \sqrt{K_w \rho_w C_w}) \tag{2.31}$$

Jensen et. al. [26] studied the mechanism governing nucleate pool boiling heat transfer in refrigerant-oil mixtures. Boiling heat transfer data were taken in mixtures of up to 10 percent oil by weight in R-113. An electrically heated tube (type 321) which was immersed in a saturated liquid at one atmosphere was 12.7 mm O.D. and 102 mm long. They observed that circumferential wall temperature measurements varied up to about $4°C$ at any one heat flux in the R-113-oil mixtures. They concluded that the circumferential wall conduction could have a significant effect on both the local and the average heat transfer coefficient in nucleate boiling.

Broussard and Westwater [27] studied the effect of heater diameter on the pool and flow boiling heat transfer of saturated Freon-113. Ranges of heater diameters were 1.59 to 7.94 mm in pool boiling and 3.18 to 12.7 mm in flow boiling. The test fluid at atmospheric pressure flowed normal to the heaters and approached at velocities 2.4, 4.0 and 6.0 m/s. For flow boiling on a horizontal tube, the heat flux is sensitive to heater size. The dependence is determined by the regime of boiling and

flow velocity. They observed that nucleate flow boiling is a weak function (almost independent) of heater size at low heat flux compared to the peak heat flux.

Breen and Westwater [28] studied the effect of diameter of horizontal tubes on film boiling heat transfer. Two test liquids (Freon-113, isopropanol) were used. During each test, boiling took place on a single steam-heated, horizontal, stainless steel tube. Tubes with 9 different outside diameters were used, varying from 0.185 to 1.895 *in*.. They observed that boiling the film heat transfer coefficient decreases rapidly to a minimum and then increases slowly to a flat plateau when the diameter of cylinder increases.

The work of Zeng and Lee [10] is the first and only one to study the effect of the circumferential conduction systematically by introducing a dimensionless number, K^*, in pool nucleate and film boiling. K^* was deduced from the governing energy differential equation [1]. Seven test sections made of stainless steel 304 with five different wall thicknesses (2.87, 1.65, 1.24, 1.02 and 0.8 *mm*), one made of Monel 400 (2.92 *mm* thickness) and an other Inconel 600 (2.29 *mm*) were used to vary the non-dimensional parameter K^* between 0.014 and 0.075. The working fluid was 99% pure commercial grade Freon-113. All the test heaters were electrically heated. They found that the heat transfer rate can significantly decrease or increase depending on the range of K^* during nucleate boiling. However, in the film boiling region, the effect of both peripheral conduction and material were very small.

As shown in the literature survey, many correlations have been proposed in the past for pool nucleate boiling. Many of the correlations differ widely one from another, and most of these correlations contain constants which must be determined experimentally for the particular surface-fluid combination. There is no a correlation which can be applied to any situation because of lack of a complete

understanding of the nucleate mechanism and effects of the surface and geometry on nucleate boiling.

For forced convection nucleate boiling, a few correlations have been proposed, and most of these correlations were based on the correlations for pool nucleate boiling and forced convection. However, most of the correlations for pool nucleate boiling do not contain the thermal properties of the heating surface, the thickness of the heating wall and the diameter of the heater. These quantities do affect nucleate boiling as shown by Bliss et. al. [24], Magrini and Nannei [25], and Zeng and Lee [2]. Zeng and Lee found that heat transfer rate can significantly decrease or increase depending on the range of K^* ($K^* = K_L r_o / K_w b$) during pool nucleate boiling. These quantities are also seldom included in the correlations for the film boiling.

Due to the nature of the asymmetrical boundary condition for a horizontal heater, the surface temperature varies with the angle. In pool nucleate and film boiling, a few studies [2] [26] recognized the effect of the variation of the surface temperature on the surface heat transfer coefficient. Due to an asymmetric fluid flow in crossflow nucleate and film boiling, heat may flow by conduction within the wall of the heater and may create a non-uniform wall temperature distribution. However, in crossflow nucleate and film boiling, no studies have been done on the effect of the variation of the surface temperature, which depends on the heater material, wall thickness, heater diameter, the specific heat generation rate of the heater, liquid flow velocity and degree of liquid subcooling.

Chapter 3

Theoretical Considerations

The overall heat transfer rate is strongly affected by the type of heating boundary when all other flow conditions are set equal. As long as there is an influence of the type of heating boundary, the effect of the peripheral wall conduction can also be expected.

The governing equation of the heater wall may be obtained from the energy equation with a source term:

$$\frac{\partial^2 T_w}{\partial r^2} + \frac{1}{r}\frac{\partial T_w}{\partial r} + \frac{1}{r^2}\frac{\partial^2 T_w}{\partial \theta^2} + \frac{\dot{q}}{K_w} = 0 \tag{3.1}$$

Here the radiation loss is assumed to be negligible.

Introducing T^+ and r^+

$$T^+ = (T_w - T_s)/(\overline{T}_w - T_s) \tag{3.2}$$

$$r^+ = r/r_o \tag{3.3}$$

Therefore Equation (3.1) becomes

$$\frac{\partial^2 T^+}{\partial r^{+2}} + \frac{1}{r^+}\frac{\partial T^+}{\partial r^+} + \frac{1}{r^{+2}}\frac{\partial^2 T^+}{\partial \theta^2} + \frac{r_o^2 \dot{q}}{K_w \Delta T} = 0 \tag{3.4}$$

Since

$$\dot{q} = \frac{\overline{q}}{b} = \frac{\overline{h}}{b}\left(\overline{T}_w - T_s\right) = \frac{\overline{h}}{b}\Delta T \tag{3.5}$$

Equation (3.4) simplifies to

$$\frac{\partial^2 T^+}{\partial r^{+2}} + \frac{1}{r^+}\frac{\partial T^+}{\partial r^+} + \frac{1}{r^{+2}}\frac{\partial^2 T^+}{\partial \theta^2} + \frac{1}{2}K^*\overline{Nu} = 0 \tag{3.6}$$

where

$$K^* = K_L r_o / K_w b \tag{3.7}$$

Equation (3.6) shows that the study on a heat transfer process in crossflow boiling must include the effect of K^*. Equation (3.6) can be solved only when the boundary condition at the outside wall of the test heater is known.

Chapter 4

Experimental Apparatus

The experimental data for the present study were obtained in a boiling heat transfer loop at University of Ottawa. The schematic diagram of the heat transfer loop is shown in Figure 4.1. The apparatus was designed to accommodate various flow channels.

4.1 Heat Transfer Loop Description

The heat transfer experimental system used in the study is a closed loop as shown in Figure 4.2. Since all the components which contact with the circulating fluid are made of Lexan, stainless steel and teflon, a variety of liquids can be used without any corrosion problem.

Circulation is provided in 3 *in.* Sch. 40 stainless steel pipes and stainless steel fittings by a centrifugal pump (Duriron Canada LTD., model 4 x 3 - 10). The pump is driven at 1750 *rpm* by a 15 HP electric motor (Westinghouse Canada Inc., model J4120). The pump discharges vertically through a 3 *in.* Sch. 40 pipe. The

fluid is circulated through two 3 *in.* globe valves (V1,V2), by-pass circuits, flow metering devices, preheaters, then to the test section, a condensing heat exchanger, a degassing chamber and then back to the pump. The pipe on the suction side of the pump is a 4 *in.* Sch. 40 pipe which provides enough liquid for the pump. The flow rate through the test section is regulated by two valves (V1 and V2) which are in the test section line and in the by-pass line as shown in Figure 4.1.

Four 15 *kW* immersion pre-heaters (Chromalox Canada Inc.) in stainless steel casings are used to give a total pre-heater power of 60 *kW*. The dimensioned drawing of the pre-heater is shown in Figure 4.3. The power supply to the preheaters is a special controller which was built by according to our specification. The controller can vary the pre-heater output power from 0 to 60 *kW*. For pre-heater protection, a flow switch (McDonnell and Miller, model FS-43) is used. The flow switch is located 43 *in.* from the pump at the suction side. This flow switch automatically turns off the pre-heaters when the flow is lost for any reason.

The condensing heat exchanger is a shell and tube type, single pass and counterflow. The cooling water is from city mains in the laboratory. Six baffles are used to force the water coolant to flow cross over the condensing tubes. Sixty-eight tubes (S.S. 304, 42 *in.* length) are used. Dimensioned drawings of the heat exchanger are shown in Figures 4.4 through 4.7.

Figure 4.8 shows the dimensioned drawing of the degassing chamber. The vent on the top of the chamber is connected to a compressed gas cylinder, the accumulator and a vacuum pump (Leybold Germany Inc., model ADEA-91-N-4) through the valves as shown in Figure 4.1. The accumulator as shown in Figure 4.9 is made of stainless steel 304 and equipped with three 6 *kW* heaters which can be used to pre-heat the test fluid entering the loop. The tank also has a safety

valve, a pressure gauge on the top and a sight glass on the side. The pressure in the accumulator is designed to be up to 2100 kPa. The accumulator is connected to the loop and the storage tank as shown in Figure 4.1. Figure 4.10 shows the dimension of the storage tank which is also made of sheet stainless steel. The volume of the storage tank is about 480 litres. The volume of the working fluid in the loop occupies about 220 litres.

The system pressure is maintained through the compressed cover gas (air) in the accumulator and by controlling the cooling water flow rate through the condenser. The system pressure is controlled automatically by a Honeywell proportional recorder-controller (Honeywell, model L91A) which operates on a motor-driven powerstat (Honeywell, model M944A) and a motor-operated cooling water valve. The inlet temperature can be controlled within $\pm 0.3°C$ by using this method. Figure 4.11 shows a schematic diagram of the pressure control system.

Figure 4.12 schematically shows the flow measurement loop. Four different flowmeters are used to cover the entire range of the test liquid flow from near zero to 32 litres per second. For the lower flows ($0 \leq Q \leq 0.8$ $litres/s$), a turbine flowmeter (Emerson Electric Co., model 1TMP) or a 3/4"-483 venturi is used. These two flowmeters are mounted together in 3/4 $in.$ line with a ball valve. For intermediate flows ($0.6 \leq Q \leq 6$ $litres/s$), a 2 $in.$ line containing a 2"-483 venturi (Vibro-Flo Inc.) and a 2 $in.$ gate valve is used. For the highest range ($4 \leq Q \leq 32$ $litres/s$), a 3 $in.$ line with a 3"-750 venturi (Vibro-Flo Inc.) and a 3 $in.$ gate valve is used. The three venturis are connected to a differential pressure transducer (Viatran Co., model 120-2-AC-5-AA-A2-0) and a special U-type mercury manometer with vernier scale (Casella England).

Because of the limited power supply, the working fluid chosen in the present

study was 99% pure commercial grade Freon-113. The contaminated Freon-113 was distilled to remove the impurities. A special distilling system was made. Figure 4.13 schematically shows the distilling system. Figure 4.14 shows the dimensioned drawing of the boiler which contains heaters, a sight glass and a pressure gauge. The heater is regulated by a temperature controller. Figure 4.15 shows a dimensioned drawing of the condenser used in the distilling system. The cooling fluid was water from the city mains.

The removable experimental test section (Figures 4.16 and 4.17) consists of a vertical boiling duct which contains an electrically heated horizontal test heater (see section 4.2 below). The inside cross-sectional dimensions of the boiling duct is 178 $mm \times 76$ mm with 760 mm in length. Two windows made of Lexan, 115 $mm \times 253$ mm and 37 mm in thickness, are provided in the middle part of the test section for visual observation. As showing in Figure 4.16, stainless steel honeycomb and straightening vanes are used to recover the pressure without flow separation, to reduce velocity fluctuations and to produce an uniform velocity profile in the near upstream of the test section.

The test heater is heated by a 30 V, 1500 $Amp.$ A.C. power supply (Hampden Limited). The electrical power input to the test heater is calculated by measuring the voltage drop between two leads embedded in the cylinder 50.8 mm (Figure 4.18) apart in the central portion and the current through the test heater. This eliminated the uncertainty in estimating the electrical lead losses and thus little error is introduced in calculating the heat flux. The probable maximum error in the wall heat flux is estimated to be about 3% as shown in Appendix B (Equation (B.9)).

4.2 Test Section

Two test heater cylinders (direct electrical resistance heating) made of stainless steel 304 with two different wall thickness (1.68 and 3.04 mm) are used. The details of the test heaters are given in Table 4.1 and Figure 4.18. The outside diameter of the test cylinders is kept at 24.5 mm to maintain an identical hydrodynamic aspect or fluid flow pattern around the test section for each test tube. The diameter of the test heaters is chosen to be within the range of practical importance in many industrial applications.

The test heaters are 172 mm in length. Nine chromel-alumel thermocouples (K-type, 24 Gauge) are spot welded onto the center of the inner wall periphery of the test heaters as shown in Figure 4.18. Four additional thermocouples are positioned on the inner wall 25.4 to 50.8 mm away from the center of the test heater to check the uniformity of both the axial temperature distribution and axial velocity distribution. In this way, the end effect of the temperature readings could be checked. The voltage drop within a 50.8 mm length in the central portion of test tube is measured with two alumel wires embedded in the cylinder (Figure 4.18).

Great care is taken to maintain each test heater surface at the same roughness by polishing it with grit sizes 80, 180 and 320 silicon-carbide paper, respectively.

The electrically heated tubes are silver-soldered onto two copper terminals. These copper terminals served as the electrical current passage. Teflon is used between test section and the heater body for electrical insulation. The copper pieces at the open end are screwed to connect with two copper bus bars. The detail of the test heater installation shows in Figure 4.19.

4.3 Temperature Measurement

The thermocouples are spot welded onto the inside wall of the test tubes. The inside surface temperature around the circumference of the test tube is measured by 24 gauge chromel-alumel thermocouples (K-type) located as shown in Figure 4.18. A Hewlett-Packard system 9000 series 200/300 computer with hard disks, 3455A Digital Voltmeter, 3495A Scanner and 37201A Extender are used to measure the thermal emf and to convert the emf into temperature values by using a system subprogram for temperature. The common cold junction temperature used is room temperature, which is measured by a thermistor built into the Hewlett Packard thermocouple reference connector (model 03495-64115). The maximum uncertainty of the temperature measurement is less than $\pm 0.5^{\circ}C$ as shown in Appendix B. It should be noted that the temperature indicated by the thermocouples, located as shown previously in Figure 4.18, will differ from the actual temperature of the outer surface of the heater tube. By solving the steady state heat conduction equation with heat generation, the outside wall temperature can be estimated by the equation as:

$$T_o = T_i - \frac{\bar{q}}{2bK_w}\left[\frac{1}{2}\left(r_o^2 - r_i^2\right) + r_i^2 \ln\frac{r_i}{r_o}\right] \tag{4.1}$$

The derivation of Equation (4.1) is in Appendix C.

4.4 Data Reduction

The average heat flux is given by:

$$\bar{q} = IV/2\pi r_o L \tag{4.2}$$

Because of circumferential heat conduction, even with electrical resistance heating the condition of constant heat flux is no longer applicable [1]. Therefore, the local heat transfer coefficient h should be calculated from (including radiation loss):

$$h = \frac{d^2T_w/d\theta^2 + \bar{q}r_o^2/K_w b}{(r_o^2/K_w b)(T_w - T_b)} - \varepsilon\dot{\sigma}(T_w^2 + T_b^2)(T_w + T_b) \tag{4.3}$$

Since the magnitude of $d^2T_w/d\theta^2$ ($\sim 10^{-3}{}^oC$) is much smaller than that of $\bar{q}r_o^2/K_w b$ ($\sim 10^{2}{}^oC$), the Equation (4.3) can be reduced to:

$$h = \frac{\bar{q}}{(T_w - T_b)} - \varepsilon\dot{\sigma}(T_w^2 + T_b^2)(T_w + T_b) \tag{4.4}$$

The seven outside surface temperatures at the middle of the test section are averaged and used to obtain the average heat transfer coefficient $\bar{h}$.

$$\bar{h} = \frac{\bar{q}}{(\bar{T}_w - T_b)} - \varepsilon\dot{\sigma}(\bar{T}_w^2 + T_b^2)(\bar{T}_w + T_b) \tag{4.5}$$

In the crossflow nucleate boiling region, the difference between T_w and T_b is less than 52 ^oC. Therefore, the radiation term in Equation (4.5) is negligible. In the crossflow film boiling region, even though the wall temperature is much higher than the liquid temperature, the emissivity is still very small. The emissivity ε for polished stainless steel is 0.074 [29]. The effect of radiation is also very small. The maximum error due to neglecting the radiation is estimated to be less than 2%. Therefore Equation (4.3) and(4.5) can be further reduced to:

$$h = \frac{\bar{q}}{(T_w - T_b)} \tag{4.6}$$

$$\bar{h} = \frac{\bar{q}}{(\bar{T}_w - T_b)} \tag{4.7}$$

The local and average Nusselt numbers are calculated from the definition:

$$Nu = hd_o/K_L \tag{4.8}$$

$$\overline{Nu} = \bar{h} d_o / K_L \tag{4.9}$$

where the conductivity K_L of Freon-113 is evaluated at the bulk temperature T_b.

The flow velocity used in the presentation of the experimental results is:

$$u = \frac{Q_{freon}}{l(W - d)} \tag{4.10}$$

where l and W are length and width of the inside test section, respectively. Calculation of Q_{freon} is in Appendix A. The Reynolds numbers are calculated from

$$Re = \frac{ud}{\nu_L} \tag{4.11}$$

The liquid bulk temperature is measured at the channel entrance 254 mm below the test heater. The test section static gage pressure is used to determine the Freon-113 saturation temperature at the test element. The pressure tap is located at 177.8 mm below the test heater. The degree of subcooling is determined from the difference between these two measurements. Heat flux is evaluated from the voltage drop across a central 50.8 mm length of the test tube and a known current flowing through the test section.

4.5 Experimental Procedure

The flow boiling loop (Figure 4.2) is filled with 99% pure commercial grade Freon-113. The overhead degassing chamber is filled up to a level 10 $in.$ from the cover. In order to remove absorbed gases from Freon-113, the degassing chamber is connected to a vacuum pump. The main globe valve (V1) and by-pass valve (V2) are partially opened and the centrifugal pump is turned on. The preheaters are turned on to raise the temperature of flowing liquid. At the same time the

cooling water which flows into the condenser is turned on too. The cooling water flow rate is controlled by a Honeywell proportional recorder-controller. In order to remove absorbed gases from the test tube and degas the Freon-113, boiling is allowed to proceed for about half an hour at higher heat flux. At the same time, the vacuum pump is turned on to remove the gases. Although the final gas content of the Freon-113 was not measured, it is believed that this procedure removes most of the gases.

After 30 minutes degassing, the vacuum pump is turned off. The flow boiling loop is closed. Another half an hour is needed to attain the desired flow velocity, bulk temperature and system pressure. The corresponding flow velocity (manometer reading) is set by adjusting either the main globe valve or by-pass valve. The bulk temperature of Freon-113 in the loop is controlled by the cooling water flow rate and heat flux of the preheaters. The system pressure is maintained through the cover gas (air) in the accumulator and by controlling the temperature of Freon-113 because the volume of Freon-113 is very sensitive to temperature.

Once the conditions of the experiment are adjusted to the desired values and steady state is established, the power to the heater is then adjusted to a desired level to start the test. About 1 to 2 minutes are allowed for the electrical components to reach steady state. All the test data are then acquired and reduced through a data acquisition system consisting of: a Hewlett-Packard system 9000 series 200/300 computer with hard disks; 3455A Digital Voltmeter; 3495A Scanner, 37201A Extender (which is required due to the relatively long distance between the data acquisition system and the computer) and HP 2225A Printer/Plotter. The raw and reduced data are stored on the disks.

Chapter 5

Results and Discussion

The results of this investigation are divided into two main sections: (1.) crossflow nucleate boiling, (2.) crossflow film boiling. The results of the experiment are presented in graphical and tabulated forms.

5.1 Visual Observations

With heat flux increased to a level sufficient to initiate boiling, nucleation starts first on the rear half of the cylinder at random locations. The number of these first nucleation sites per unit area is small, and there is no observable tendency for them to activate neighboring sites. As the heat flux is increased, the density of sites increases and becomes more uniform, and nucleation spreads to the forward half of the cylinder. Bubbles thus initiated on the forward half grow and move around the cylinder as a result of liquid drag and buoyant effects. They separate individually from the cylinder somewhere downstream of the 90-degree position. With further increase in the heat flux, the percentage of vapor in the two phase mixture in the

cylinder wake increases to the point that a vapor cavity forms in this region. The transition from individual bubble separation to this type of cavity formation takes place gradually. In the forward region of the cylinder, the influence of moving fluid is evident. In the crossflow nucleate boiling, an increase in both crossflow velocity and degree of liquid subcooling decreases the bubble diameter as shown in Figures 5.1, 5.2 and 5.3.

In the crossflow film boiling, the rear half portion of the heating tube was coated with a thin, dark deposit after each set of runs because Freon-113 was decomposed to the products of carbon, chlorine and fluorine at heating surface temperatures above 350 ^{o}C. Whenever the tube was seen to be discolored, it was cleaned and polished. The other procedures of the experiment described in Chapter 4.

5.2 Crossflow Nucleate Boiling

The experimental data of crossflow nucleate boiling are presented by Tables 5.1 through 5.14. The temperature readings of thermocouples are checked before each experiment. As shown in Figure 5.4, the differences between wall thermocouple temperature readings is less than $0.2^{o}C$ before an experiment. The uniformity of the flow velocity over the test heater has been checked indirectly and verified by the difference of the horizontal axial temperatures at the forward stagnation point. In Figure 5.5, the difference of the axial temperatures is very small at the center of test heater. Therefore, we can assume that the flow velocity is fairly uniform over the test tube. If Freon is not completely de-gassed, the heat transfer coefficient increases as shown Figure 5.6. The increase of the heat transfer observed may be due to two effects: (1.) the agitation of vapor bubbles and the possible thin film

evaporation at the tube surface [30] and (2.) the slight increase of the flow velocity due to mixture gases in Freon-113. Increasing the gases in Freon-113 decreases the mixture density. From Equation (A.12), it is obvious that flow rate increases with decreasing mixture density at the same U-tube manometer reading.

The reproducibility of the test results in crossflow nucleate boiling is excellent as can be seen in Figure 5.7. Distributions of the non-dimensional temperature T^+ are plotted in Figure 5.8 for different flow velocities and Figure 5.9 for different liquid subcooling. The physical meaning of T^+ may be interpreted as the ratio of the local heat transfer coefficient to the average heat transfer coefficient. These figures show that the variations of the local surface temperature are significant and increase with increasing flow velocity and degree of liquid subcooling.

Figures 5.10 and 5.11 represent the effect of the flow velocity on the surface heat flux in the crossflow nucleate boiling region for a fixed value of K*. It can be seen that the effects of flow velocity are significant. An increase in flow velocity improves the nucleate boiling heat transfer, and the curves shift up with increasing flow velocity. This is in agreement qualitatively with observations by Yilmaz and Westwater [9] and Mckee and Bell [31].

The working fluid at a test section is held at the degree of liquid subcooling ranging from 18.1 to 37.1°C. These degrees of liquid subcooling minimize cavitation at the pump and assure that no vapor generation is caused by both heat input of the pump and heat input of the preheaters. The heat flux versus temperature difference ΔT is plotted in Figure 5.12 and 5.13 for different degrees of liquid subcooling. These demonstrate typical boiling curves measured with the cylinder normal to the flow for different degrees of subcooling. Both the surface heat flux and the average heat transfer coefficient increase as the degree of subcooling increases. The effect

of the liquid subcooling is significant.

Figure 5.14 shows the effect of system pressure on the surface heat flux. In Figure 5.14, the different degrees of subcooling are corrected to $21.3°C$ by using the empirical correlation obtained from the present experiment. The correlation is shown in Figure 5.15. The heat flux increases as the system pressure increases. This may be due to the decrease of the surface tension acting between the liquid and vapor during the bubble formation when system pressure increases.

From Figure 5.16 to 5.19, local nucleate boiling curves ($\bar{q}$ versus ΔT) are shown for four values of cross flow velocity. Wall temperature measurements indicate large (up to about $6°C$) variation in the circumferential wall temperature in Freon-113. The figures show that the minimum value of the surface temperature occurs at the forward stagnation point as observed in pool boiling on a horizontal cylinder [10]. The maximum value of the surface temperature seems to occur around the backward stagnation point for the cross flow velocity of 0.11 m/s. The point of maximum temperature moves toward the angle of about 150° with increasing flow velocity (up to about 0.52 m/s). This is quite similar to those observed in a single phase flow study [1]. With further increase in the flow velocity, the point of maximum temperature moves toward the angle of about 60° for higher heat flux as shown in Figure 5.19. This may be due to the laminar boundary layer transition to turbulence. Figure 5.20 shows local heat transfer coefficient curves (h_θ versus ΔT) for 0.3 m/s velocity.

Typical local heat transfer coefficients are illustrated in Figure 5.21, 5.22 and 5.23 for different flow velocities, degrees of liquid subcooling and heat fluxes. It can be seen that effect of the flow velocity, degree of liquid subcooling and heat flux on the distribution of heat transfer coefficient is significant for a fixed value of K^*. As

shown in these figures, the variation of the heat transfer coefficient increases with increasing flow velocity, degree of liquid subcooling and heat flux.

Experimental nucleate flow boiling results of the present study are tested against the correlation proposed by Rohsenow [20] which relates nucleate flow boiling heat flux to single phase crossflow heat flux and nucleate pool boiling heat flux as shown in Figure 5.24:

$$\bar{q}_{tot} = \bar{q}_{PNB} + \bar{q}_{FC} \tag{5.1}$$

This method requires a knowledge of nucleate pool boiling. For crossflow nucleate boiling, values of $\bar{q}_{tot}$ are greater than the critical values for pool boiling. Thus using $\bar{q}_{PNB}$ in Equation 5.1 at heat fluxes higher than the critical value for nucleate pool boiling may yield inaccurate results. In our experimental data, $\bar{q}_{tot}$ does not exceed the critical heat flux for nucleate pool boiling. Figures 5.25 through 5.29 show comparison of experimental crossflow nucleate boiling curves with Rohsenow's prediction. For the single phase crossflow heat flux, Perkins and Leppert's correlation [15] is used. For the nucleate pool boiling heat flux, both McNelly's correlation [7] and Stephan's correlation [6] are used. From these figures, the superposition of McNelly's correlation and Perkins and Leppert's correlation shows fairly good agreement with the present experimental curves, especially at low flow velocities.

The present results are also compared with those of Zeng [10] for nucleate pool boiling heat transfer. To see if our data is comparable to Zeng's nucleate pool boiling results, our results are corrected for the cross flow velocity, the degree of fluid subcooling and system pressure. For the corrections of flow velocity, liquid subcooling and system pressure, the empirical correlations obtained from our experiment have been used as shown in Figure 5.15, 5.30 and 5.31. The deduced results are shown in Figures 5.32 through 5.35 and the agreement is fairly good. The difference

may be due to the different flow regimes involved and due to the error of the empirical correlations. These demonstrate that we can approximately estimate crossflow nucleate boiling heat flux from nucleate pool boiling by using the corrections for the flow velocity, liquid subcooling and system pressure.

5.3 Crossflow Film Boiling

The experimental data of crossflow film boiling is presented by Tables 5.15 through 5.20. As shown in Figure 5.36, the reproducibility of the experimental results in crossflow film boiling is excellent. The non-dimensional temperature T^+ is illustrated in Figure 5.37 and 5.38. Compared with crossflow nucleate boiling, the experimental results in crossflow film boiling have very small relative temperature variations and small variations of the local heat transfer coefficient.

Figure 5.39 represents the effect of flow velocity on the surface heat flux in crossflow film boiling. An increase in flow velocity improves the film boiling heat transfer. The effect of liquid subcooling is shown in Figure 5.40. An increase in liquid subcooling also increases the film boiling heat transfer. It can be seen that the effect of flow velocity and liquid subcooling is significant. These effects can be explained as follows. For crossflow film boiling, liquid is forced past the heating surface and a vapor film is formed to separate the liquid from the heating surface. With increasing liquid flow velocity, the vapor film becomes thinner which results in an increase in the heat transfer rate across the vapor film. When the liquid is subcooled, some energy is transferred into the bulk liquid. The vapor film thickness is less and the heat transfer rate across the vapor film will be augmented. Figure 5.41 shows the effect of system pressure on crossflow film boiling. The heat transfer

rate is increased with increasing system pressure. Increased heat transfer at elevated pressure results from an increased vapor density of the film which in turn leads to increased heat transfer. In Figure 5.41, the liquid subcooling is corrected by the empirical correlations obtained from the present experiment.

Table 5.27 shows the experimental data of crossflow film boiling with the empirical curves in the form

$$\bar{q} = a(\Delta T)^b \tag{5.2}$$

The arbitrary constants a and b are determined by least-squares fit. Equations such as these are useful in design work. The coefficient a increases steadily as the flow velocity and the degree of subcooling increase. The exponent b decreases steadily.

Figure 5.42 shows the crossflow film boiling heat transfer coefficient $\bar{h}$ versus flow velocity V for different ΔT. As shown in Figure 5.42, the average film boiling heat transfer coefficient is proportional to V at flow velocities from 0.11 to 0.52 m/s. Yilmaz and Westwater [19] found that the crossflow film boiling heat transfer coefficient was proportional to $V^{0.56}$ at flow velocities from 2.4 to 6.8 m/s.

Figures 5.43 through 5.46 show local film boiling curves ($\bar{q}$ versus ΔT) for different flow conditions. The figures show that the minimum value of the surface temperature always occurs at the forward stagnation point where liquid pressure is a maximum and the vapor film is thinnest. The maximum value of surface temperature seems to occur at an angle of about 150° for the different velocities. Such difference in surface temperature can be partially explained by the variation of vapor film thickness with angle. The local heat flux is approximately constant around the heater, which gives

$$\bar{q} = K_v \Delta T/\delta + constant \tag{5.3}$$

Therefore a comparison between the stagnation point ($\theta = 0°$) and 90° position

would give

$$\frac{\Delta T_w \mid_{\theta=90^\circ}}{\Delta T_w \mid_{\theta=0^\circ}} = \frac{\delta \mid_{\theta=90^\circ}}{\delta \mid_{\theta=0^\circ}} \tag{5.4}$$

The flow film boiling analysis [32] predicts that the film thickness increases significantly around the cylinder. Thus ΔT should increase when the angle increases as shown in Figures 5.43 through 5.46.

Typical local film boiling heat transfer coefficients are plotted in Figure 5.47 and 5.48 for different flow velocities and degree of liquid subcooling. It can be seen that the variation of the heat transfer coefficient increases with increasing flow velocity. The variation of the heat transfer coefficient does not seem to be affected by the liquid subcooling.

5.4 Effect of K^* on Crossflow Nucleate Boiling

In the nucleate pool boiling region, Zeng and Lee [10] found that the effect of K^* is significant and a critical K^* exists. If conditions other than the heater wall thickness, b, are set equal, the effect of K^* is equivalent to the effect of wall thickness. Their explanation for the existence of a critical K^* is as follows [10]: The thinner wall would have a larger bubble population which would produce a stronger stirring motion near the wall surface and hence result in a higher heat transfer rate at the same surface heat flux. On the other hand, a larger wall thickness has a low thermal resistance to the transverse heat flux. In this case, the growing bubble extracts heat from not only the wall beneath the bubble base but also from the surrounding area of the bubble and hence results in a higher heat transfer rate at same surface heat flux.

In the crossflow nucleate boiling region, Fand et. al. [18] found from a photo-

graphic study that the number of nucleation sites on a heated cylinder decreases with an increase in system pressure, flow velocity and degree of subcooling. Vliet and Leppert [33] stated that the effect of wall thickness should be most significant where large bubbles form on the heater surface. McKee and Bell [17] stated that an increase in flow velocity decreases the bubble diameter. Bankoff and Mikesell [34] indicated that the number of nucleation sites on a heated surface and the bubble diameter decrease as the flow velocity and degree of liquid subcooling increase.

In crossflow nucleate boiling, the bubble diameter decreases as the flow velocity and degree of liquid subcooling increase as shown in Figures 5.1 through 5.3. The smaller bubbles will produce less stirring motion near the wall surface than the larger bubbles. The smaller bubbles will extract less heat from the surrounding area of the bubbles than the larger bubbles. Therefore, the effect of thickness b (or K^*) in crossflow nucleate boiling may be much less than that in nucleate pool boiling. Figures 5.49 through 5.51 show the effect of K^* in crossflow nucleate boiling. As it can be seen in these figures, the effect of K^* seems to disappear in crossflow nucleate boiling.

Vliet and Leppert [33] found that there is little effect of heater tube wall thickness on the peak heat flux from 0.006 *in* to solid rod, at least for low flow velocity and liquid subcooling where the bubble size is largest Under the conditions of low flow velocity and liquid subcooling, the bubble diameter becomes larger. It is felt that the effect of wall thickness b (or K^*) may be significant at low flow velocity and liquid subcooling.

Chapter 6

Conclusions and Recommendations

Conclusions

1. For Freon-113 boiling outside a horizontal tube, the boiling curve is sensitive to flow velocity, degree of subcooling and pressure.

2. The heat transfer rate increases with increasing flow velocity, degree of subcooling and pressure.

3. Increasing flow velocity, degree of subcooling and heat flux always cause an increase in the variation of the local heat transfer coefficient, especially for crossflow nucleate boiling.

4. At low flow velocities, crossflow nucleate boiling heat flux was successfully correlated by using Rohsenow's superposition method.

5. Crossflow nucleate boiling can be approximately estimated from nucleate pool boiling by using empirical corrections for flow velocity, liquid subcooling and

system pressure.

6. From the photographic studies of the crossflow nucleate boiling, the diameter of the bubbles decreased with increasing crossflow velocity and the degree of liquid subcooling. The results is in agreement with Bankoff and Mikesell [34] for water.

7. The effect of K^* seems to disappear in crossflow nucleate boiling from the preliminary study.

Recommendations

1. In order to find out the effect of K^* in crossflow boiling, more tests are necessary for wide range of K^*, especially at the low flow velocity and liquid subcooling.

2. The non-dimensional parameter, $K^* = K_L r_o / K_w b$, is also changed by the diameter of the heater and the conductivity of the liquid. Therefore, different diameters of the heater and liquids should be studied.

Appendix A

Calculation of Flow Rate

Bernoulli equation:

$$\frac{P_2 - P_1}{\rho} + \frac{V_2^2 - V_1^2}{2} + g\Delta H_c = 0 \tag{A.1}$$

From the continuity equation for constant density flow

$$Q = V_1 A_1 = V_2 A_2 \tag{A.2}$$

$$V_1 = \frac{V_2 A_2}{A_1} \tag{A.3}$$

because horizontal position of venturi

$$\Delta H_c = 0 \tag{A.4}$$

substitute Equation (A.3) and A.4) into Equation (A.1)

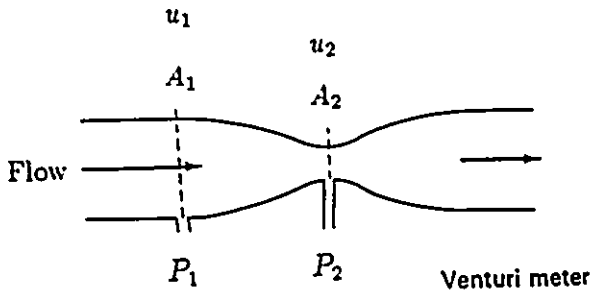

$$V_2 = \sqrt{\frac{2}{\rho} \cdot \frac{P_1 - P_2}{1 - A_2^2/A_1^2}} \tag{A.5}$$

therefor

$$Q = A_2\sqrt{\frac{2}{\rho} \cdot \frac{P_1 - P_2}{1 - A_2^2/A_1^2}} \tag{A.6}$$

assuming $(P_1 - P_2)_{water} = (P_1 - P_2)_{freon}$, we have

$$\frac{Q_{water}}{Q_{freon}} = \sqrt{\frac{\rho_{freon}}{\rho_{water}}} \tag{A.7}$$

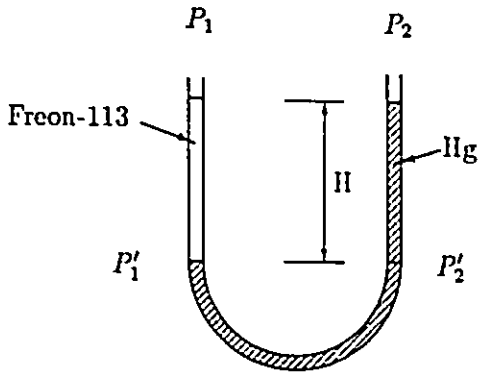

Manometer

$$P_1' = P_2' \tag{A.8}$$

therefore

$$P_1 + H\rho_{freon} = P_2 + H\rho_{Hg} \tag{A.9}$$

$$P_1 - P_2 = H(\rho_{Hg} - \rho_{freon}) \tag{A.10}$$

The height of water for $(P_1 - P_2)$ will be

$$H_{water} = \frac{H(\rho_{Hg} - \rho_{freon})}{\rho_{water}} \tag{A.11}$$

H is read from manometer. Q_{water} is taken from Figure A.1 and A.2 according to H_{water}.

$$Q_{freon} = Q_{water}\sqrt{\frac{\rho_{water}}{\rho_{freon}}} \tag{A.12}$$

Appendix B

Estimation of Experimental Errors

The experimental uncertainty can be estimated by using the standard method of uncertainty analysis [35]. In mathematical form, this method is as follows:

Let the result Y be a function of n independent variables:$X_1, X_2, \cdots, X_n$.

$$Y = Y(X_1, X_2, \cdots, X_n) \tag{B.1}$$

Then the uncertainty of the result Y is given by:

$$\Delta Y = \left[\left(\frac{\partial Y}{\partial X_1}\Delta X_1\right)^2 + \left(\frac{\partial Y}{\partial X_2}\Delta X_2\right)^2 + \cdots + \left(\frac{\partial Y}{\partial X_n}\Delta X_n\right)^2\right]^{1/2} \tag{B.2}$$

If Y is the form of $Y = A \cdot X_1^{m_1} \cdot X_2^{m_2} \cdots X_n^{m_n}$, where A is a constant and $m_1, m_2, \cdots$ and m_n are either 1 or -1, then the uncertainty of Y can be expressed as:

$$\frac{\Delta Y}{Y} = \left[\left(\frac{\Delta X_1}{X_1}\right)^2 + \left(\frac{\Delta X_2}{X_2}\right)^2 + \cdots + \left(\frac{\Delta X_n}{X_n}\right)^2\right]^{1/2} \tag{B.3}$$

The source of errors and their influence on the presented results will be considered here.

Flow velocity

The dimensions of the maximum flow channel area in the test section are (17.8 ± 0.1 cm) by (7.6 ± 0.1 cm) and the area is therefore 135.3 cm^2 in ± 2 percent. The mercury manometer indicates an uncertainty that varies between approximately ± 1 and ± 2 percent for the high and low flow rate ranges, respectively. The maximum uncertainty in the velocity is:

$$\left[(2)^2 + (2)^2\right]^{1/2} = \pm 3 \; percent \tag{B.4}$$

Liquid temperature

The liquid temperature is measured by K-type thermocouple. The standard limit of error for the K-type thermocouple is $\pm 0.4°C$ [36]. The estimated uncertainty in reading the potentiometer is $\pm 0.1°C$ [37]. The uncertainty in the liquid temperature due to the fluctuation is approximately $\pm 0.3°C$. The uncertainty in liquid temperature is therefore:

$$\left[(0.4)^2 + (0.1)^2 + (0.3)^2\right]^{1/2} = \pm 0.5°C \tag{B.5}$$

Wall temperature

The uncertainty in wall temperature is:

$$\left[(0.4)^2 + (0.1)^2\right]^{1/2} = \pm 0.5°C \tag{B.6}$$

Saturation temperature

The uncertainty in test section gage pressure is ± 0.5 psi. It results in an uncertainty of $\pm 0.5°C$ in Freon-113 saturation temperature.

Liquid subcooling

From the uncertainties in bulk liquid and saturation temperatures, the uncertainty

in liquid subcooling (ΔT_{sub}) is:

$$\left[(0.5)^2 + (0.5)^2\right]^{1/2} = \pm 0.7°C \tag{B.7}$$

Heat flux

The uncertainty in length of voltage drop is ±2 percent and in heater diameters ±0.4 percent. The uncertainty in area is:

$$\left[(2)^2 + (0.4)^2\right]^{1/2} = \pm 2\ percent \tag{B.8}$$

Voltage and current measurements are made at approximately ±0.5 percent and ±2 percent uncertainties, respectively. The uncertainty in heat flux is:

$$\left[(0.5)^2 + (2)^2 + (2)^2\right]^{1/2} = \pm 3\ percent \tag{B.9}$$

End effect

The end effect in the test heaters can be produced by heat being conducted away by the bus bars. The heat conducted away from the ends could be estimated by:

$$\bar{q} = \pi d b K_w \frac{dT}{dx} \tag{B.10}$$

In crossflow nucleate boiling, the maximum axial temperature gradient (dT/dx) is about 3 $°C$ per inch for test tube #1 ($K^* = 0.0212$). It is found that the maximum error due to the end effect is less than 1 percent in crossflow nucleate boiling, so that the end effect would be negligible in crossflow nucleate boiling. In the crossflow film boiling, the maximum temperature gradient (dT/dx) is about 80 $°C$ per inch for test tube #2 ($K^* = 0.0384$). The maximum error due to the end effect is about 10 percent in crossflow film boiling.

Radiation effect

The heat loss due to radiation may be calculated by:

$$\bar{q}_{rad} = \varepsilon \dot{\sigma} (T_w^4 - T_b^4) \tag{B.11}$$

where the emissivity ε is 0.074 for stainless steel.

In the crossflow nucleate boiling region, the uncertainty of heat flux due to radiation is less than 0.05 percent. In the crossflow film boiling region, the uncertainty of heat flux due to radiation is less than 2 percent. Therefore, it may be stated that the error due to neglecting radiation is negligibly small in both crossflow nucleate boiling and crossflow film boiling regions.

Appendix C

Derivation of Outside Surface Temperature

Considering a general case, a two dimensional conduction equation can be written as:

$$r\frac{\partial}{\partial r}\left(r\frac{\partial T}{\partial r}\right)+\frac{\partial^2 T}{\partial \theta^2}+\frac{r^2\dot{q}}{K_w}=0 \tag{C.1}$$

Experimental results show that $\partial^2 T/\partial\theta^2$ is on the order of 10^{-3}, while $r\frac{\partial}{\partial r}\left(r\frac{\partial T}{\partial r}\right)$ on the order of 10^2.

Therefore, Equation (C.1) can be further reduced to

$$\frac{d^2T}{dr^2}+r\frac{dT}{dr}+\frac{\dot{q}}{K_w}=0 \tag{C.2}$$

Equation (C.2) is a typical Euler equation.

Let $r=e^y$, $y=\ln r$,

$$\frac{dT}{dr}=\frac{dT}{dy}\frac{dy}{dr}=\frac{1}{r}\frac{dT}{dy} \tag{C.3}$$

$$\frac{d^2T}{dr^2}=\frac{d}{dy}\left(\frac{1}{r}\frac{dT}{dr}\right)\frac{dy}{dr}=\frac{1}{r^2}\frac{d^2T}{d^2y}-\frac{1}{r^2}\frac{dT}{dy} \tag{C.4}$$

Substituting Equation (C.3) and (C.4) into Equation (C.2)

$$\frac{d^2T}{dy^2} + \frac{\dot{q}}{K_w}e^{2y} = 0 \tag{C.5}$$

The general solution of Equation (C.5) is

$$T = B_o + B_1 y - \frac{\dot{q}}{4K_w}e^{2y} \tag{C.6}$$

Assuming $dT/dr|_{r_i} = 0$ then

$$B_1 = \frac{\dot{q}}{2K_w}r_i^2 \tag{C.7}$$

$$T_o = T_i - \frac{\dot{q}}{2K_w}\left[\frac{1}{2}\left(r_o^2 - r_i^2\right) + r_i^2 \ln\frac{r_i}{r_o}\right] \tag{C.8}$$

$$T_o = T_i - \frac{\bar{q}}{2bK_w}\left[\frac{1}{2}\left(r_o^2 - r_i^2\right) + r_i^2 \ln\frac{r_i}{r_o}\right] \tag{C.9}$$

List of References

[1] Y. Lee and S. Kakade, Effect of Peripheral Wall Conduction on Heat Transfer from a Cylinder in Cross Flow, *Int. J. Heat Mass Transfer* **19**, 1031-1037(1976).

[2] Y. Zeng and Y. Lee, The Effect of Peripheral Wall Conduction in Pool Boiling, *Heat Transfer Science and Technology, Hemisphere,* 445-454(1987).

[3] S. Nukiyaman, The Maximum and Minimum Values of Heat Transmitted from Metal to Boiling Water under Atmospheric Pressure, *Journal Japan Society of Mechanical Engineering* **37**, 367-374(1934).

[4] W. M. Rohsenow, A Method of Correlating Heat Transfer Data for Surface Boiling Liquids, *Trans. ASME J. Heat Transfer* **74**, 969- (1952).

[5] B. B. Mikic and W. M. Rohsenow, A New Correlation of Pool-Boiling Data Including the Effect of Heating Surface Characteristics, *Trans. ASME J. Heat Transfer* **91**, 245-250(1969).

[6] K. Stephan and H. Auracher, Correlations for Nucleate Boiling Heat Transfer in Forced Convection, *Int. J. Heat Mass Transfer* **24**, 99-107(1981).

[7] M. J. McNelly, Heat Transfer in Nucleate Boiling, *J. Imp. Coll. Chem. Engng. Soc.* **7**, 18-34(1953).

[8] K. Stephan and M. Abdelsalam, Heat-Transfer Correlations for Natural Convection Boiling, *Int. J. Heat Mass Transfer* **23**, 73-87(1980).

[9] S. Yilmaz and J. W. Westwater, Effect of Velocity on Heat Transfer to Boiling Freon-113, *Trans. ASME J. Heat Transfer* **102**, 26-31(1980).

[10] Y. Zeng, Effect of Peripheral wall Conduction in Pool Boiling, *Master Thesis*, University of Ottawa, (1985).

[11] L. A. Bromley, Heat Transfer in Stable Film Boiling, *Chemical Engineering Progress* **46**, 221-227(1950).

[12] B. P. Breen and J. W. Westwater, Effect of Diameter of Horizontal Tubes on Film Boiling Heat Transfer, *Chemical Engineering Progress* **58**, 67-72(1962).

[13] N. Bakhru and J. H. Lienhard, Boiling from Small Cylinders, *Int. J. Heat Mass Transfer* **15**, 2011-2025(1972).

[14] R. M. Fand, Heat Transfer by Forced Convection from a Cylinder to Water in Crossflow, *Int. J. Heat Mass Transfer* **8**, 995-1010(1965).

[15] H. C. Perkins and G. Leppert, Forced Convection Heat Transfer from a Uniformly Heated Cylinder, *Trans. ASME J. Heat Transfer* **84**, 257-263(1962).

[16] G. C. Vliet, Local Boiling Peak Heat Flux for Water Flowing Normal to Cylinders, *Ph.D. Thesis*, Mechanical Engng. Dept., Stanford University(1962).

[17] H. R. McKee and K. J. Bell, Forced Convection Boiling from a Cylinder Normal to the Flow, *Chemical Engineering Progress Symposium Series* **65**, 222-230(1969).

[18] R. M. Fand, K. K. Keswani, M. M. Jotwani and R. C. C. Ho, Simultaneous Boiling and Forced Convection Heat Transfer from a Horizontal Cylinder to Water, *Trans. ASME J. Heat Transfer* **98**, 395-400(1976).

[19] S. Yilmaz, Effect of Velocity on Heat Transfer to Boiling Freon-113, *Ph.D. Thesis*, University of Illinois at Urbana-Champaign(1979).

[20] W. M. Rohsenow, Heat Transfer with Evaporation, Chapter *in Heat Transfer*, University of Michigan Press(1953).

[21] S. S. Kutateladze, Boiling Heat Transfer, *Int. J. Heat Mass Transfer* 4, 31-45(1961).

[22] L. A. Bromley, N. R. LeRoy and J. A. Robbers, Heat Transfer in Forced Convection Film Boiling, *Industrial and Engineering Chemistry* **45**, 2639-2646(1953).

[23] E. I. Motte, L. A. Bromley, Film Boiling of Flowing Subcooled Liquids, *Industrial and Engineering Chemistry* **49**, 1921-1928(1957).

[24] F. E. Bliss, S. T. Hsu and M. Crawford, An Investigation into the Effects of Various Platings on the Film Coefficient during Nucleate Boiling from Horizontal Tubes, *Int. J. Heat Mass Transfer* **12**, 1061-1072(1969).

[25] U. Magrini and E. Nannei, On the Influence of the Thickness and Thermal Properties of Heating Walls on the Heat Transfer Coefficients in Nucleate Pool Boiling, *Int. J. Heat Mass Transfer* **97**, 173-178(1975).

[26] M. K. Jensen and D. L. Jackman, Predication of Nucleate Pool Boiling Heat Transfer Coefficients of Refrigerant-oil mixtures, *Trans. ASME J. Heat Transfer* **106**, 184-190(1984).

[27] R. A. Broussard and J. W. Westwater, Boiling Heat Transfer of Freon-113 Flowing Normal to a Tube: Effect of Tube Diameter, *AIAA 19th Thermophysics Conference*, Snowmass, 1-7(1984).

[28] B. P. Breen and J. W. Westwater, Effect of Diameter of Horizontal Tubes on Film Boiling Heat Transfer, *Chemical Engineering Progress* **58**, 67-72(1962).

[29] J. P. Holman, Heat Transfer, 5*th* Edition, McGraw-Hill Company (1981).

[30] K. L. Bennett, B. L. Hertaler and C. E. Kalb, Down-flow Shell-Side Forced Convection Boiling, *ASME Symp.*, Vol. HTD-44, 1-9(1985).

[31] H. R. Mckee, Forced Convection Boiling from a Cylinder Normal to the Flow, *Ph.D Thesis*, Oklahoma State University, (1967).

[32] L. C. Witte and J. A. Orozco, The Effect of Vapor Velocity on Film Boiling from Cylinders, *ASME Paper 82-Ht-28*, 1-6(1982).

[33] G. C. Vliet and G. Leppert, Local Boiling Peak Heat Flux for Water Flowing Normal to Cylinders, *Ph.D. Thesis*, Stanford University (1962).

[34] S. G. Bankoff and R. D. Mikesell, Bubble Growth Rates in Highly Subcooled Nucleate Boiling, *Chemical Engineering Progress Symposium Series*55, 95-102.

[35] W. Gellert, H. Kustner and M. Hellwich, The Vnr Encyclopedia of Mathematics, *Van Nostrand Reinhold Company*, 617(1977).

[36] Temperature Handbook 85, *OMEGA Engineering*, Inc., (1984).

[37] Manual of Digital Voltmeter 3455A, *Hewlett-Packard Company*, (1976).

Table 4.1 Characteristics of Test Tubes

NO.	Material	O.D. m	Thickness m	Conductivity K_w $W/m \cdot °C$	$K^* = K_L r_o / K_w b$
1	S.S. 304	0.0254	0.00304	13.98	0.0212
2	S.S. 304	0.0254	0.00168	13.98	0.0384

The conductivity K_w was taken from Mark's Standard Handbook for Mechanical Engineers.

The conducivity of Freon-113 was taken from ASHRAE Handbook & Product directory (1977 Fundamentals).

Table 5.1 Experimental Data In Crossflow Nucleate Boiling

Test Tube #1 S.S.304 Working Fluid = R-113

$K^* = 0.0212$ $V = 0.11\ m/s$ $\Delta T_{sub} = 22.6\,℃$ $P = 0.189\ Mpa$ $T_{sat} = 67.6\,℃$

No.	$\bar{q}$	T_o (℃)							$\overline{T}_o$	$\overline{T}_o - T_s$	$\bar{h}$	$\overline{Nu}$
	KW/m^2	0°	30°	60°	90°	120°	150°	180°	℃	℃	$W/m^2 \cdot °C$	
1	10.8	60.2	61.1	63.4	63.9	65.1	65.2	65.2	63.4	-4.2	588	211
2	13.2	62.4	63.2	65.2	63.9	66.5	67.2	67.3	65.3	-2.3	650	233
3	15.8	64.3	64.9	66.2	66.0	67.6	68.3	68.4	66.6	-1.0	731	262
4	17.3	65.3	65.5	66.8	66.8	68.6	69.7	69.9	67.6	0.1	764	274
5	18.9	65.7	66.1	67.3	67.8	69.5	70.7	70.8	68.4	0.8	809	290
6	20.4	66.4	66.4	67.7	68.3	69.9	71.1	71.3	68.8	1.2	859	308
7	22.1	66.8	66.8	68.2	68.8	70.5	71.6	77.7	69.3	1.7	910	326
8	23.7	67.5	67.6	69.1	69.7	71.4	72.6	72.7	70.2	2.6	942	337
9	25.5	68.1	68.0	69.5	69.9	72.0	73.2	73.3	70.7	3.1	994	356
10	27.3	68.4	68.2	69.7	70.2	72.3	73.7	73.8	71.0	3.4	1051	376
11	29.2	68.9	68.7	70.2	71.0	72.9	74.3	74.3	71.5	4.0	1101	394
12	31.2	69.1	68.9	70.4	71.4	73.3	74.7	74.7	71.9	4.3	1162	416
13	35.3	69.9	69.7	71.2	72.1	74.1	75.7	75.6	72.7	5.2	1274	456
14	39.5	70.4	70.2	71.7	72.4	74.7	76.2	76.0	73.2	5.6	1403	502
15	44.2	70.9	70.8	72.2	72.9	75.3	76.9	76.7	73.8	6.2	1534	549
16	49.2	71.2	71.2	72.5	72.9	75.6	77.3	77.1	74.1	6.6	1691	605
17	54.6	72.1	72.2	73.4	74.3	76.4	78.2	78.0	75.0	7.5	1818	651
18	59.8	72.8	73.0	74.1	75.1	77.0	78.8	78.6	75.7	8.2	1945	696
19	66.1	73.8	74.0	75.0	75.5	77.7	79.5	79.2	76.5	8.9	2099	751
20	72.0	74.6	74.8	75.7	76.0	78.2	80.0	79.7	77.2	9.6	2239	802
21	78.5	75.4	75.7	76.6	76.8	78.7	80.3	80.1	77.8	10.2	2395	857
22	85.1	76.1	76.4	77.2	77.4	79.2	80.6	80.4	78.3	10.8	2553	914
23	92.2	76.3	76.7	77.5	76.9	79.2	80.5	80.1	78.4	10.8	2762	989
24	99.7	76.8	77.2	77.9	77.0	79.3	80.4	80.1	78.6	11.1	2966	1062

Table 5.2 Experimental Data In Crossflow Nucleate Boiling

Test Tube #1 S.S.304 Working Fluid = R-113

$K^* = 0.0212$ $V = 0.20\ m/s$ $\Delta T_{sub} = 22.6\,℃$ $P = 0.189\ Mpa$ $T_{sat} = 67.6\,℃$

No.	$\bar{q}$	T_o (℃)							$\overline{T}_o$	$\overline{T}_o - T_s$	$\bar{h}$	$\overline{Nu}$
	KW/m^2	0°	30°	60°	90°	120°	150°	180°	℃	℃	$W/m^2 \cdot ℃$	
1	13.1	58.3	59.0	61.2	62.4	62.0	62.1	61.9	60.8	-6.8	834	298
2	14.5	59.5	60.3	62.2	61.8	63.0	63.3	63.3	61.9	-5.6	859	308
3	15.7	60.2	60.9	62.9	62.2	63.8	64.2	64.3	62.7	-4.8	887	317
4	17.2	61.2	62.0	63.7	62.6	64.8	65.5	65.4	63.8	-3.8	918	329
5	18.7	62.3	63.0	64.6	63.7	66.1	66.9	66.8	64.9	-2.6	939	336
6	20.3	63.0	63.7	65.1	64.8	67.0	68.1	68.1	65.8	-1.8	975	349
7	21.9	63.6	64.2	65.6	65.7	67.8	68.9	69.0	66.5	-1.0	1016	364
8	23.6	64.5	65.1	66.4	66.5	68.6	69.4	69.4	67.3	-0.3	1059	379
9	25.5	65.1	65.7	67.1	67.2	69.3	70.2	70.1	67.9	0.4	1110	398
10	27.2	65.8	66.3	67.7	67.9	70.0	70.9	70.8	68.6	1.0	1155	416
11	29.1	66.3	66.8	68.3	68.6	70.4	71.2	71.2	69.0	1.5	1211	434
12	31.1	66.7	67.2	68.8	69.0	70.9	71.6	71.4	69.4	1.9	1271	455
13	33.1	67.2	67.7	69.3	69.5	71.5	72.3	72.0	70.0	2.4	1324	474
14	35.3	67.8	68.2	69.8	70.0	71.9	72.7	72.4	70.5	2.9	1384	495
15	36.7	68.0	68.3	70.0	70.5	72.3	73.1	72.9	70.8	3.2	1426	511
16	39.5	68.5	68.9	70.5	70.8	72.8	73.6	73.3	71.3	3.7	1505	539
17	44.1	69.2	69.5	71.1	71.3	73.5	74.3	73.8	71.9	4.4	1639	587
18	49.3	69.9	70.2	71.7	71.9	74.5	75.5	75.0	72.8	5.2	1774	635
19	54.4	70.4	70.7	72.1	72.5	75.1	76.2	75.7	73.4	5.8	1918	687
20	59.8	71.0	71.2	72.7	73.2	75.8	76.9	76.3	74.0	6.4	2065	739
21	65.5	71.6	71.8	73.2	73.9	76.6	77.7	77.0	74.7	7.1	2208	7905
22	71.9	72.3	72.7	74.1	74.5	77.4	78.7	78.0	75.5	8.0	2357	844
23	78.3	73.0	73.3	74.7	75.2	78.0	79.1	78.3	76.1	8.5	2522	903
24	85.2	73.9	74.2	75.5	75.7	78.7	79.8	79.0	76.9	9.3	2677	958
25	92.3	74.7	75.1	76.3	76.4	79.2	80.4	79.6	77.5	10.0	2838	1016
26	100.3	75.6	76.0	77.1	77.3	79.8	80.2	80.0	78.2	10.7	3017	1080

Table 5.3 Experimental Data In Crossflow Nucleate Boiling

Test Tube #1 S.S.304 Working Fluid = R-113

$K^* = 0.0212$ $V = 0.30\ m/s$ $\Delta T_{sub} = 22.6\,℃$ $P = 0.189\ Mpa$ $T_{sat} = 67.6\,℃$

No.	$\bar{q}$	T_o (℃)							$\overline{T}_o$	$\overline{T}_o - T_s$	$\bar{h}$	$\overline{Nu}$
	KW/m^2	0°	30°	60°	90°	120°	150°	180°	℃	℃	$W/m^2 \cdot ℃$	
1	17.1	58.5	59.4	61.5	61.0	61.6	61.7	61.5	60.7	-6.9	1089	390
2	18.7	59.6	60.4	62.4	61.8	62.4	62.8	62.7	61.7	-5.6	1117	400
3	20.2	60.5	61.3	63.2	62.0	63.3	63.9	63.8	62.7	-4.9	1146	410
4	21.9	61.4	62.3	64.0	62.7	64.1	64.7	64.8	63.6	-4.0	1179	422
5	23.6	62.3	63.2	64.8	63.4	65.4	66.2	66.3	64.7	-2.9	1198	429
6	25.4	63.4	64.2	65.7	64.7	66.5	67.4	67.5	65.8	-1.8	1222	437
7	27.2	64.2	65.1	66.4	65.8	67.4	68.4	68.5	66.7	-0.9	1254	449
8	29.2	65.2	66.1	67.3	66.8	68.5	69.5	69.5	67.7	0.1	1288	461
9	31.1	65.9	66.6	68.0	67.7	69.3	70.2	70.0	68.3	0.8	1332	477
10	33.2	66.6	67.3	68.6	68.3	70.0	70.8	70.7	69.0	1.4	1385	496
11	35.0	66.9	67.6	68.9	69.0	70.5	71.2	70.9	69.3	1.8	1439	515
12	37.4	67.6	68.2	69.6	69.4	71.1	71.7	71.4	69.9	2.4	1500	537
13	39.5	68.0	68.6	70.0	69.9	71.6	72.3	72.0	70.4	2.9	1553	556
14	41.8	68.4	68.9	70.4	70.4	72.1	72.8	72.5	70.9	3.3	1618	579
15	44.3	68.9	69.4	70.8	70.8	72.6	73.2	72.7	71.3	3.7	1686	603
16	46.7	69.2	69.7	71.1	71.3	73.1	73.7	73.3	71.7	4.1	1750	626
17	49.2	69.5	70.0	71.5	71.6	73.5	74.2	73.7	72.1	4.5	1816	650
18	54.4	70.1	70.7	72.2	72.1	74.4	75.0	74.4	72.8	5.2	1957	700
19	59.8	70.6	71.1	72.6	72.8	75.3	76.0	75.1	73.5	5.9	2101	752
20	65.7	71.2	71.6	73.1	73.5	76.3	77.0	76.3	74.3	6.7	2247	805
21	72.0	71.7	72.2	73.7	74.1	77.0	77.6	76.8	74.9	7.3	2411	863
22	78.3	72.4	72.8	74.4	74.7	77.8	78.4	77.6	75.6	8.0	2562	917
23	85.0	73.0	73.4	75.0	75.4	78.6	79.1	78.1	76.2	8.6	2725	976
24	92.2	73.8	74.2	75.8	76.1	79.5	70.1	79.2	77.1	9.5	2873	1028
25	99.7	74.5	75.0	76.6	76.7	80.2	80.8	79.8	77.8	10.3	3039	1088

Table 5.4 Experimental Data In Crossflow Nucleate Boiling

Test Tube #1 S.S.304 Working Fluid = R-113

$K^* = 0.0212$ $V = 0.52\,m/s$ $\Delta T_{sub} = 22.6\,℃$ $P = 0.189\,Mpa$ $T_{sat} = 67.6\,℃$

No.	$\bar{q}$	T_o (℃)							$\overline{T}_o$	$\overline{T}_o - T_s$	$\bar{h}$	$\overline{Nu}$
	KW/m^2	0°	30°	60°	90°	120°	150°	180°	℃	℃	$W/m^2 \cdot °C$	
1	23.3	57.0	58.8	60.5	60.4	59.7	60.3	60.4	59.6	-8.0	1599	572
2	25.2	58.9	59.8	61.6	60.0	60.6	61.3	61.5	60.6	-6.9	1612	572
3	27.1	60.1	61.1	62.9	60.8	61.8	62.9	62.8	61.9	-5.6	1598	572
4	29.1	61.1	62.2	64.1	61.9	62.8	64.0	63.9	63.0	-4.6	1614	578
5	31.0	62.0	63.1	65.1	62.9	63.8	65.0	64.9	64.0	-3.6	1631	584
6	32.9	63.0	64.0	66.0	63.8	64.7	66.1	66.0	65.0	-2.6	1650	591
7	35.1	64.1	65.2	67.3	65.0	66.0	67.6	67.3	66.2	-1.3	1652	591
8	37.1	64.9	66.2	68.3	66.1	66.8	68.4	68.2	67.1	-0.4	1675	600
9	39.5	66.2	67.4	69.4	67.1	68.0	69.2	69.2	68.2	0.7	1700	608
10	41.7	66.9	68.2	70.1	68.1	68.8	69.8	70.0	69.0	1.4	1738	622
11	44.1	67.6	68.8	70.8	68.8	69.6	70.4	70.6	69.6	2.1	1789	640
12	46.4	68.0	69.1	71.2	69.5	70.2	70.8	71.1	70.1	2.5	1851	663
13	49.2	68.5	69.6	71.8	69.9	70.9	71.4	71.7	70.6	3.1	1919	687
14	51.9	69.1	70.2	72.3	70.6	71.6	71.9	72.3	71.2	3.7	1979	708
15	54.6	69.3	70.5	72.5	71.0	72.2	72.2	72.8	71.6	4.0	2053	735
16	59.7	69.7	70.9	72.7	71.6	72.9	72.9	73.6	72.1	4.6	2200	788
17	65.5	70.3	71.4	72.9	72.0	73.9	73.7	74.4	72.8	5.2	2359	844
18	71.5	70.7	71.8	73.2	72.6	74.8	74.5	75.2	73.4	5.8	2522	903
19	78.0	71.3	72.3	73.6	73.2	75.6	75.1	76.1	74.0	6.4	2690	963
20	85.0	71.8	72.9	74.1	73.6	76.6	76.2	77.2	74.8	7.3	2851	1021
21	91.9	72.3	73.3	74.5	74.3	77.2	76.7	77.7	75.3	7.7	3032	1085
22	99.5	72.9	73.8	75.1	74.7	77.9	77.4	78.4	76.0	8.4	3215	1151

Table 5.5 Experimental Data In Crossflow Nucleate Boiling

Test Tube #1 S.S.304 Working Fluid = R-113

$K^* = 0.0212$ $V = 0.84\ m/s$ $\Delta T_{sub} = 22.6\,℃$ $P = 0.189\ Mpa$ $T_{sat} = 67.6\,℃$

No.	$\bar{q}$	T_o (℃)							$\overline{T}_o$	$\overline{T}_o - T_s$	$\bar{h}$	$\overline{Nu}$
	KW/m^2	0°	30°	60°	90°	120°	150°	180°	℃	℃	$W/m^2 \cdot °C$	
1	39.1	61.0	62.0	63.9	64.8	63.2	65.4	65.6	63.5	-4.1	2114	757
2	41.6	61.9	63.0	65.0	63.9	64.3	66.6	66.9	64.6	-3.0	2124	760
3	44.1	63.1	64.3	66.2	64.6	65.5	67.7	67.9	65.8	-1.8	2121	759
4	46.6	63.9	65.1	67.1	65.6	66.3	68.5	68.5	66.6	-1.0	2160	773
5	48.9	64.8	66.0	67.9	66.4	66.9	69.0	69.0	67.2	-0.3	2201	788
6	51.7	65.7	67.0	68.9	67.1	67.8	69.6	69.5	68.1	0.5	2241	802
7	54.4	66.5	67.8	69.7	68.0	68.5	69.9	69.8	68.7	1.1	2294	821
8	57.1	67.4	68.6	70.5	68.6	69.1	70.2	70.1	69.3	1.7	2348	841
9	59.7	67.9	69.2	71.1	69.1	69.6	70.4	70.3	69.8	2.2	2413	864
10	62.6	68.7	70.0	71.9	69.6	70.1	70.7	70.5	70.3	2.7	2474	886
11	66.3	69.2	70.7	72.6	70.2	70.7	71.0	70.8	70.8	3.3	2567	919
12	71.6	69.9	71.5	73.5	70.5	71.2	71.2	70.9	71.4	3.8	2714	972
13	78.0	70.6	72.2	74.4	71.5	71.8	71.7	71.3	72.0	4.4	2890	1034
14	84.8	71.3	73.2	75.6	72.1	72.5	72.4	71.8	72.8	5.2	3049	1092
15	92.2	72.0	74.2	76.3	72.8	73.3	73.2	72.6	73.6	6.0	3225	1155
16	99.4	72.5	74.7	76.4	73.3	73.9	73.8	73.2	74.1	6.5	3419	1224

Table 5.6 Experimental Data In Crossflow Nucleate Boiling

Test Tube #1 S.S.304 Working Fluid = R-113

$K^* = 0.0212$ $\Delta T_{sub} = 18.1\,℃$ $V = 0.30\,m/s$ $P = 0.189\,Mpa$ $T_{sat} = 67.6\,℃$

No.	$\bar{q}$	T_o (℃)							$\overline{T}_o$	$\overline{T}_o - T_s$	$\bar{h}$	$\overline{Nu}$
	KW/m^2	0°	30°	60°	90°	120°	150°	180°	℃	℃	$W/m^2 \cdot °C$	
1	11.9	58.9	59.5	61.1	61.1	61.3	61.3	60.0	60.5	-7.1	1076	390
2	13.1	59.9	60.7	62.4	61.2	62.6	62.6	62.3	61.7	-5.8	1071	388
3	14.7	61.1	61.9	63.7	62.1	63.8	63.9	63.7	63.0	-4.6	1087	394
4	15.8	61.9	62.7	64.5	63.0	64.4	64.8	64.7	63.8	-3.8	1106	531
5	17.2	62.8	63.6	65.5	63.7	65.4	65.7	65.6	64.8	-2.8	1126	409
6	18.8	64.0	64.9	66.7	65.0	66.3	66.8	66.8	65.9	-1.7	1145	415
7	20.5	66.2	66.1	67.8	65.8	67.6	68.3	68.2	67.2	-0.4	1161	421
8	21.[illegible]	65.9	66.9	68.5	67.0	68.2	69.0	69.0	67.9	0.3	1189	431
9	23.6	66.6	67.5	69.1	67.8	69.0	69.8	69.8	68.6	1.0	1236	448
10	25.5	67.4	68.2	69.9	68.8	69.9	70.7	70.5	69.4	1.8	1278	464
11	27.4	67.8	68.8	70.5	69.3	70.6	71.4	71.2	70.1	2.5	1332	483
12	29.2	68.2	69.1	70.9	69.7	71.2	71.8	71.6	70.5	2.9	1393	505
13	31.1	68.5	69.3	71.1	70.2	71.7	72.4	72.0	70.8	3.2	1456	528
14	33.1	68.8	69.7	71.5	70.7	72.4	72.9	72.5	71.3	3.7	1518	551
15	35.3	69.2	70.0	71.7	71.1	72.9	73.4	73.0	71.7	4.2	1592	577
16	37.3	69.4	70.2	71.7	71.4	73.3	73.7	73.2	71.9	4.3	1662	603
17	39.6	69.7	70.6	72.0	71.8	73.7	74.4	73.8	72.4	4.8	1732	628
18	41.9	70.1	70.8	72.3	72.2	74.2	74.8	74.2	72.7	5.1	1803	654
19	44.2	70.3	71.1	72.5	72.5	74.6	75.3	74.7	73.1	5.5	1873	679
20	49.3	70.9	71.6	73.0	72.9	75.5	76.2	75.5	73.8	6.2	2033	531
21	54.6	71.4	72.1	73.5	73.5	76.3	77.0	76.3	74.4	6.9	2188	794
22	59.7	71.9	72.5	73.9	74.0	76.9	77.6	76.7	74.9	7.3	2351	853
23	65.8	72.6	73.1	74.5	74.7	77.7	78.4	77.5	75.6	8.0	2520	914
24	71.9	73.3	73.8	75.1	75.4	78.4	79.1	78.2	76.3	8.7	2684	974
25	78.7	73.9	74.4	75.6	75.8	79.0	79.6	78.7	76.9	9.3	2876	1043
26	85.2	74.5	75.0	76.3	76.4	79.5	80.1	79.2	77.4	9.8	3052	1107
27	92.1	75.2	75.6	76.9	79.8	79.9	80.5	79.5	77.9	10.3	3243	1176
28	100.6	76.1	76.6	77.7	77.6	80.5	81.0	80.1	78.6	11.1	3451	1252

Table 5.7 Experimental Data In Crossflow Nucleate Boiling

Test Tube #1 S.S.304 Working Fluid = R-113

$K^* = 0.0212$ $\Delta T_{sub} = 22.6\,℃$ $V = 0.30\,m/s$ $P = 0.189\,Mpa$ $T_{sat} = 67.6\,℃$

No.	$\bar{q}$	T_o (℃)							$\overline{T}_o$	$\overline{T}_o - T_s$	$\bar{h}$	$\overline{Nu}$
	KW/m^2	0°	30°	60°	90°	120°	150°	180°	℃	℃	$W/m^2 \cdot °C$	
1	17.1	58.5	59.4	61.5	61.0	61.6	61.7	61.5	60.7	-6.9	1089	390
2	18.7	59.6	60.4	62.4	61.8	62.4	62.8	62.7	61.7	-5.6	1117	400
3	20.2	60.5	61.3	63.2	62.0	63.3	63.9	63.8	62.7	-4.9	1146	410
4	21.9	61.4	62.3	64.0	62.7	64.1	64.7	64.8	63.6	-4.0	1179	422
5	23.6	62.3	63.2	64.8	63.4	65.4	66.2	66.3	64.7	-2.9	1198	429
6	25.4	63.4	64.2	65.7	64.7	66.5	67.4	67.5	65.8	-1.8	1222	437
7	27.2	64.2	65.1	66.4	65.8	67.4	68.4	68.5	66.7	-0.9	1254	449
8	29.2	65.2	66.1	67.3	66.8	68.5	69.5	69.5	67.7	0.1	1288	461
9	31.1	65.9	66.6	68.0	67.7	69.3	70.2	70.0	68.3	0.8	1332	477
10	33.2	66.6	67.3	68.6	68.3	70.0	70.8	70.7	69.0	1.4	1385	496
11	35.0	66.9	67.6	68.9	69.0	70.5	71.2	70.9	69.3	1.8	1439	515
12	37.4	67.6	68.2	69.6	69.4	71.1	71.7	71.4	69.9	2.4	1500	537
13	39.5	68.0	68.6	70.0	69.9	71.6	72.3	72.0	70.4	2.9	1553	556
14	41.8	68.4	68.9	70.4	70.4	72.1	72.8	72.5	70.9	3.3	1618	579
15	44.3	68.9	69.4	70.8	70.8	72.6	73.2	72.7	71.3	3.7	1686	603
16	46.7	69.2	69.7	71.1	71.3	73.1	73.7	73.3	71.7	4.1	1750	626
17	49.2	69.5	70.0	71.5	71.6	73.5	74.2	73.7	72.1	4.5	1816	650
18	54.4	70.1	70.7	72.2	72.1	74.4	75.0	74.4	72.8	5.2	1957	700
19	59.8	70.6	71.1	72.6	72.8	75.3	76.0	75.1	73.5	5.9	2101	752
20	65.7	71.2	71.6	73.1	73.5	76.3	77.0	76.3	74.3	6.7	2247	805
21	72.0	71.7	72.2	73.7	74.1	77.0	77.6	76.8	74.9	7.3	2411	863
22	78.3	72.4	72.8	74.4	74.7	77.8	78.4	77.6	75.6	8.0	2562	917
23	85.0	73.0	73.4	75.0	75.4	78.6	79.1	78.1	76.2	8.6	2725	976
24	92.2	73.8	74.2	75.8	76.1	79.5	70.1	79.2	77.1	9.5	2873	1028
25	99.7	74.5	75.0	76.6	76.7	80.2	80.8	79.8	77.8	10.3	3039	1088

Table 5.8 Experimental Data In Crossflow Nucleate Boiling

Test Tube #1 S.S.304 Working Fluid = R-113

$K^* = 0.0215$ $\Delta T_{sub.} = 27.1\,℃$ $V = 0.30\,m/s$ $P = 0.189\,Mpa$ $T_{sat} = 67.6\,℃$

No.	$\bar{q}$	T_o (℃)							$\overline{T}_o$	$\overline{T}_o - T_s$	$\bar{h}$	$\overline{Nu}$
	KW/m^2	0°	30°	60°	90°	120°	150°	180°	℃	℃	$W/m^2 \cdot °C$	
1	23.3	58.9	59.9	62.7	61.5	63.0	63.1	62.8	61.7	-5.8	1098	388
2	25.2	60.1	61.1	63.5	62.0	63.9	64.4	64.1	62.9	-4.7	1129	399
3	27.1	61.1	62.1	64.2	62.7	64.5	64.2	64.1	63.7	-3.8	1168	413
4	29.1	62.3	63.1	65.0	63.9	66.0	67.0	66.8	65.0	-2.5	1185	419
5	30.8	63.0	63.8	65.4	64.6	66.4	67.5	67.6	65.6	-1.9	1228	434
6	32.9	64.0	64.7	66.1	65.6	67.4	68.5	68.5	66.5	-1.0	1266	447
7	35.1	65.0	65.5	66.8	66.3	68.3	69.2	69.1	67.3	-0.2	1310	463
8	37.2	65.6	66.1	67.4	67.2	67.0	69.8	69.5	67.9	0.4	1358	480
9	39.4	66.2	66.7	68.0	67.8	69.7	70.6	70.3	68.6	1.0	1405	497
10	41.8	66.8	67.3	68.6	68.5	70.5	71.1	70.7	69.2	1.6	1457	515
11	44.3	67.4	67.9	69.3	69.1	71.1	71.6	71.1	69.8	2.2	1515	536
12	46.5	67.6	68.0	69.5	69.4	71.4	72.0	71.4	70.0	2.4	1578	558
13	49.2	68.2	68.7	70.2	69.9	72.1	72.6	72.1	70.6	3.1	1631	576
14	51.7	68.6	69.1	70.6	70.4	72.7	73.2	72.6	71.1	3.6	1689	597
15	54.5	69.0	69.5	71.0	70.8	73.1	73.6	72.9	71.5	4.0	1757	621
16	59.6	69.5	70.0	71.5	71.3	74.0	74.6	73.8	72.2	4.7	1881	665
17	65.6	70.0	70.5	72.0	72.0	74.8	75.5	74.7	72.9	5.4	2023	715
18	71.2	70.5	71.0	72.6	72.6	75.6	76.4	75.5	73.6	6.1	2150	760
19	78.1	71.0	71.4	73.1	73.1	76.4	77.0	76.1	74.2	6.6	2321	820
20	84.3	71.7	72.1	73.8	74.3	77.1	77.9	77.1	75.0	7.4	2448	865
21	92.1	72.4	72.9	74.5	74.6	78.1	78.9	77.8	75.8	8.2	2611	923
22	98.9	72.9	73.3	75.0	75.2	78.7	79.4	78.6	76.3	8.8	2764	977

Table 5.9 Experimental Data In Crossflow Nucleate Boiling

Test Tube #1 S.S.304 Working Fluid = R-113

$K^* = 0.0212$ $\Delta T_{sub} = 33.1\,℃$ $V = 0.30\,m/s$ $P = 0.189\,Mpa$ $T_{sat} = 67.6\,℃$

No.	$\bar{q}$	T_o (℃)							$\overline{T}_o$	$\overline{T}_o - T_s$	$\bar{h}$	$\overline{Nu}$
	KW/m^2	0°	30°	60°	90°	120°	150°	180°	℃	℃	$W/m^2 \cdot °C$	
1	26.9	56.1	57.6	61.7	60.2	62.5	62.5	61.7	60.4	-7.2	1040	361
2	28.8	57.6	59.1	63.1	60.3	63.5	62.5	62.8	61.6	-5.9	1065	370
3	30.9	59.1	60.5	64.3	61.3	64.2	64.3	63.9	62.7	-4.8	1095	380
4	33.0	60.7	62.2	65.6	62.5	65.5	65.9	65.5	64.2	-3.3	1111	386
5	35.4	62.7	64.0	66.9	63.9	66.3	66.9	66.7	65.6	-1.9	1137	395
6	37.2	63.5	64.7	67.2	65.0	66.6	67.3	66.9	66.0	-1.5	1179	410
7	39.4	64.9	66.0	68.0	65.9	67.3	68.0	67.7	67.0	-0.5	1213	422
8	41.6	66.0	67.2	68.7	66.8	68.2	68.8	68.4	67.9	0.4	1245	433
9	44.1	66.1	67.1	68.7	67.4	68.6	69.3	68.9	68.1	0.6	1312	456
10	46.6	66.7	67.5	69.3	67.9	69.4	70.0	69.5	68.7	1.2	1362	473
11	49.0	67.2	67.8	69.5	68.3	70.0	70.6	70.1	69.2	1.7	1412	491
12	51.6	67.4	68.1	69.8	68.8	70.6	71.0	70.4	69.5	2.0	1474	512
13	54.2	67.6	68.3	69.9	68.9	71.0	71.4	70.9	69.9	2.4	1533	533
14	57.0	68.2	38.8	70.3	69.5	71.6	71.9	71.3	70.4	2.9	1591	553
15	59.8	68.0	68.5	70.2	69.7	71.8	72.8	72.3	71.5	2.9	1666	579
16	62.6	68.6	68.9	70.6	70.0	72.5	72.9	72.0	70.9	3.4	1720	597
17	65.6	69.0	69.4	71.0	70.3	73.1	73.5	72.7	71.4	3.9	1776	617
18	71.6	69.3	69.6	71.3	70.8	73.8	74.3	73.3	72.0	4.5	1912	665
19	78.1	70.2	70.5	72.2	71.5	75.0	75.5	74.5	73.0	5.5	2031	706
20	84.8	70.5	70.8	72.5	72.2	75.8	76.4	75.3	73.5	6.0	2171	754
21	91.6	70.9	71.2	73.1	72.8	76.5	77.3	76.3	74.2	6.7	2308	802
22	99.1	71.8	72.1	73.9	73.4	77.6	78.4	77.2	75.2	7.7	2437	847
23	107.3	72.1	72.5	74.4	74.9	78.0	78.8	77.9	75.6	8.1	2610	907

Table 5.10 Experimental Data In Crossflow Nucleate Boiling

Test Tube #1 S.S.304 Working Fluid = R-113

$K^* = 0.0212$ $\Delta T_{sub} = 37.1\,℃$ $V = 0.30\,m/s$ $P = 0.189\,Mpa$ $T_{sat} = 67.6\,℃$

No.	$\bar{q}$	T_o (℃)							$\overline{T}_o$	$\overline{T}_o - T_s$	$\bar{h}$	$\overline{Nu}$
	KW/m^2	0°	30°	60°	90°	120°	150°	180°	℃	℃	$W/m^2 \cdot °C$	
1	30.7	55.2	56.8	61.3	59.0	62.1	62.0	61.1	59.7	-7.7	1050	361
2	32.6	56.5	58.1	62.6	59.5	63.3	63.2	62.4	61.0	-6.5	1070	368
3	31.9	58.2	59.7	64.1	60.9	64.4	64.3	63.7	62.4	-5.1	1091	375
4	36.9	59.6	61.2	65.3	62.2	65.0	65.0	64.4	63.4	-4.1	1121	385
5	39.3	61.4	62.8	66.7	63.8	66.0	66.1	65.7	64.8	-2.7	1146	394
6	41.7	62.8	64.3	67.1	64.8	66.2	66.8	66.2	65.6	-1.9	1189	409
7	43.9	64.2	65.3	67.7	65.5	66.7	67.2	66.9	66.3	-1.2	1225	421
8	46.4	66.1	67.1	68.8	66.4	67.7	68.3	67.9	67.6	0.2	1249	429
9	49.0	67.8	68.7	69.5	67.3	68.2	68.8	68.5	68.6	1.1	1288	443
10	51.4	66.3	67.4	69.0	67.7	68.6	69.3	68.9	68.2	0.7	1363	468
11	54.2	66.5	67.3	69.1	67.8	69.0	69.7	69.2	68.5	1.0	1427	490
12	56.9	66.9	67.6	69.3	68.1	69.7	70.3	69.8	68.9	1.5	1480	509
13	59.7	67.2	68.0	69.6	68.7	70.4	70.9	70.3	69.4	1.9	1536	528
14	62.5	67.6	68.2	69.9	69.1	70.7	71.2	70.7	69.7	2.3	1592	547
15	65.5	67.8	68.3	70.1	69.4	71.1	71.6	71.0	70.0	2.5	1659	570
16	71.4	68.3	68.7	70.4	69.8	72.0	72.5	71.8	70.6	3.1	1780	611
17	77.7	69.1	69.5	71.2	70.4	73.2	73.6	72.8	71.6	4.1	1894	651
18	84.6	69.6	69.9	71.5	71.0	74.1	74.6	73.6	72.2	4.7	2029	697
19	91.4	70.0	70.4	72.1	71.8	75.0	75.7	74.6	73.0	5.5	2153	740
20	99.1	71.0	71.2	73.0	72.5	76.1	77.0	75.9	74.0	6.6	2276	782
21	106.9	71.6	71.8	73.7	73.1	77.1	78.1	77.1	74.9	7.4	2408	827

Table 5.11 Experimental Data In Crossflow Nucleate Boiling

Test Tube #1 S.S.304 Working Fluid = R-113

$K^* = 0.0212$ $P = 0.158\ Mpa$ $V = 0.30\ m/s$ $T_b = 40.5\,℃$ $T_{sat} = 61.8\,℃$

No.	$\bar{q}$	T_o (℃)							$\overline{T}_o$	$\overline{T}_o - T_s$	$\bar{h}$	$\overline{Nu}$
	KW/m^2	0°	30°	60°	90°	120°	150°	180°	℃	℃	$W/m^2 \cdot °C$	
1	18.2	55.0	55.8	57.7	57.5	57.9	58.2	58.0	57.1	-4.7	1113	393
2	20.1	56.1	56.9	58.7	57.6	59.0	59.6	59.4	58.3	-3.5	1133	400
3	21.8	57.0	57.8	59.5	58.4	60.1	60.9	60.8	59.3	-2.5	1157	409
4	23.4	57.8	58.2	60.3	59.2	61.4	62.5	62.3	60.5	-1.3	1172	414
5	25.1	58.4	59.4	60.1	60.6	62.7	63.7	63.6	61.5	-0.3	1195	422
6	27.0	59.6	60.3	61.8	61.6	63.8	64.9	62.6	62.5	0.7	1230	435
7	28.8	60.3	60.9	62.3	62.4	64.4	65.4	65.2	63.1	1.3	1277	451
8	31.0	61.3	61.7	63.1	63.0	65.4	66.3	65.9	64.0	2.2	1322	467
9	32.8	62.0	62.4	63.7	63.7	66.0	66.9	66.4	64.5	2.7	1366	483
10	34.9	62.5	62.8	64.2	64.6	66.4	67.2	66.8	65.0	3.2	1425	504
11	37.1	63.0	63.5	64.8	64.9	67.0	67.7	67.2	65.5	3.8	1482	524
12	39.0	63.4	63.9	65.2	65.5	67.5	68.3	67.8	66.0	4.2	1528	540
13	43.9	64.2	64.7	66.2	66.2	68.7	69.4	68.7	67.0	5.2	1658	586
14	49.0	64.8	65.5	67.1	67.1	69.8	70.5	69.7	67.9	6.1	1789	632
15	54.0	65.4	66.0	67.6	67.7	70.5	71.2	70.4	68.7	6.7	1926	681
16	59.5	65.9	66.5	68.2	68.3	71.5	72.3	71.4	69.3	7.5	2087	731
17	65.6	66.6	67.2	68.8	68.9	72.4	73.2	72.2	70.1	8.3	2218	784
18	71.5	67.2	67.7	69.3	69.6	73.1	73.9	73.0	70.7	8.9	2367	837
19	77.8	67.7	68.2	69.9	70.3	73.7	74.5	73.5	71.2	9.4	2532	895
20	84.6	68.4	68.9	70.6	70.7	74.4	75.1	74.0	71.9	10.1	2695	952
21	92.0	69.2	69.7	71.4	71.5	75.0	75.7	74.6	72.6	10.8	2867	1013
22	99.0	70.0	70.4	72.0	71.7	75.3	75.9	74.9	73.1	11.3	3038	1074

Table 5.12 Experimental Data In Crossflow Nucleate Boiling

Test Tube #1 S.S.304 Working Fluid = R-113

$K^* = 0.0212$ $P = 0.189\ Mpa$ $V = 0.30\ m/s$ $T_b = 40.5\,℃$ $T_{sat} = 67.6\,℃$

No.	$\bar{q}$	T_o (℃)							$\overline{T}_o$	$\overline{T}_o - T_s$	$\bar{h}$	$\overline{Nu}$
	KW/m^2	0°	30°	60°	90°	120°	150°	180°	℃	℃	$W/m^2 \cdot °C$	
1	23.3	58.9	59.9	62.7	61.5	63.0	63.1	62.8	61.7	-5.8	1098	388
2	25.2	60.1	61.1	63.5	62.0	63.9	64.4	64.1	62.9	-4.7	1129	399
3	27.1	61.1	62.1	64.2	62.7	64.5	64.2	64.1	63.7	-3.8	1168	413
4	29.1	62.3	63.1	65.0	63.9	66.0	67.0	66.8	65.0	-2.5	1185	419
5	30.8	63.0	63.8	65.4	64.6	66.4	67.5	67.6	65.6	-1.9	1228	434
6	32.9	64.0	64.7	66.1	65.6	67.4	68.5	68.5	66.5	-1.0	1266	447
7	35.1	65.0	65.5	66.8	66.3	68.3	69.2	69.1	67.3	-0.2	1310	463
8	37.2	65.6	66.1	67.4	67.2	67.0	69.8	69.5	67.9	0.4	1358	480
9	39.4	66.2	66.7	68.0	67.8	69.7	70.6	70.3	68.6	1.0	1405	497
10	41.8	66.8	67.3	68.6	68.5	70.5	71.1	70.7	69.2	1.6	1457	515
11	44.3	67.4	67.9	69.3	69.1	71.1	71.6	71.1	69.8	2.2	1515	536
12	46.5	67.6	68.0	69.5	69.4	71.4	72.0	71.4	70.0	2.4	1578	558
13	49.2	68.2	68.7	70.2	69.9	72.1	72.6	72.1	70.6	3.1	1631	576
14	51.7	68.6	69.1	70.6	70.4	72.7	73.2	72.6	71.1	3.6	1689	597
15	54.5	69.0	69.5	71.0	70.8	73.1	73.6	72.9	71.5	4.0	1757	621
16	59.6	69.5	70.0	71.5	71.3	74.0	74.6	73.8	72.2	4.7	1881	665
17	65.6	70.0	70.5	72.0	72.0	74.8	75.5	74.7	72.9	5.4	2023	715
18	71.2	70.5	71.0	72.6	72.6	75.6	76.4	75.5	73.6	6.1	2150	760
19	78.1	71.0	71.4	73.1	73.1	76.4	77.0	76.1	74.2	6.6	2321	820
20	84.3	71.7	72.1	73.8	74.3	77.1	77.9	77.1	75.0	7.4	2448	865
21	92.1	72.4	72.9	74.5	74.6	78.1	78.9	77.8	75.8	8.2	2611	923
22	98.9	72.9	73.3	75.0	75.2	78.7	79.4	78.6	76.3	8.8	2764	977

Table 5.13 Experimental Data In Crossflow Nucleate Boiling

Test Tube #1 S.S.304 Working Fluid = R-113

$K^* = 0.0212$ $P = 0.230\ Mpa$ $V = 0.30\ m/s$ $T_b = 40.5\,℃$ $T_{sat} = 74.6\,℃$

No.	$\bar{q}$	T_o (℃)							$\overline{T}_o$	$\overline{T}_o - T_s$	$\bar{h}$	$\overline{Nu}$
	KW/m^2	0°	30°	60°	90°	120°	150°	180°	℃	℃	$W/m^2 \cdot °C$	
1	32.9	66.5	67.8	71.0	69.6	71.6	71.9	71.4	70.0	-4.5	1115	394
2	35.1	67.9	69.0	71.2	69.9	71.4	72.2	71.9	70.6	-4.0	1166	412
3	37.4	69.1	70.0	71.9	70.4	72.5	73.3	73.0	71.6	-2.9	1201	425
4	39.5	70.3	71.1	72.7	71.2	73.3	74.2	74.0	72.6	-2.0	1233	436
5	42.0	71.7	72.3	73.3	72.1	74.1	74.8	74.6	73.4	-1.1	1276	451
6	44.4	72.6	73.1	73.8	73.0	74.8	75.5	75.2	74.2	-0.4	1319	466
7	46.9	73.3	73.5	74.4	73.6	75.5	76.3	75.8	74.8	0.2	1369	484
8	49.3	73.6	73.7	74.7	74.1	75.9	76.4	76.0	75.1	0.5	1427	504
9	52.2	74.2	74.4	75.6	74.5	76.9	77.4	76.9	75.9	1.3	1474	521
10	54.8	74.3	74.6	75.8	75.2	77.3	77.7	77.1	76.1	1.6	1537	543
11	57.3	74.6	74.9	76.1	75.5	77.7	78.0	77.4	76.5	1.9	1593	563
12	60.1	74.6	74.9	76.3	75.9	78.1	78.4	77.7	76.7	2.1	1663	588
13	63.0	75.3	75.6	76.9	76.3	78.7	79.0	78.3	77.3	2.7	1713	605
14	66.1	75.5	75.8	77.2	76.6	79.2	79.4	78.6	77.6	3.0	1781	630
15	72.1	75.8	76.0	77.6	77.0	80.0	80.4	79.4	78.2	3.6	1910	675
16	78.9	76.6	76.9	78.4	77.7	81.2	81.7	80.8	79.3	4.7	2034	719
17	85.3	77.0	77.3	78.8	78.4	81.8	82.5	81.5	79.8	5.2	2170	767
18	92.5	77.5	77.8	79.4	79.3	82.7	83.5	82.4	80.6	6.0	2310	816
19	99.6	78.2	78.5	80.2	79.6	83.5	84.3	83.3	81.3	6.8	2439	862

Table 5.14 Experimental Data In Crossflow Nucleate Boiling

Test Tube #1 S.S.304 Working Fluid = F-113

$K^* = 0.0212$ $P = 0.258\,Mpa$ $V = 0.30\,m/s$ $T_b = 40.5\,℃$ $T_{sat} = 78.9\,℃$

No.	$\bar{q}$	T_o (℃)							$\overline{T}_o$	$\overline{T}_o - T_s$	$\bar{h}$	$\overline{Nu}$
	KW/m^2	0°	30°	60°	90°	120°	150°	180°	℃	℃	$W/m^2 \cdot °C$	
1	39.6	71.6	73.0	76.1	75.3	76.5	77.2	76.6	75.1	-3.7	1143	404
2	42.0	73.0	74.3	76.6	75.0	76.9	77.6	77.1	75.9	-3.0	1188	420
3	44.5	74.5	75.6	77.1	75.4	77.4	78.0	77.8	76.7	-2.1	1230	436
4	46.9	75.8	76.7	77.6	76.3	77.9	78.6	78.1	77.4	-1.4	1270	449
5	49.5	76.9	77.7	78.1	77.0	78.5	79.2	78.8	78.2	-0.6	1313	464
6	52.2	77.4	77.9	78.5	77.6	79.2	79.8	79.3	78.7	-0.2	1368	484
7	55.0	77.7	78.1	80.1	78.2	80.0	80.5	80.0	79.2	0.4	1420	502
8	57.6	77.8	78.2	79.1	78.5	80.2	80.7	80.1	79.4	0.5	1482	524
9	60.4	78.4	78.6	79.7	78.8	80.9	81.3	80.7	79.9	1.1	1532	541
10	63.2	78.6	78.8	79.9	79.3	81.2	81.6	80.9	80.2	1.3	1594	563
11	66.2	78.9	79.1	80.2	79.6	81.7	82.0	81.3	80.5	1.7	1655	585
12	69.3	78.8	79.0	80.3	79.8	82.0	82.3	81.5	80.6	1.8	1726	610
13	72.2	79.1	79.3	80.5	80.1	82.3	82.6	81.9	81.0	2.1	1784	630
14	78.9	80.0	80.2	81.5	80.4	83.6	83.9	83.1	82.1	3.2	1898	671
15	85.8	80.5	80.7	82.0	81.1	84.2	84.8	83.8	82.7	3.8	2034	719
16	92.8	80.9	81.2	82.6	81.9	85.3	85.6	84.6	83.3	4.5	2166	765
17	100.3	81.6	81.8	83.3	82.4	86.3	86.8	85.6	84.2	5.4	2294	811

Table 5.15 Experimental Data In Crossflow Film Boiling

Test Tube #2 S.S 304 Working Fluid = R-113

$K^* = 0.0384$ $V = 0.20\ m/s$ $\Delta T_{sub} = 23.7\ ℃$ $P = 0.196\ Mpa$ $T_{sat} = 68.7\ ℃$

No.	$\bar{q}$	T_o (℃)							$\overline{T}_o$	$\overline{T}_o - T_s$	$\bar{h}$	$\overline{Nu}$
	KW/m^2	0°	30°	60°	90°	120°	150°	180°	℃	℃	$W/m^2 \cdot ℃$	
1	125.8	616.0	616.4	623.4	638.6	652.6	650.9	647.9	635.1	566.3	213.2	76.3
2	121.5	601.3	601.0	606.7	620.3	633.7	632.5	629.2	617.8	549.0	212.0	75.9
3	113.5	568.6	567.8	573.2	586.8	601.0	600.0	597.3	584.9	516.2	210.0	75.2
4	107.5	550.7	550.4	555.9	569.4	583.5	583.2	581.1	567.8	499.0	205.7	73.6
5	101.3	523.4	522.4	527.4	541.2	556.3	556.7	554.5	540.3	471.5	204.5	73.2
6	95.2	500.6	499.5	504.3	517.8	533.4	534.8	532.9	517.6	448.8	201.4	72.1
7	88.1	470.2	469.5	474.1	487.7	504.0	507.1	504.8	488.2	419.4	198.8	71.2
8	83.1	441.3	440.1	444.1	457.6	474.5	478.3	476.3	458.9	390.1	200.9	71.9

Table 5.16 Experimental Data In Crossflow Film Boiling

Test Tube #2 S.S 304 Working Fluid = R-113

$K^* = 0.0384$ $V = 0.30\ m/s$ $\Delta T_{sub} = 23.7\ ℃$ $P = 0.196\ Mpa$ $T_{sat} = 68.7\ ℃$

No.	$\bar{q}$	T_o (℃)							$\overline{T}_o$	$\overline{T}_o - T_s$	$\bar{h}$	$\overline{Nu}$
	KW/m^2	0°	30°	60°	90°	120°	150°	180°	℃	℃	$W/m^2 \cdot °C$	
1	125.7	572.0	576.6	589.6	616.6	625.4	619.0	618.6	602.5	533.7	225.4	80.7
2	119.3	555.2	559.1	571.6	597.5	606.7	599.8	600.2	584.3	515.2	221.1	79.2
3	112.3	528.0	532.6	545.0	570.8	581.0	574.6	573.9	558.0	489.2	218.9	78.4
4	105.9	504.1	509.0	521.7	548.1	558.4	552.2	551.6	535.0	466.2	216.2	77.4
5	100.2	480.2	484.6	496.6	521.8	535.0	528.7	527.4	510.6	441.8	215.3	77.1
6	92.6	447.2	451.2	462.8	488.4	501.9	496.1	495.1	477.5	408.7	214,1	76.6
7	84.5	404.0	408.0	418.8	443.7	456.6	451.3	449.8	433.2	364.4	217.7	77.9

Table 5.17 Experimental Data In Crossflow Film Boiling

Test Tube #2 S.S 304 Working Fluid = R-113

$K^* = 0.0384$ $V = 0.52\ m/s$ $\Delta T_{sub} = 23.7\ ℃$ $P = 0.196\ Mpa$ $T_{sat} = 68.7\ ℃$

No.	$\bar{q}$	T_o (℃)							$\overline{T}_o$	$\overline{T}_o - T_s$	$\bar{h}$	$\overline{Nu}$
	KW/m^2	0°	30°	60°	90°	120°	150°	180°	℃	℃	$W/m^2 \cdot °C$	
1	142.2	537.2	553.6	580.2	608.5	606.5	612.8	613.1	587.4	518.6	262.2	93.9
2	137.1	524.1	540.8	567.8	595.8	594.3	600.1	601.0	574.8	506.1	258.8	92.6
3	129.7	499.3	515.3	541.9	569.5	567.9	574.0	575.1	549.0	480.2	257.3	92.1
4	122.4	474.4	490.5	516.5	543.5	541.5	546.9	547.5	523.0	454.2	256.2	91.7
5	115.1	450.5	465.6	491.0	517.8	516.6	522.0	522.4	498.0	429.2	254.1	91.0
6	107.8	418.8	433.2	457.9	483.4	482.0	487.2	487.4	464.3	395.5	257.1	92.0
7	99.9	387.3	401.1	424.8	451.9	451.3	458.0	457.8	433.2	364.4	257.4	92.1

Table 5.18 Experimental Data In Crossflow Film Boiling

Test Tube #2 S.S 304 Working Fluid = R-113

$K^* = 0.0384$ $\Delta T_{sub.} = 23.7\,℃$ $V = 0.30\,m/s$ $P = 0.196\,Mpa$ $T_{sat} = 68.7\,℃$

No.	$\bar{q}$	T_o (℃)							$\overline{T}_o$	$\overline{T}_o - T_s$	$\bar{h}$	$\overline{Nu}$
	KW/m^2	0°	30°	60°	90°	120°	150°	180°	℃	℃	$W/m^2 \cdot ^oC$	
1	125.7	572.0	576.6	589.6	616.6	625.4	619.0	618.6	602.5	533.7	225.4	80.7
2	119.3	555.2	559.1	571.6	597.5	606.7	599.8	600.2	584.3	515.2	221.1	79.2
3	112.3	528.0	532.6	545.0	570.8	581.0	574.6	573.9	558.0	489.2	218.9	78.4
4	105.9	504.1	509.0	521.7	548.1	558.4	552.2	551.6	535.0	466.2	216.2	77.4
5	100.2	480.2	484.6	496.6	521.8	535.0	528.7	527.4	510.6	441.8	215.3	77.1
6	92.6	447.2	451.2	462.8	488.4	501.9	496.1	495.1	477.5	408.7	214,1	76.6
7	84.5	404.0	408.0	418.8	443.7	456.6	451.3	449.8	433.2	364.4	217.7	77.9

Table 5.19 Experimental Data In Crossflow Film Boiling

Test Tube #2 S.S 304 Working Fluid = R-113

$K^* = 0.0384$ $\Delta T_{sub.} = 32.7\,℃$ $V = 0.30\,m/s$ $P = 0.196\,Mpa$ $T_{sat} = 68.7\,℃$

No.	$\bar{q}$	T_o (℃)							$\overline{T}_o$	$\overline{T}_o - T_s$	h	$\overline{Nu}$
	KW/m^2	0°	30°	60°	90°	120°	150°	180°	℃	℃	$W/m^2 \cdot ℃$	
1	129.8	561.7	569.7	584.3	612.1	619.3	610.3	609.3	595.2	526.5	232.1	81.0
2	124.5	546.5	553.6	567.6	595.0	602.4	593.7	593.6	578.9	510.2	229.4	80.0
3	117.2	519.6	526.9	540.8	568.2	576.4	567.9	567.6	552.5	483.8	226.9	79.2
4	111.1	494.6	502.2	516.3	544.0	552.8	544.3	543.3	528.2	459.5	225.7	78.8
5	105.1	464.3	472.0	485.8	513.8	521.6	514.0	512.8	497.8	429.0	227.6	79.4
6	96.6	426.4	434.0	447.1	474.4	482.0	474.8	474.7	459.1	390.3	228.3	79.7

Table 5.20 Experimental Data In Crossflow Film Boiling

Test Tube #2 S.S 304 Working Fluid = R-113

$K^* = 0.0384$ $\Delta T_{sub.} = 38.7\,℃$ $V = 0.30\,m/s$ $P = 0.196\,Mpa$ $T_{sat} = 68.7\,℃$

No.	q	T_o (℃)							$\overline{T}_o$	$\overline{T}_o - T_s$	$\bar{h}$	$\overline{Nu}$
	KW/m^2	0°	30°	60°	90°	120°	150°	180°	℃	℃	$W/m^2 \cdot °C$	
1	149.3	582.0	587.4	599.3	624.8	637.0	628.7	627.2	612.3	543.6	256.3	88.0
2	142,5	563.1	568.3	579.8	605.7	617.6	609.2	607.7	593.1	524.4	253.2	86.9
3	134.5	531.0	536.9	549.0	574.8	588.2	580.7	578.3	562.74	494.0	252,5	86,6
4	125.8	494.7	500.5	513.3	539.4	553.1	544.5	542.3	526,8	458.1	253.2	86.9
5	137.6	544.8	552.2	565.0	594.0	608.0	599.8	598.8	580.4	511.7	250.0	85.8
6	130.5	520.7	528.1	540.6	568.7	583.5	574.8	573.5	555.7	487.0	248.2	85.2
7	121.5	486.0	493.5	508.0	533.6	549.2	541.2	539.2	521.2	452.5	247.4	84.9
8	104.6	400.7	418.4	434.3	462.6	478.2	468.2	463.0	447.6	379.0	250.5	86.0

Table 5.21 Experimental Data In Crossflow Film Boiling

Test Tube #2 S.S 304 Working Fluid = R-113

$K^* = 0.0384$ $P = 0.157\ Mpa$ $V = 0.30\ m/s$ $T_b = 30\,℃$ $T_{sat} = 61.7\,℃$

No.	$\bar{q}$	T_o (℃)							$\overline{T}_o$	$\overline{T}_o - T_s$	$\bar{h}$	$\overline{Nu}$
	KW/m^2	0°	30°	60°	90°	120°	150°	180°	℃	℃	$W/m^2 \cdot °C$	
1	118.0	534.7	541.7	555.6	584.8	596.6	588.0	585.4	569.5	507.8	218.8	75.1
2	112.6	516.2	523.0	536.6	565.6	577.3	569.4	567.4	550.8	489.1	216.3	74.2
3	104.9	485.7	492.6	505.8	534.5	545.9	530.7	536.2	519.9	458.2	214.2	73.5
4	98.4	454.1	460.6	473.1	500.9	514.2	506.9	504.8	487.8	426.1	214.9	73.7
5	90.9	413.6	420.0	432.2	460.1	470.9	465.4	463.9	446.6	384.9	218.2	74.9

Table 5.22 Experimental Data In Crossflow Film Boiling

Test Tube #2 S.S 304 Working Fluid = R-113

$K^* = 0.0384$ $P = 0.196\ Mpa$ $V = 0.30\ m/s$ $T_b = 30\,℃$ $T_{sat} = 68.7\,℃$

No.	$\bar{q}$	T_o (℃)							$\overline{T}_o$	$\overline{T}_o - T_s$	$\bar{h}$	$\overline{Nu}$
	KW/m^2	0°	30°	60°	90°	120°	150°	180°	℃	℃	$W/m^2 \cdot °C$	
1	149.3	582.0	587.4	599.3	624.8	637.0	628.7	627.2	612.3	543.6	256.5	88.0
2	142,5	563.1	568.3	579.8	605.7	617.6	609.2	607.7	593.1	524.4	253.2	86.9
3	134.5	531.0	536.9	549.0	574.8	588.2	580.7	578.3	562.74	494.0	252,5	86,6
4	125.8	494.7	500.5	513.3	539.4	553.1	544.5	542.3	526,8	458.1	253.2	86.9
5	137.6	544.8	552.2	565.0	594.0	608.0	599.8	598.8	580.4	511.7	250.0	85.8
6	130.5	520.7	528.1	540.6	568.7	583.5	574.8	573.5	555.7	487.0	248.2	85.2
7	121.5	486.0	493.5	508.0	533.6	549.2	541.2	539.2	521.2	452.5	247.4	84.9
8	104.6	400.7	418.4	434.3	462.6	478.2	468.2	463.0	447.6	379.0	250.5	86.0

Table 5.23 Experimental Data In Crossflow Film Boiling

Test Tube #2 S.S 304 Working Fluid = R-113

$K^* = 0.0384$ $P = 0.230\ Mpa$ $V = 0.30\ m/s$ $T_b = 30\,℃$ $T_{sat} = 74.5\,℃$

No.	$\bar{q}$	T_o (℃)							$\overline{T}_o$	$\overline{T}_o - T_s$	$\bar{h}$	$\overline{Nu}$
	KW/m^2	0°	30°	60°	90°	120°	150°	180°	℃	℃	$W/m^2 \cdot °C$	
1	166.7	611.5	617.3	629.7	658.9	875.7	667.0	665.1	646.6	572.1	270.4	92.8
2	157.9	589.1	594.7	607.7	639.3	654.3	646.1	644.3	625.1	550.6	265.3	91.0
3	151.1	567.0	573.0	586.1	617.3	633.0	624.3	622.7	603.3	528.8	263.6	90.4
4	142.8	537.8	543.9	556.6	587.4	604.0	594.4	592.6	573.8	499.3	262.5	90.0
5	135.8	511.0	517.2	529.8	560.4	576.0	567.9	566.4	547.0	472.5	262.6	90.1
6	127.0	481.6	467.5	499.7	529.7	543.9	535.6	534.7	516.1	441.6	261.3	89.7

Table 5.24 Experimental Data In Crossflow Nucleate Boiling

Test Tube #2 S.S.304 Working Fluid = R-113

$K^* = 0.0384$ $V = 0.11\ m/s$ $\Delta T_{sub} = 22.6\,℃$ $P = 0.189\ Mpa$ $T_{sat} = 67.6\,℃$

No.	$\bar{q}$	T_o (℃)							$\overline{T}_o$	$\overline{T}_o - T_s$	$\bar{h}$	$\overline{Nu}$
	KW/m^2	0°	30°	60°	90°	120°	150°	180°	℃	℃	$W/m^2 \cdot °C$	
1	17.9	63.2	63.7	64.3	66.4	66.0	67.1	71.9	66.0	-1.5	851	305
2	19.8	64.0	64.5	65.1	67.2	66.6	67.7	72.4	66.7	-0.9	911	326
3	21.7	64.9	65.4	66.0	68.0	67.5	68.5	73.1	67.6	0.0	959	343
4	23.6	65.7	66.2	66.8	68.8	68.3	69.2	73.8	68.3	0.8	1013	362
5	25.8	66.5	67.1	67.7	69.4	69.1	70.0	74.2	69.1	1.5	1070	383
6	28.2	67.4	68.0	68.5	70.0	69.8	70.5	74.7	69.8	2.3	1136	407
7	30.6	68.1	68.8	69.2	70.5	70.4	71.1	75.5	70.5	3.0	1200	430
8	33.0	68.9	69.6	69.9	71.1	71.0	71.6	76.0	71.2	3.6	1261	452
9	35.3	69.4	70.0	70.3	71.4	71.4	72.0	76.5	71.6	4.0	1325	474
10	41.0	70.4	71.2	71.5	72.4	72.3	72.9	77.4	72.6	5.1	1485	532
11	46.8	71.5	72.3	72.6	73.4	73.4	73.8	78.5	73.7	6.1	1631	583
12	52.6	72.3	73.2	73.6	74.4	74.3	74.7	79.1	74.5	7.0	1781	638
13	59.2	73.5	74.4	74.7	75.5	75.3	75.6	80.0	75.6	8.0	1937	694
14	66.4	74.7	75.6	75.8	76.5	76.3	76.7	80.7	76.6	9.1	2100	752
15	74.0	75.9	76.8	77.0	77.5	77.4	77.7	81.4	77.7	10.1	2263	810
16	81.9	76.6	77.6	77.7	78.2	78.1	78.3	81.6	78.3	10.7	2456	879
17	90.1	77.5	78.6	78.8	79.1	79.1	79.1	82.0	79.2	11.6	2636	944
18	98.8	78.4	79.5	79.5	79.9	79.9	79.8	82.6	80.0	12.4	2826	1012

Table 5.25 Experimental Data In Crossflow Nucleate Boiling

Test Tube #2 S.S.304 Working Fluid = R-113

$K^* = 0.0384$ $V = 0.30\ m/s$ $\Delta T_{sub} = 22.6\ ℃$ $P = 0.189\ Mpa$ $T_{sat} = 67.6\ ℃$

No.	$\bar{q}$	T_o (℃)							$\overline{T}_o$	$\overline{T}_o - T_s$	$\bar{h}$	$\overline{Nu}$
	KW/m^2	0°	30°	60°	90°	120°	150°	180°	℃	℃	$W/m^2 \cdot °C$	
1	21.6	61.4	62.2	63.1	64.3	64.1	64.7	68.9	64.3	-3.5	1137	407
2	25.9	63.3	63.8	64.6	66.3	65.8	66.6	70.7	65.8	-1.8	1245	446
3	30.5	65.1	65.5	66.2	68.2	67.6	68.4	72.1	67.5	-0.1	1359	486
4	32.9	65.8	66.3	67.0	69.0	68.3	69.2	72.3	68.2	0.6	1419	508
5	35.2	66.4	66.9	67.6	69.6	69.0	69.8	72.8	68.7	1.2	1483	531
6	38.1	67.4	67.9	68.6	70.5	69.9	70.6	73.6	69.7	2.1	1545	553
7	40.6	67.9	68.4	69.2	71.1	70.5	71.1	74.0	70.2	2.6	1614	578
8	43.8	68.8	69.5	70.0	71.9	71.3	71.9	74.7	71.0	3.5	1684	603
9	46.2	69.3	70.1	70.5	72.4	71.7	72.3	75.4	71.6	4.0	1753	627
10	49.7	69.8	70.8	71.2	73.1	72.4	72.9	75.6	72.1	4.5	1834	656
11	52.6	70.0	71.1	71.6	73.5	72.7	73.3	76.2	72.5	4.9	1913	685
12	59.1	70.9	72.2	72.5	74.4	73.7	74.2	77.3	73.5	5.9	2074	742
13	66.5	71.9	73.2	73.6	75.6	74.7	75.3	78.5	74.5	7.0	2254	807
14	73.7	72.7	74.0	74.5	76.5	75.6	76.2	79.4	75.4	7.8	2427	869
15	81.6	73.5	74.8	75.4	77.5	76.5	77.1	80.1	76.2	8.7	2613	935
16	90.1	74.5	75.8	76.3	78.5	77.4	78.0	81.2	77.2	9.6	2800	1002
17	98.5	75.3	76.6	77.2	79.2	78.3	78.8	81.7	78.0	10.4	2988	1070

Table 5.26 Experimental Data In Crossflow Nucleate Boiling

Test Tube #2 S.S.304 Working Fluid = R-113

$K^* = 0.0384$ $V = 0.52\,m/s$ $\Delta T_{sub} = 22.6\,℃$ $P = 0.189\,Mpa$ $T_{sat} = 67.6\,℃$

No.	$\bar{q}$	T_o (℃)							$\overline{T}_o$	$\overline{T}_o - T_s$	$\bar{h}$	$\overline{Nu}$
	KW/m^2	0°	30°	60°	90°	120°	150°	180°	℃	℃	$W/m^2 \cdot °C$	
1	30.1	62.3	63.8	65.2	63.9	65.4	64.9	68.3	65.0	-2.6	1507	540
2	32.6	63.3	64.7	66.1	65.2	66.4	65.8	69.5	66.0	-1.6	1556	557
3	35.3	64.4	65.8	67.0	66.3	67.3	66.9	70.0	66.9	-0.7	1611	577
4	37.8	65.4	66.7	67.6	67.2	68.2	67.8	70.8	67.8	0.2	1663	595
5	40.6	66.3	67.7	68.4	68.1	68.9	68.6	71.5	68.5	1.0	1725	618
6	43.5	67.1	68.6	69.1	68.9	69.6	69.4	72.1	69.3	1.8	1790	641
7	46.4	67.8	69.4	69.7	69.7	70.1	70.0	72.5	69.9	2.4	1861	666
8	49.7	68.4	70.2	70.5	70.5	70.7	70.8	73.0	70.6	3.0	1941	695
9	52.7	69.1	70.8	71.0	71.2	71.2	71.3	73.7	71.2	3.6	2015	721
10	55.4	69.4	71.3	71.3	71.6	71.5	71.7	73.8	71.5	3.9	2093	749
11	59.2	69.7	71.9	72.0	72.4	72.1	72.3	74.7	72.1	4.6	2183	782
12	66.3	70.7	72.7	72.7	73.5	72.9	73.3	75.5	73.0	5.4	2368	848
13	73.7	71.4	73.5	73.5	74.6	73.9	74.3	76.8	73.9	6.3	2553	914
14	81.8	72.3	74.2	74.3	75.7	74.8	75.3	77.9	74.8	7.2	2748	984
15	89.5	72.8	74.8	74.8	76.6	75.5	76.0	78.5	75.4	7.8	2946	1054
16	98.7	73.7	75.5	75.7	77.8	76.5	77.0	79.5	76.3	8.8	3152	1128

Table 5.27 Correlations of Experimental Data
In Crossflow Film Boiling

$$\bar{q} = a(\Delta T)^b$$

$$K^* = 0.038\text{-}4$$

	a	b
$\Delta T_{sub.} = 23.7\,^\circ C$ $P = 0.196\,Mpa$ $V = 0.20\,m/s$	89.7	1.142
$\Delta T_{sub.} = 23.7\,^\circ C$ $P = 0.196\,Mpa$ $V = 0.30\,m/s$	180.6	1.039
$\Delta T_{sub.} = 23.7\,^\circ C$ $P = 0.196\,Mpa$ $V = 0.52\,m/s$	292.8	0.988
$\Delta T_{sub.} = 32.7\,^\circ C$ $P = 0.196\,Mpa$ $V = 0.30\,m/s$	286.7	0.974
$\Delta T_{sub.} = 38.7\,^\circ C$ $P = 0.196\,Mpa$ $V = 0.30\,m/s$	335.4	0.966

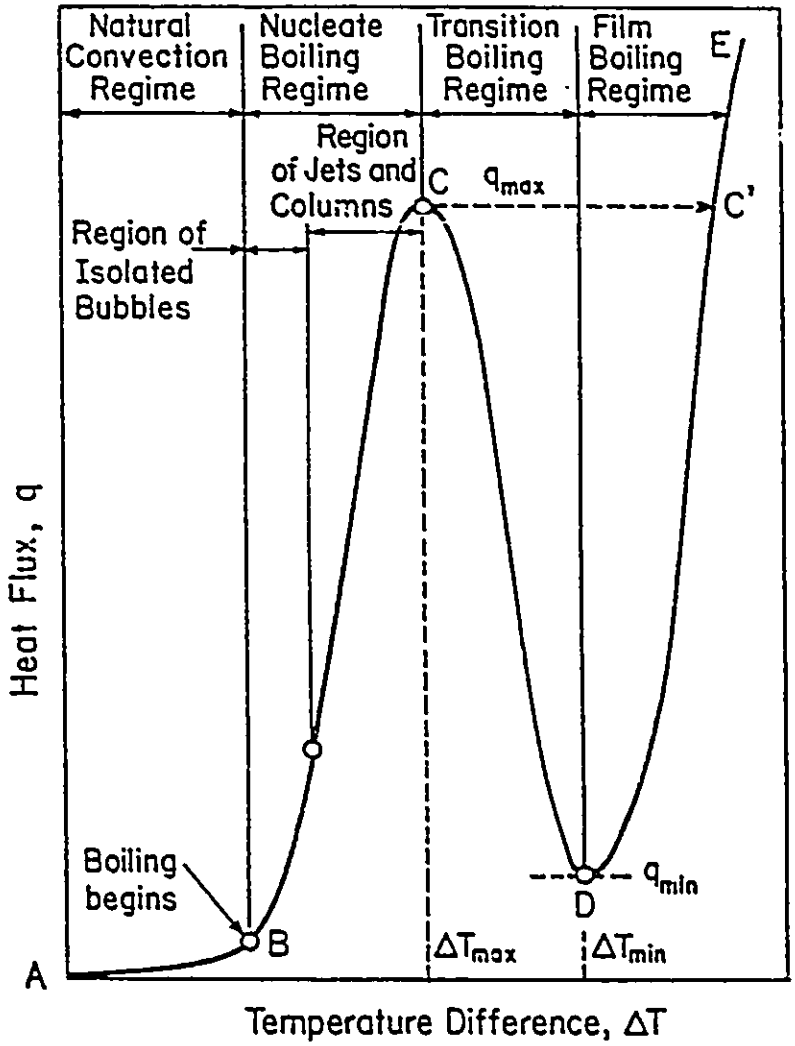

Figure 2.1 Characteristic Boiling Curves and Regimes on Boiling

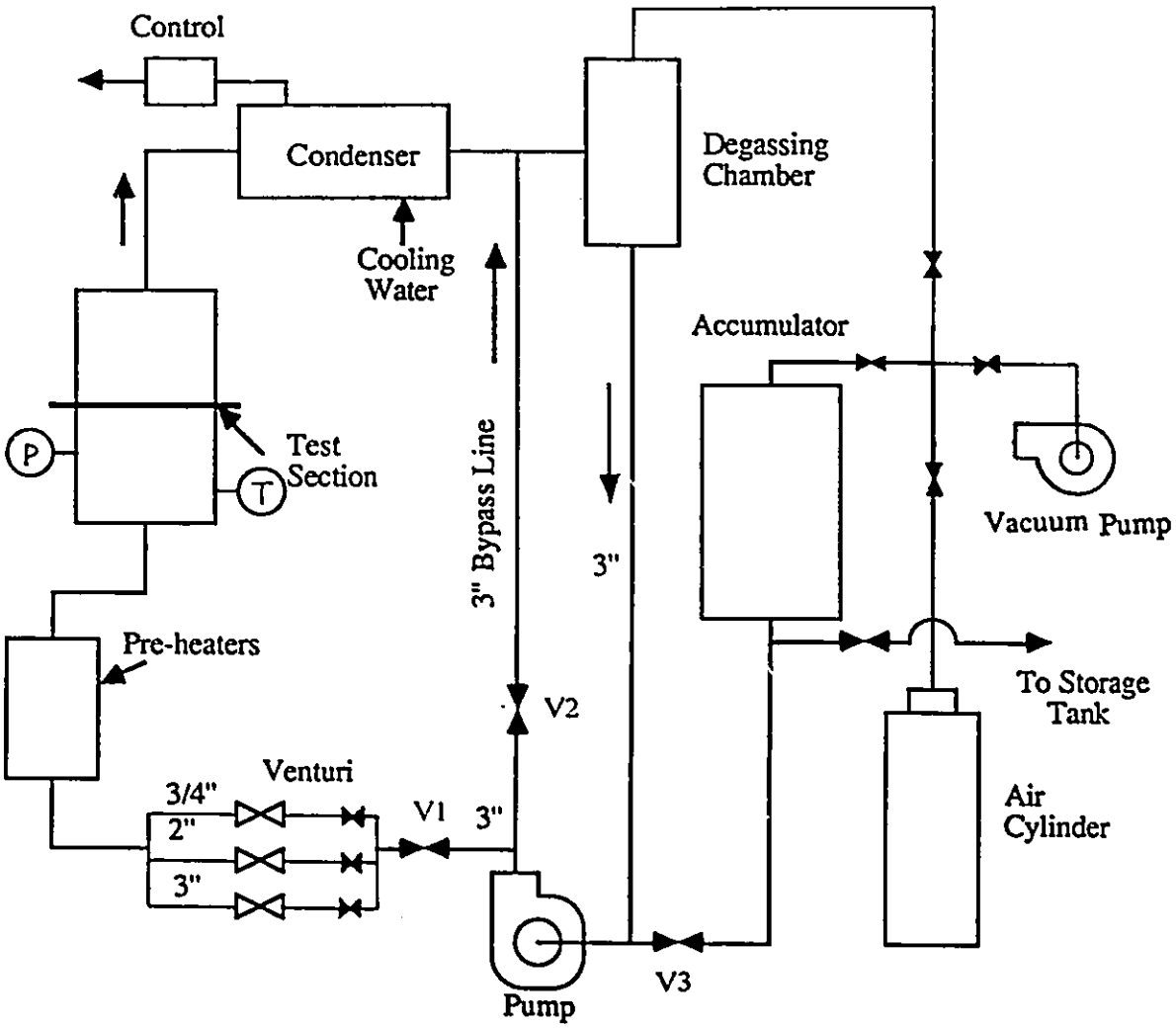

Figure 4.1 Schematic Diagram of Heat Transfer Loop

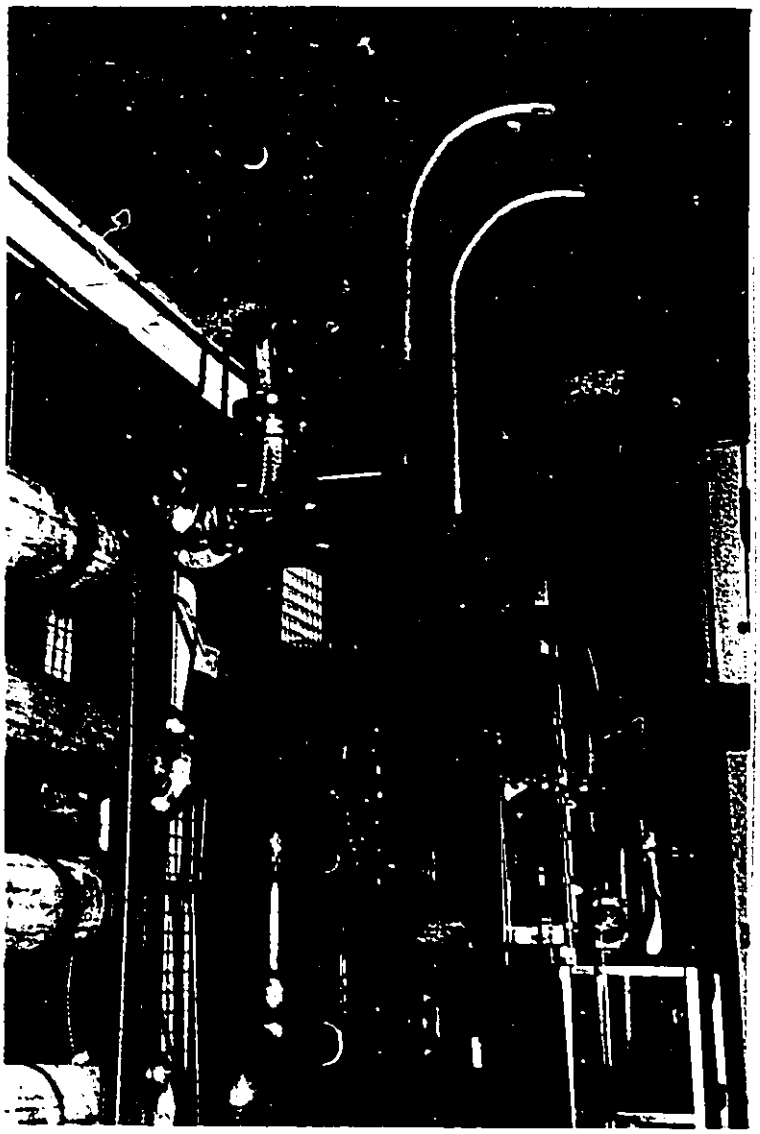

Figure 4.2 Photograph of Heat Transfer Loop

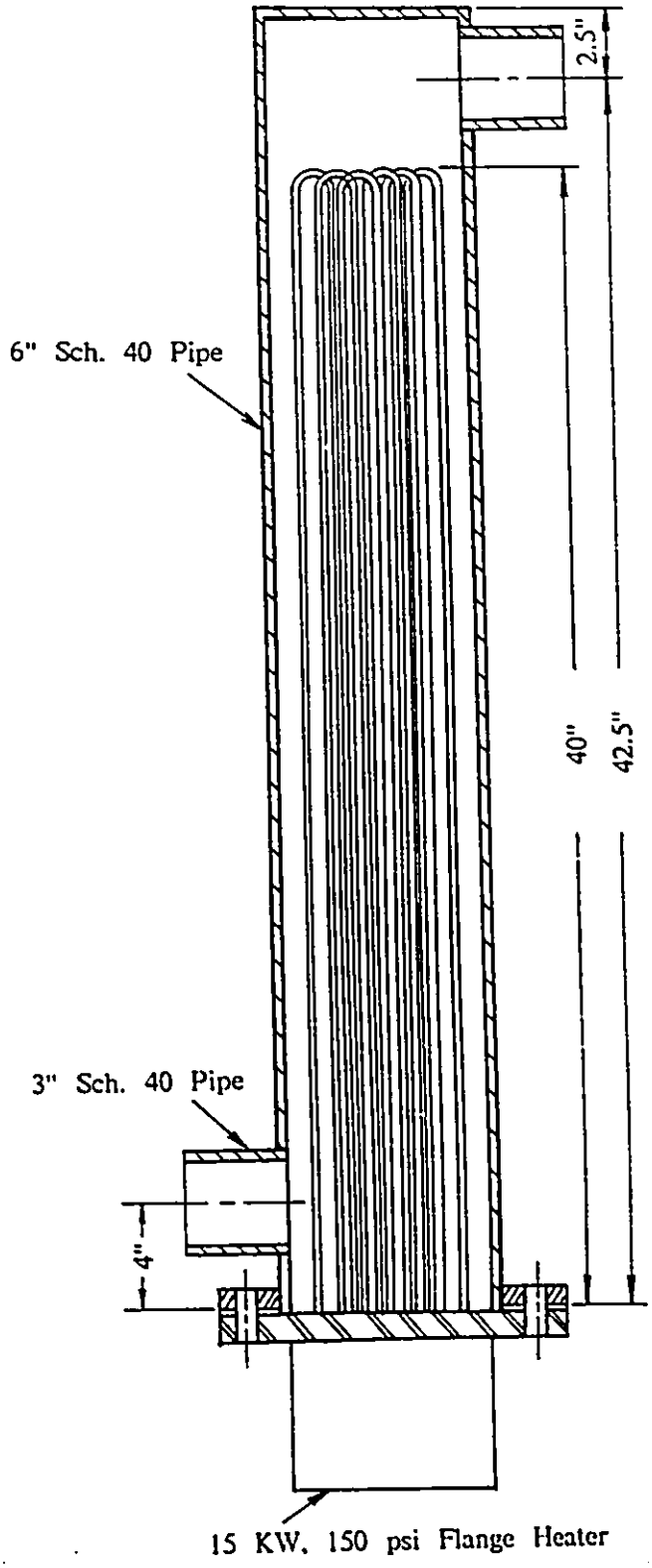

Figure 4.3 Dimensioned Drawing of Pre-heater

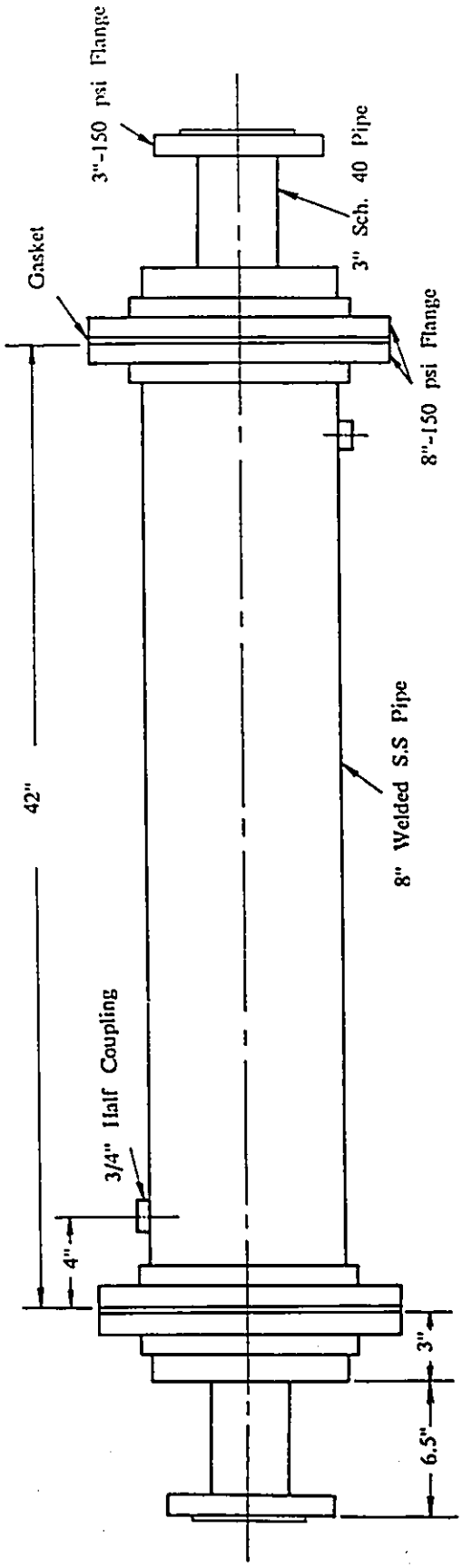

Figure 4.4 Dimensioned Drawing of Condenser (a)

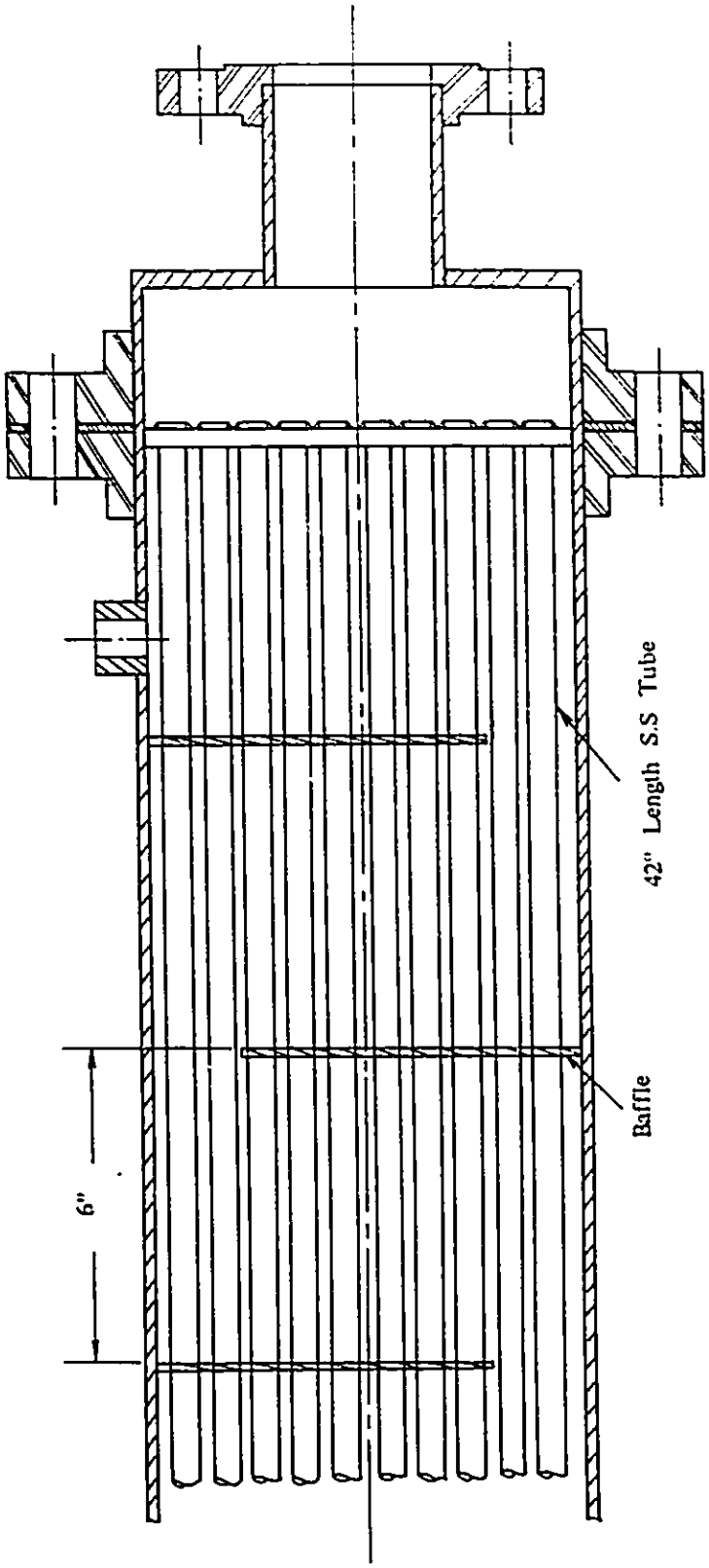

Figure 4.5 Dimensioned Drawing of Condenser (b)

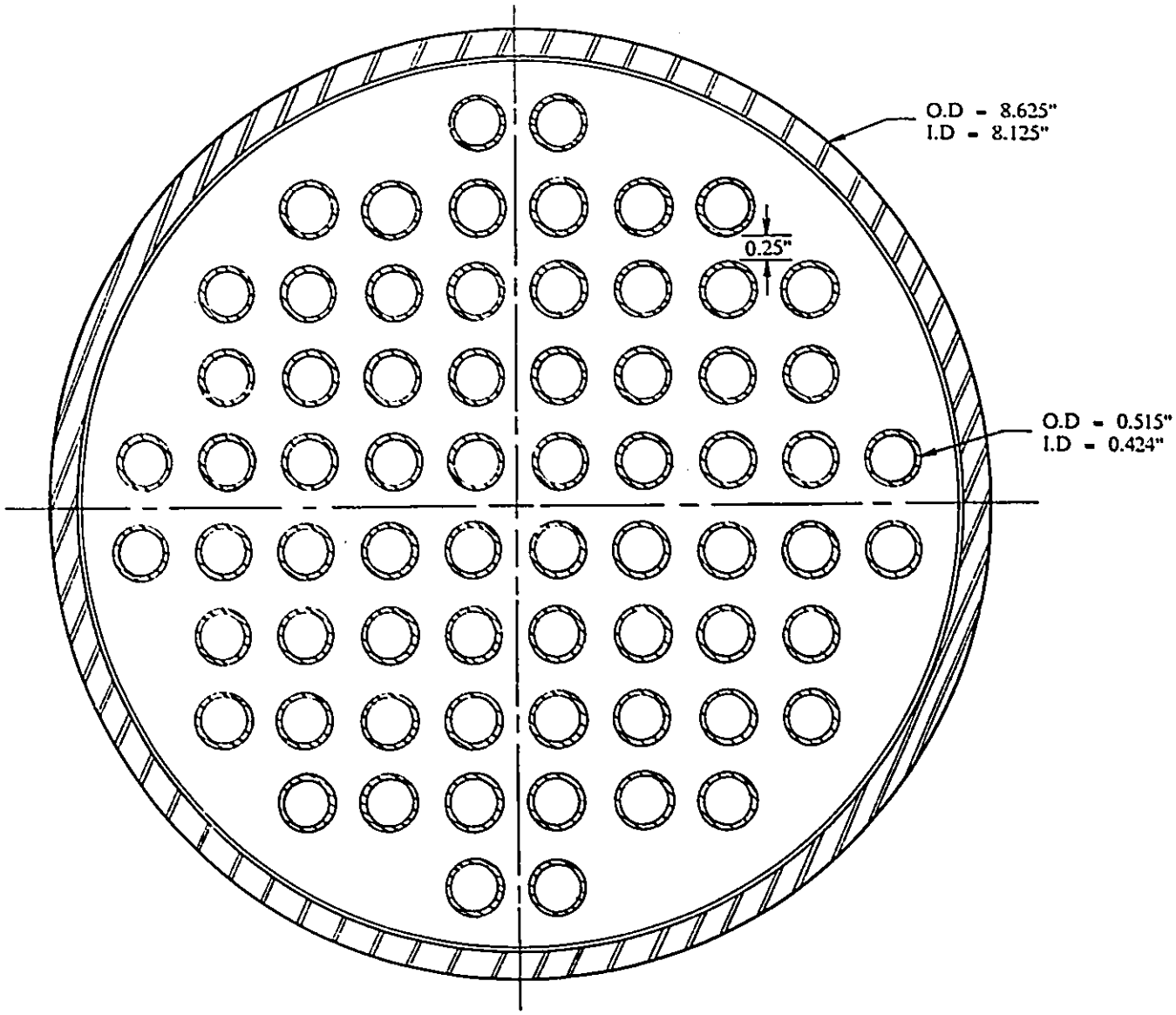

Figure 4.6 Dimensioned Drawing of Condenser Baffle Plates (a)

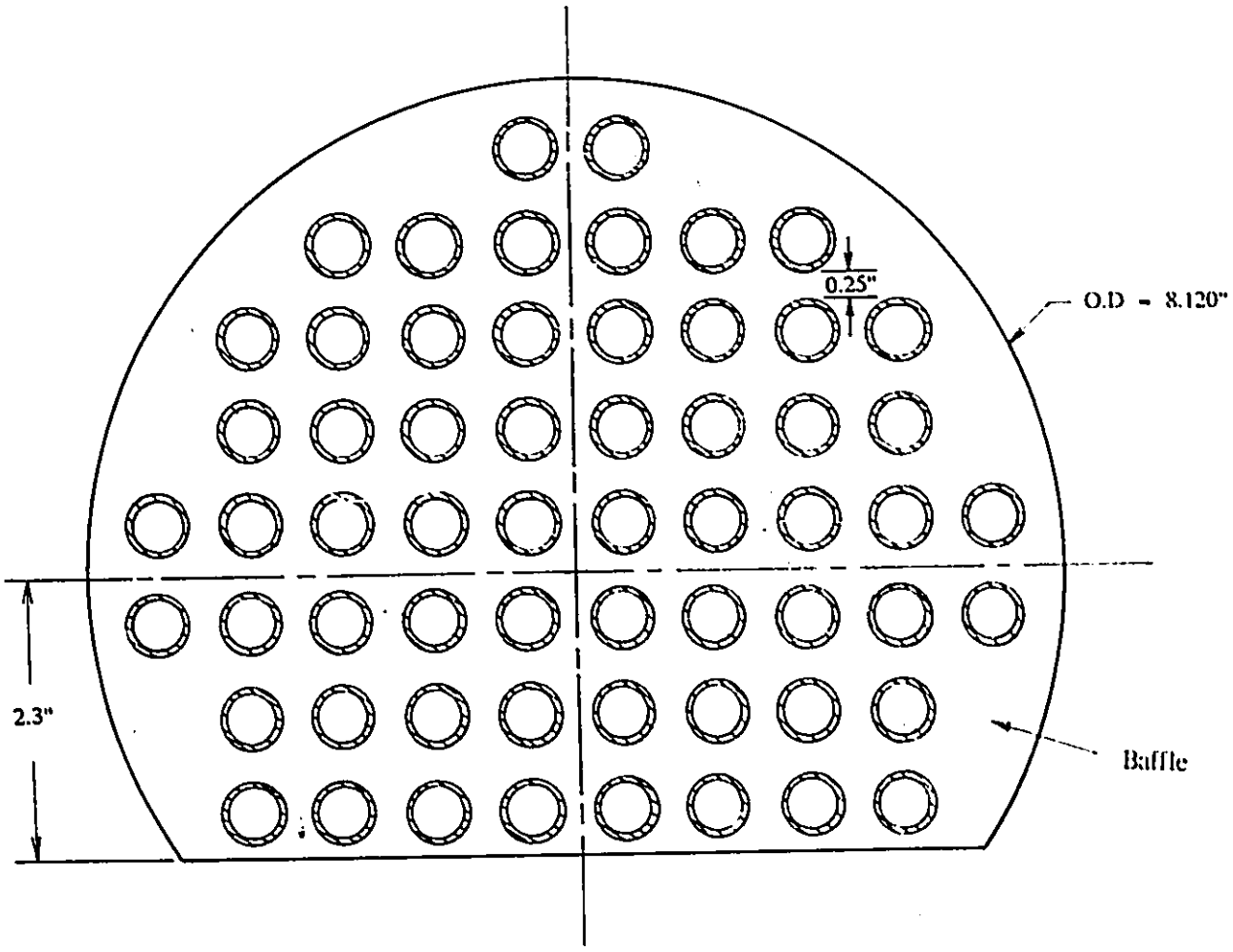

Figure 4.7 **Dimensioned Drawing of Condenser Baffle Plates (b)**

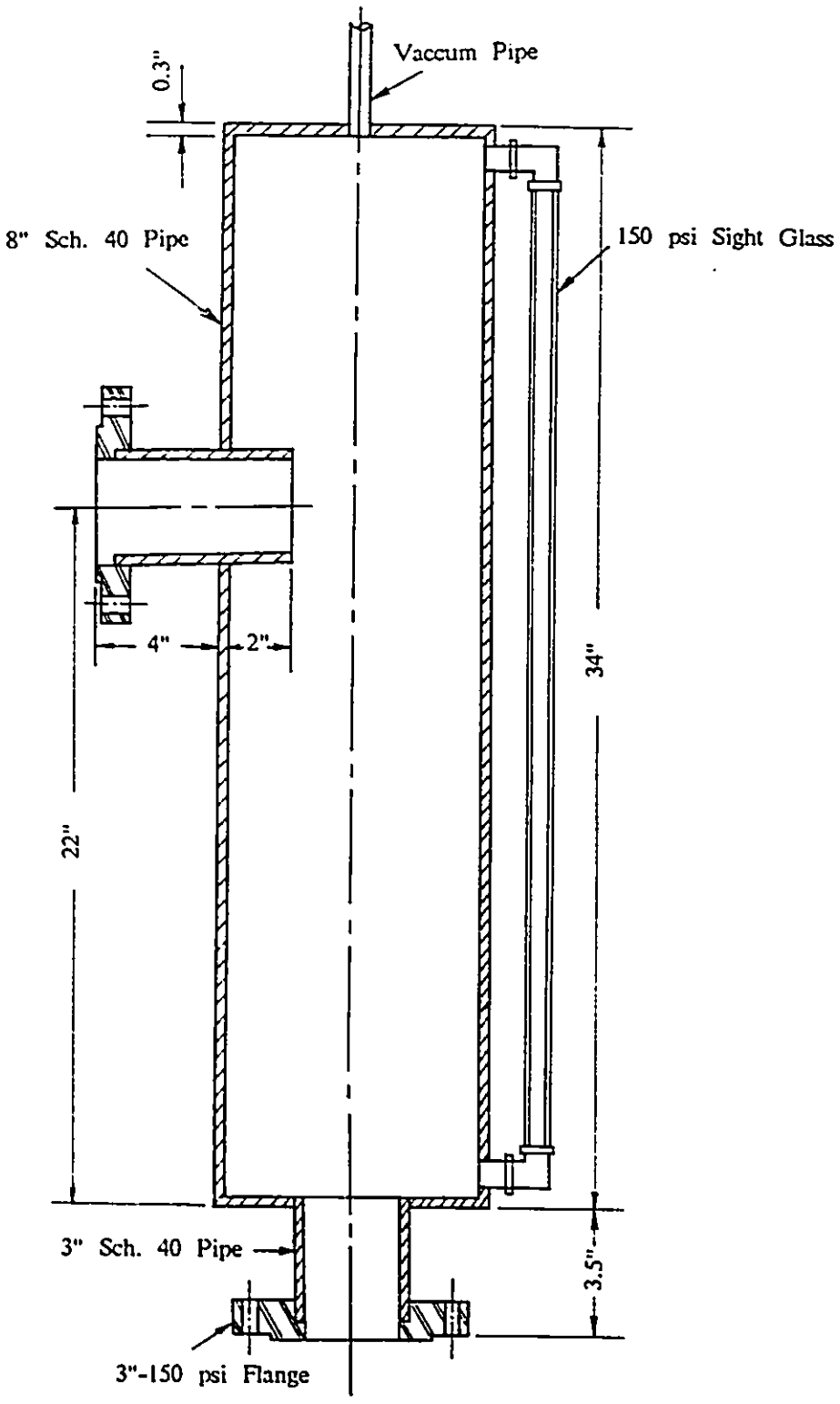

Figure 4.8 Dimensioned Drawing of Degassing Chamber

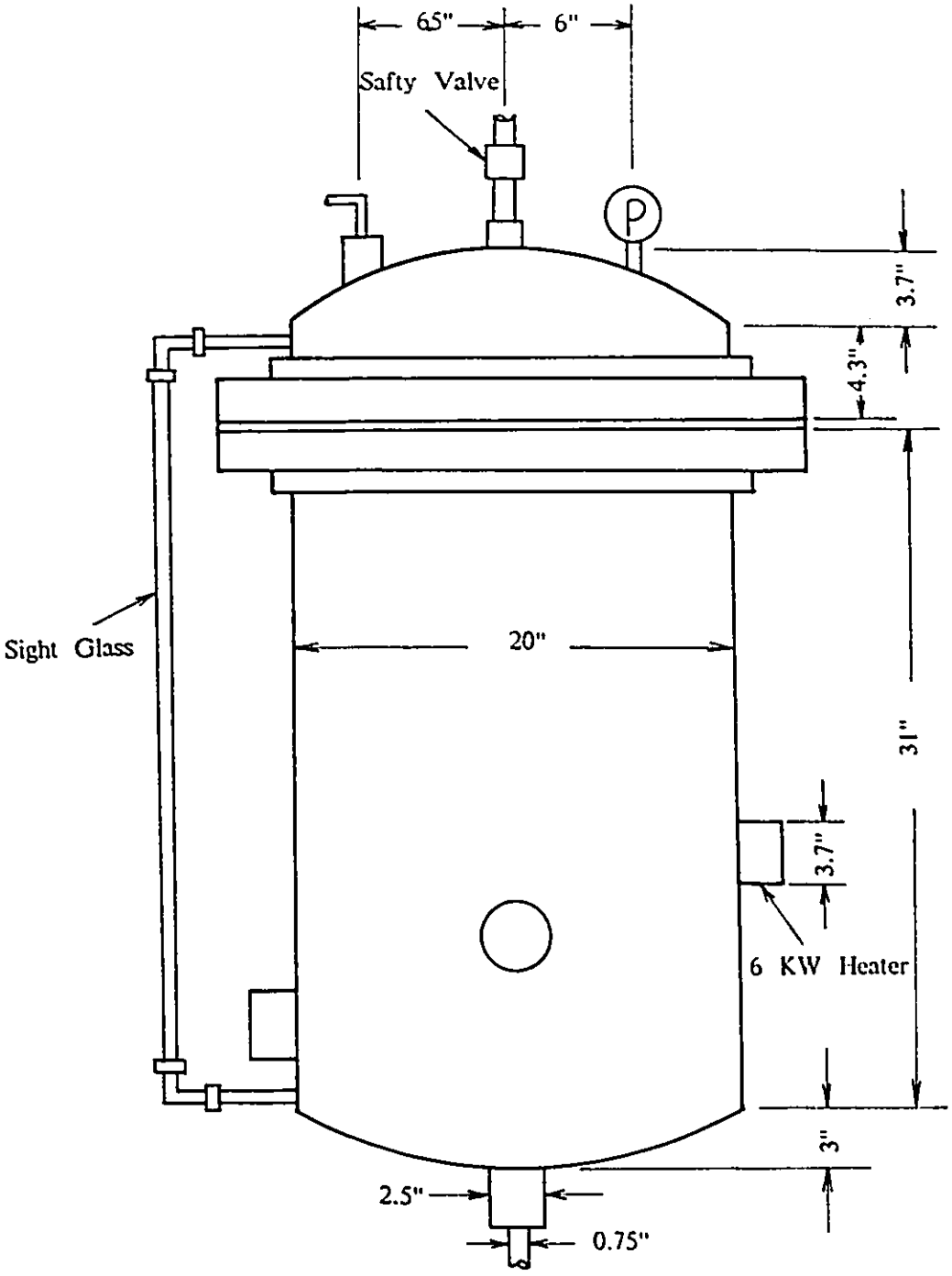

Figure 4.9 Dimensioned Drawing of Accumulator

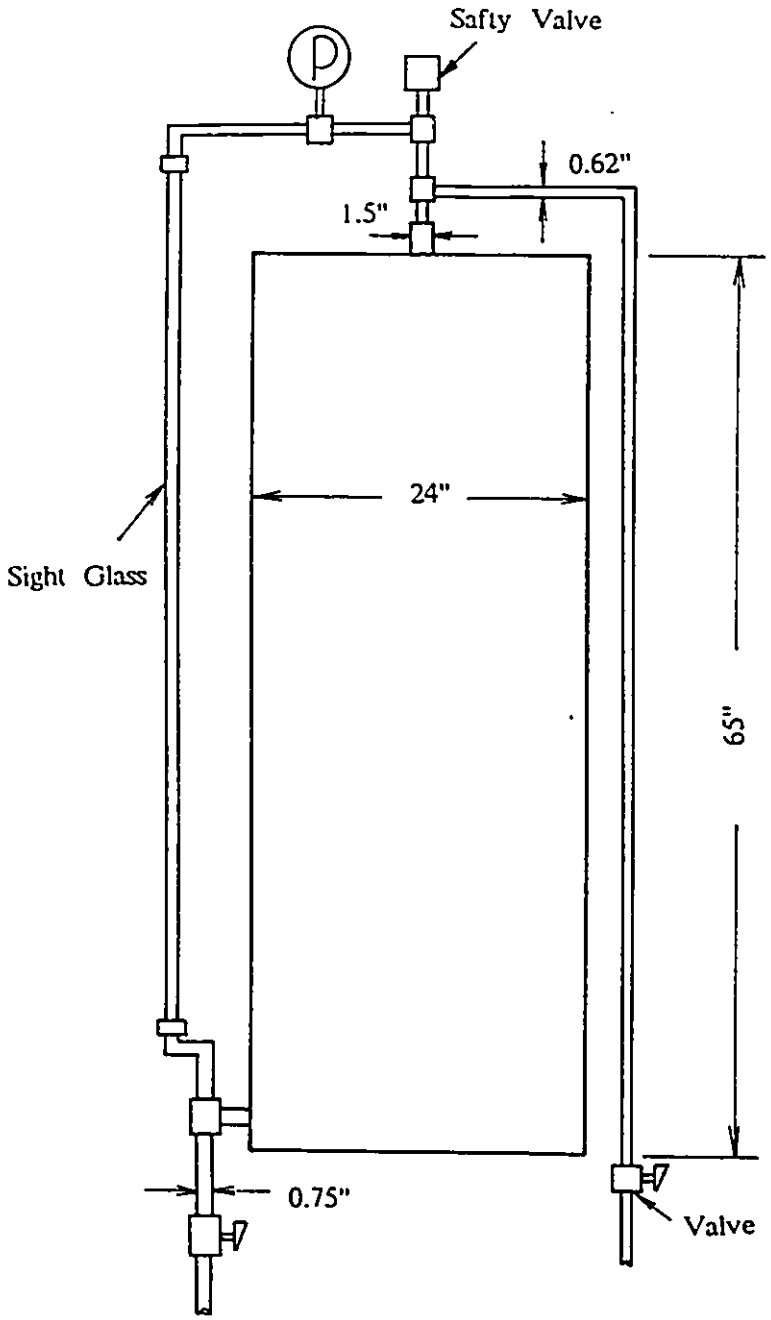

Figure 4.10 Dimensioned Drawing of Storage Tank

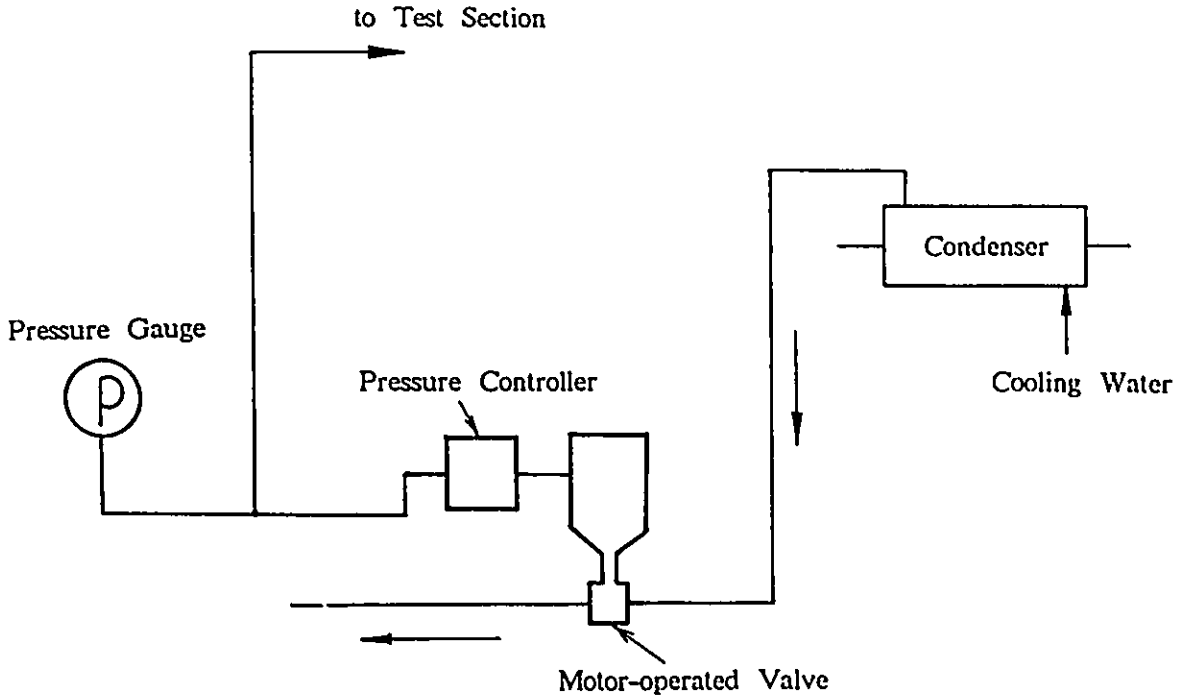

Figure 4.11 Schematic Diagram of Pressure Control System

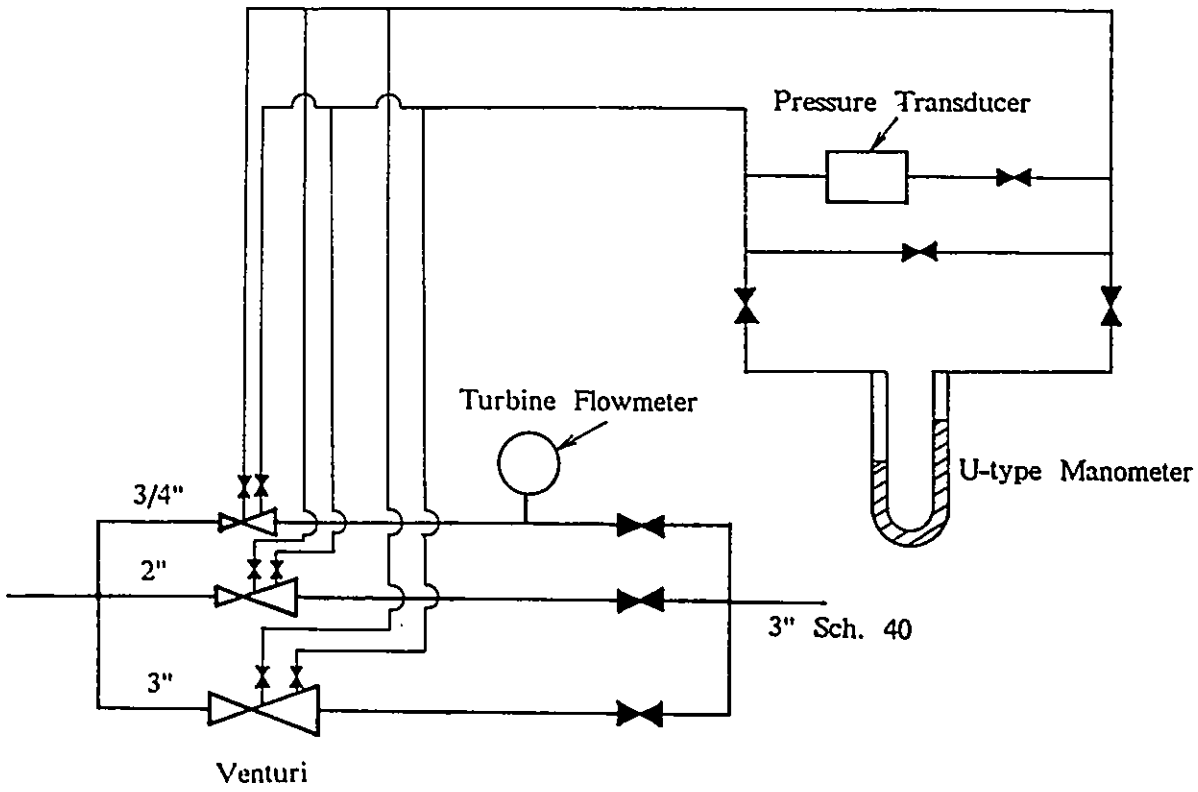

Figure 4.12 Schematic Diagram of Flow Measurement Loop

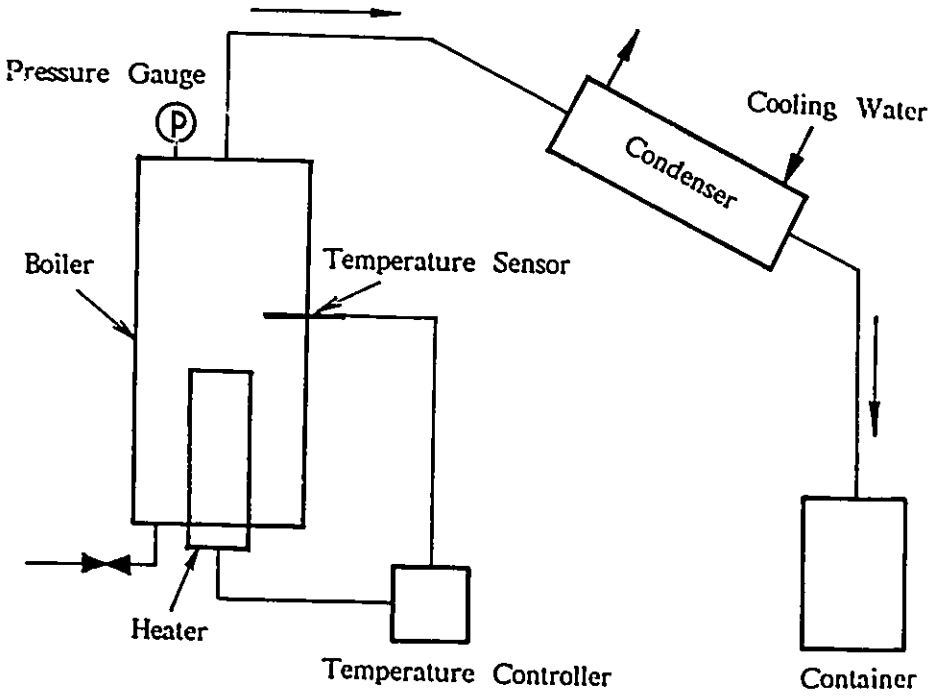

Figure 4.13 Schematic Diagram of Distilling System

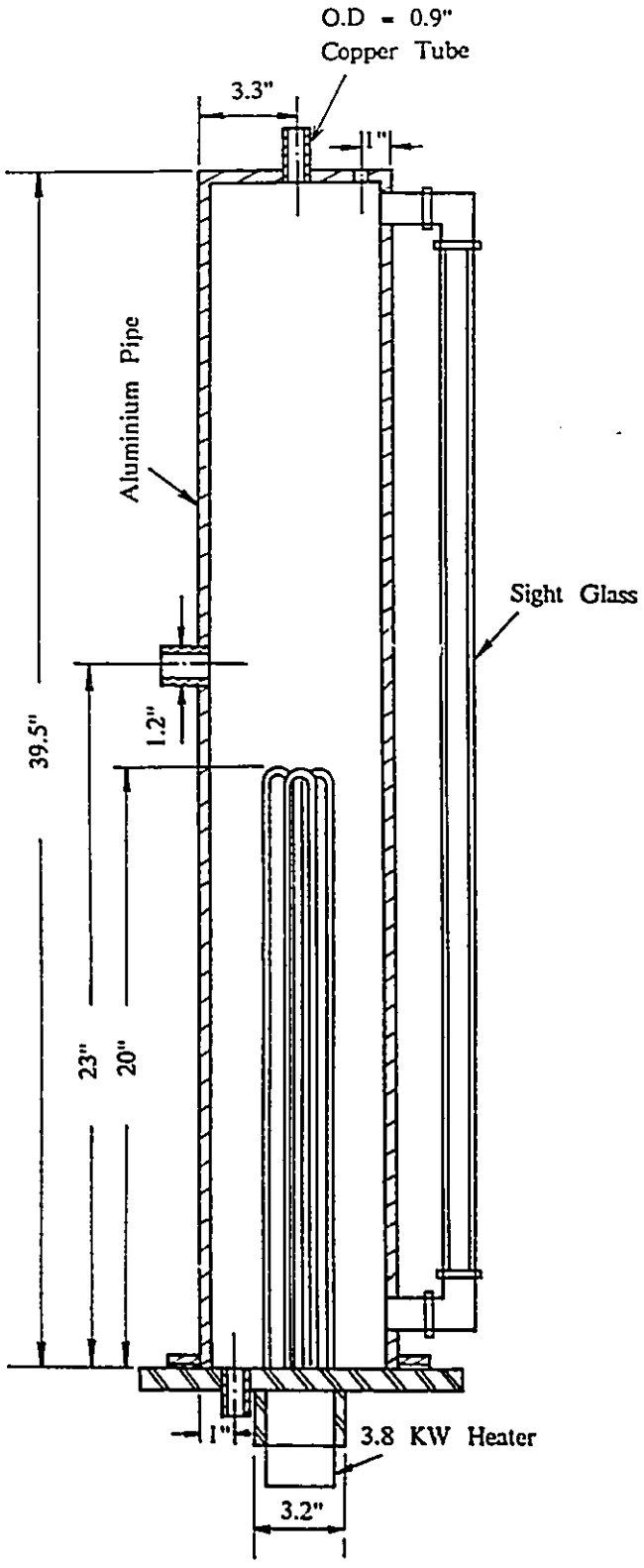

Figure 4.14 Dimensioned Drawing of Boiler Used in Distilling System

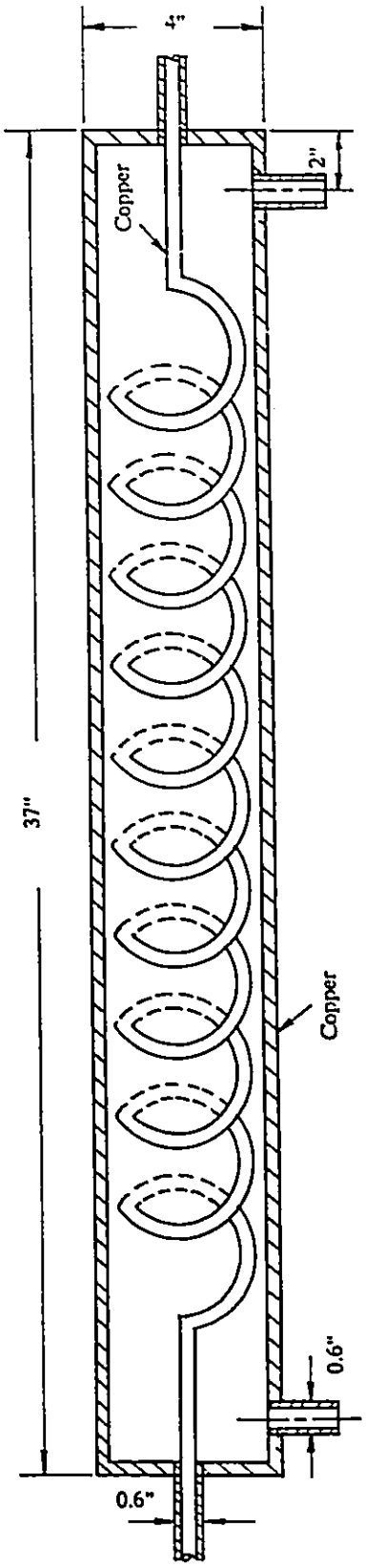

Figure 4.15 Dimensioned Drawing of Condenser Used in Distilling System

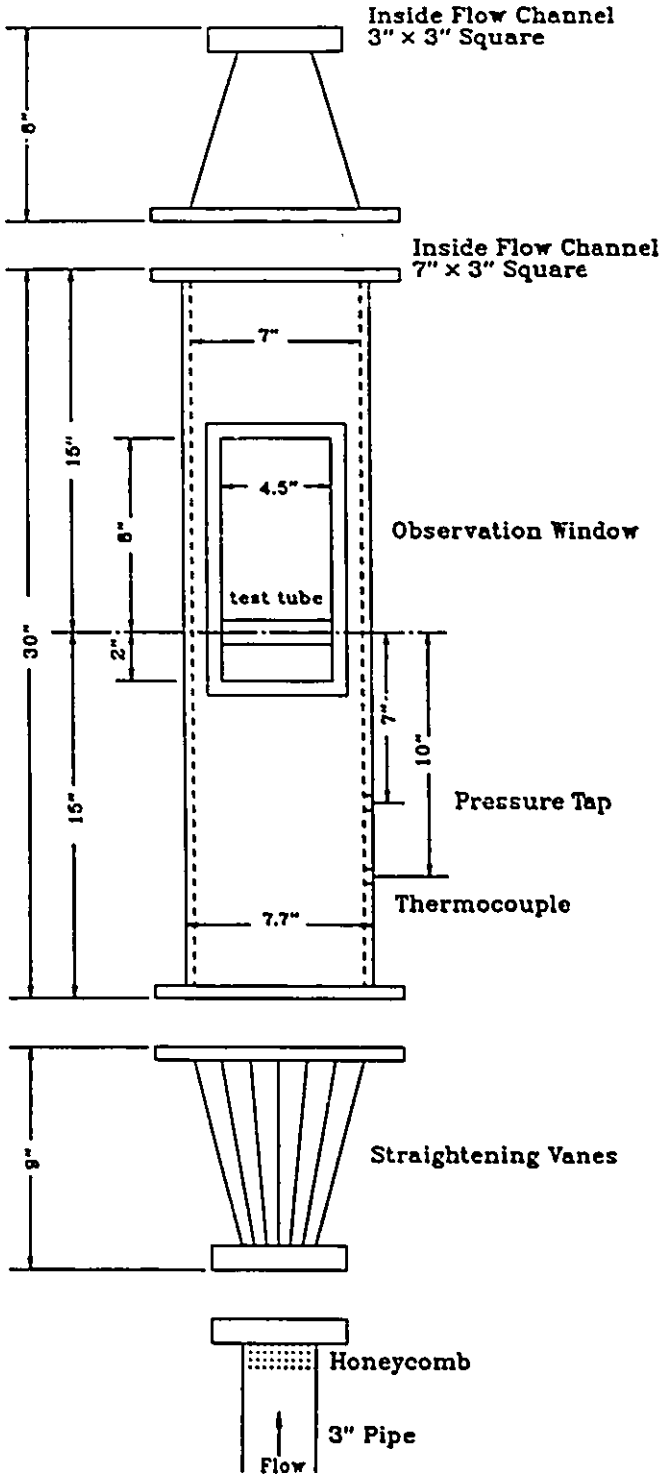

Figure 4.16 Dimensioned Drawing of Test Section

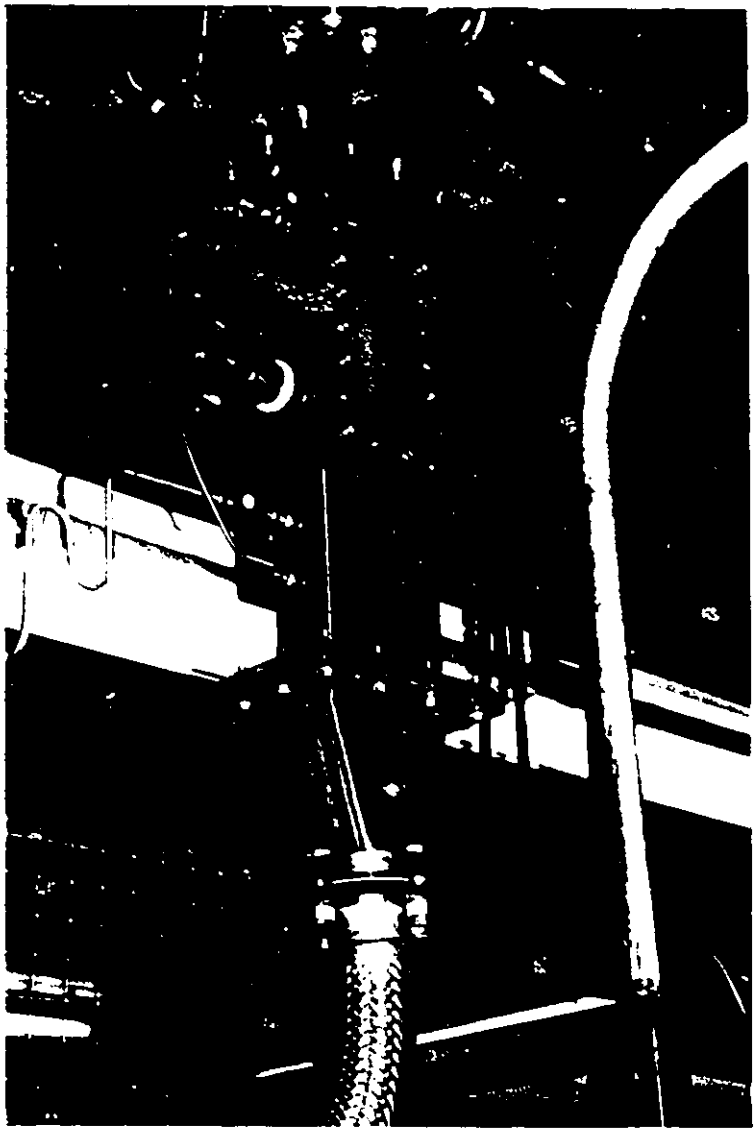

Figure 4.17 Photograph of Test Section

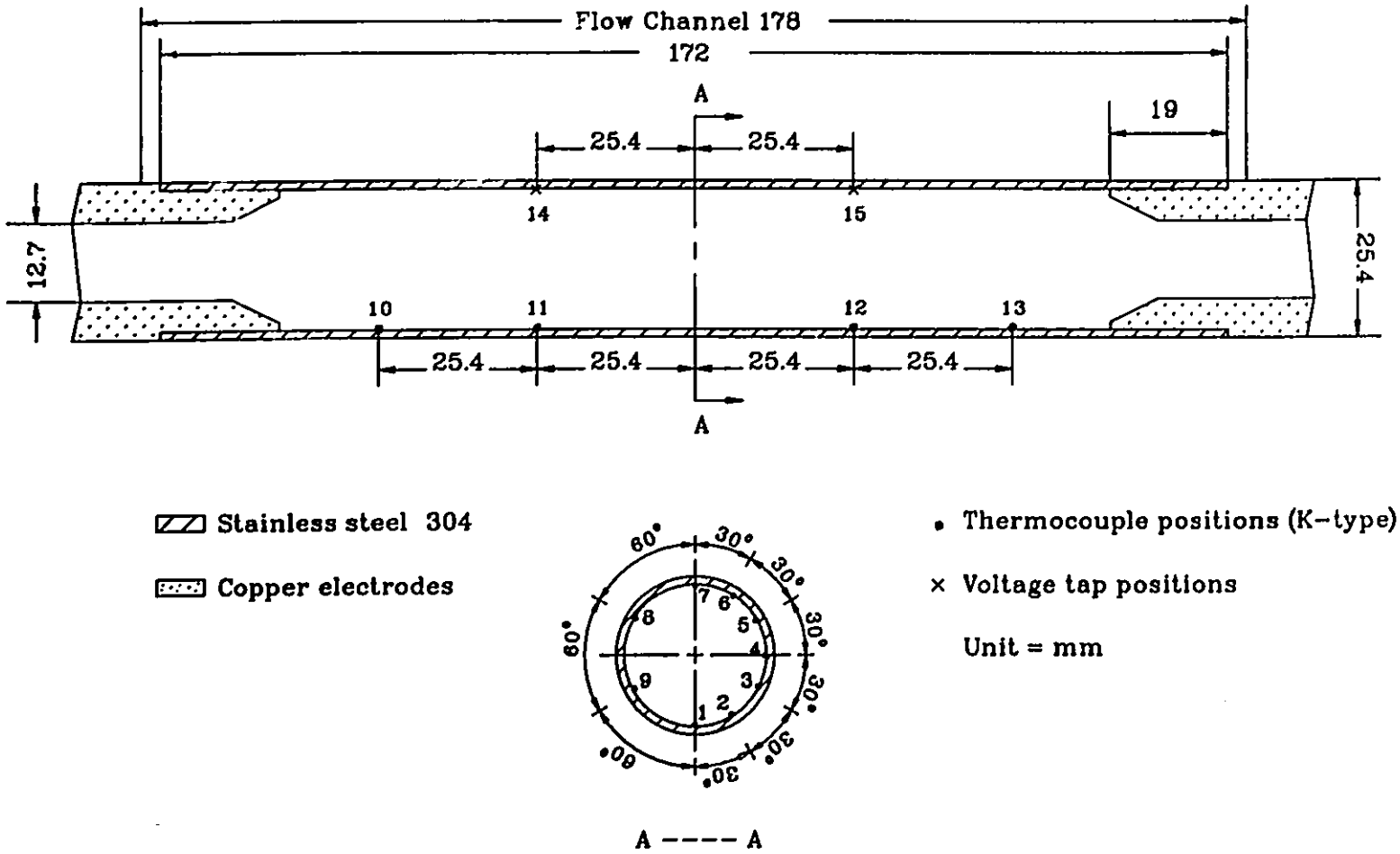

Figure 4.18 Test Heater and the Location of Thermocouples

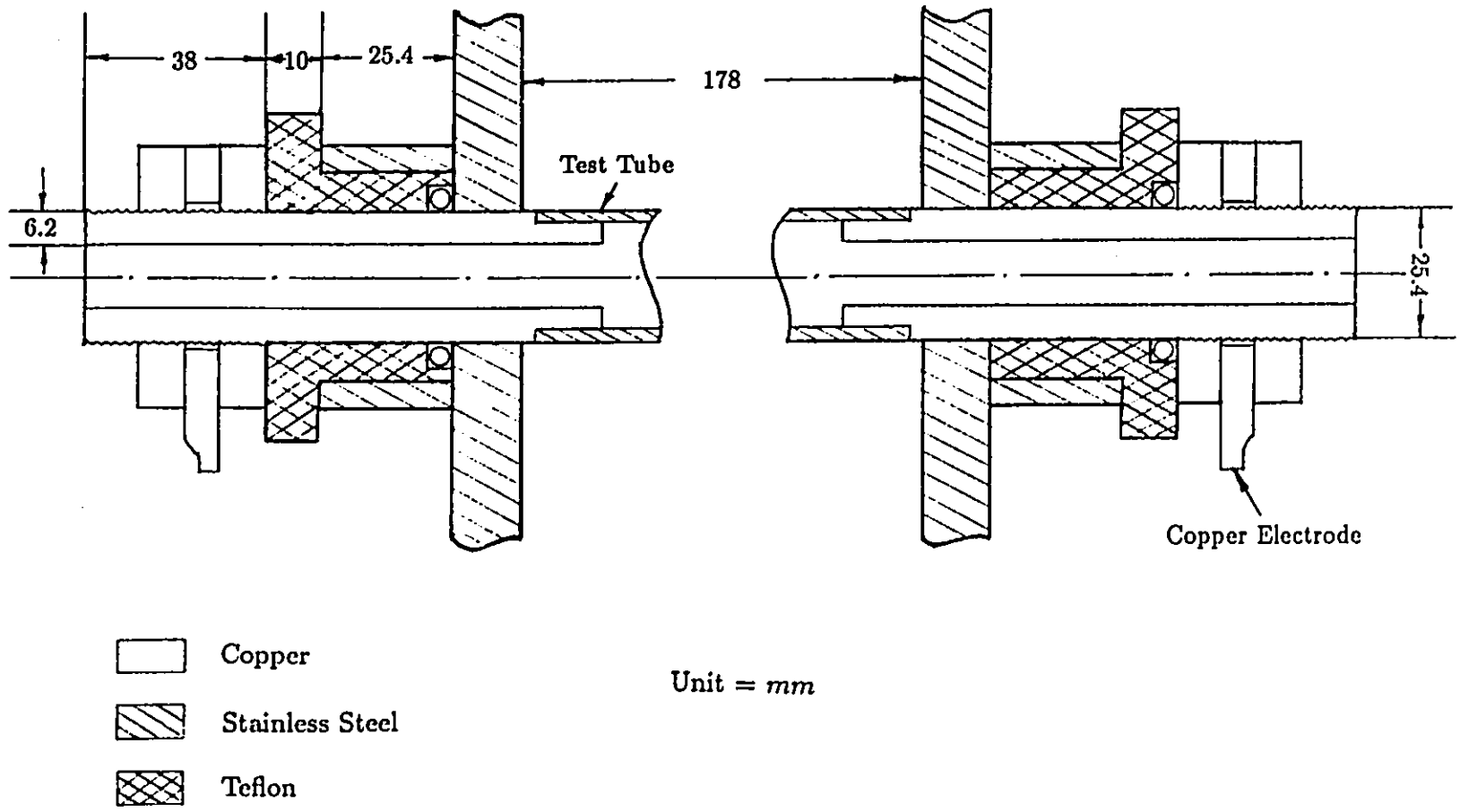

Figure 4.19 Details of Test Tube Conductors

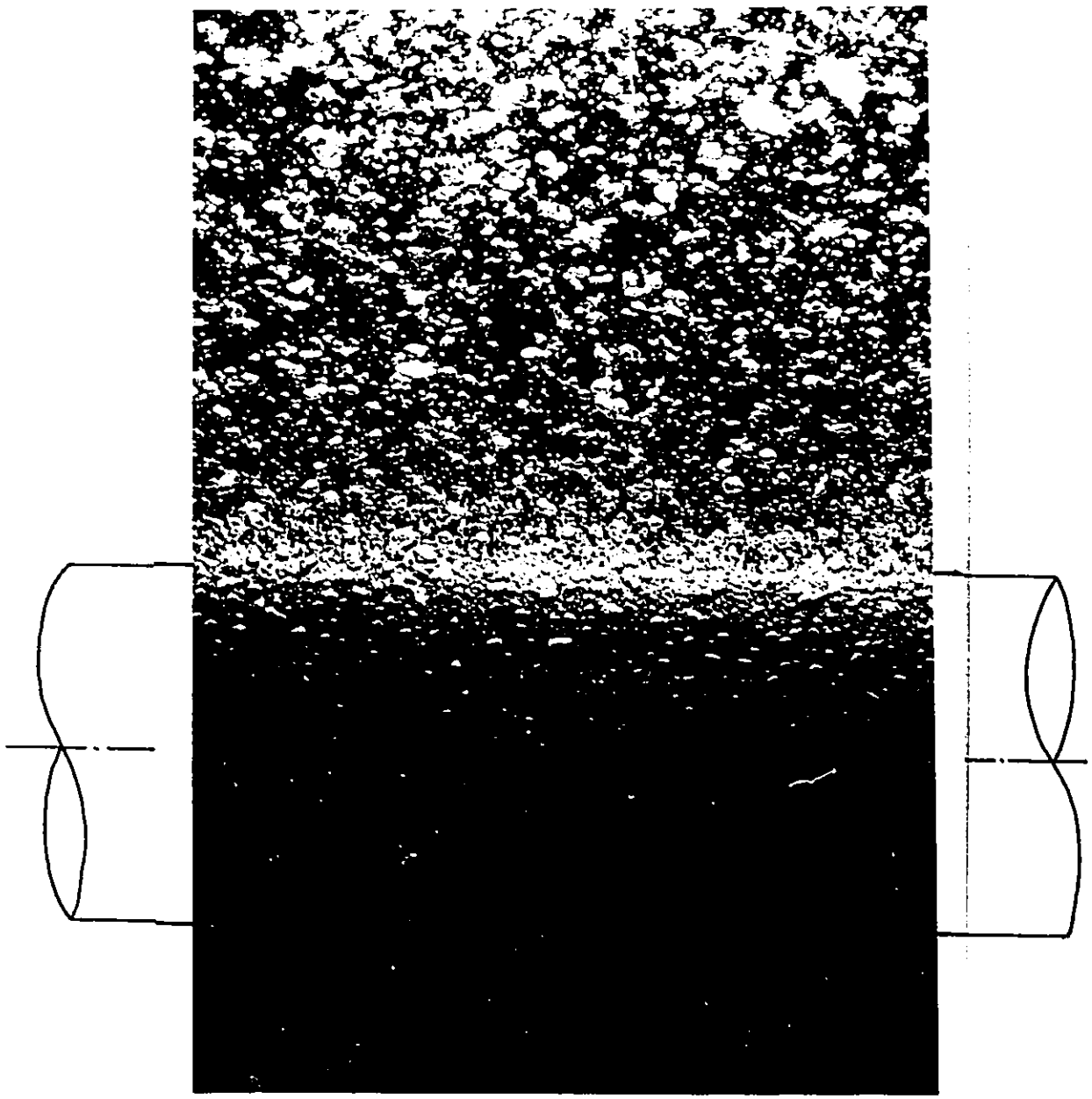

$K^* = 0.0212$
$\Delta T_{sub.} = 22.6°C$
$V = 0$ m/s
$P = 0.189$ Mpa
$\bar{q} = 49$ kw/m^2

Figure 5.1 Photograph of Forced Convection Nucleate Boiling

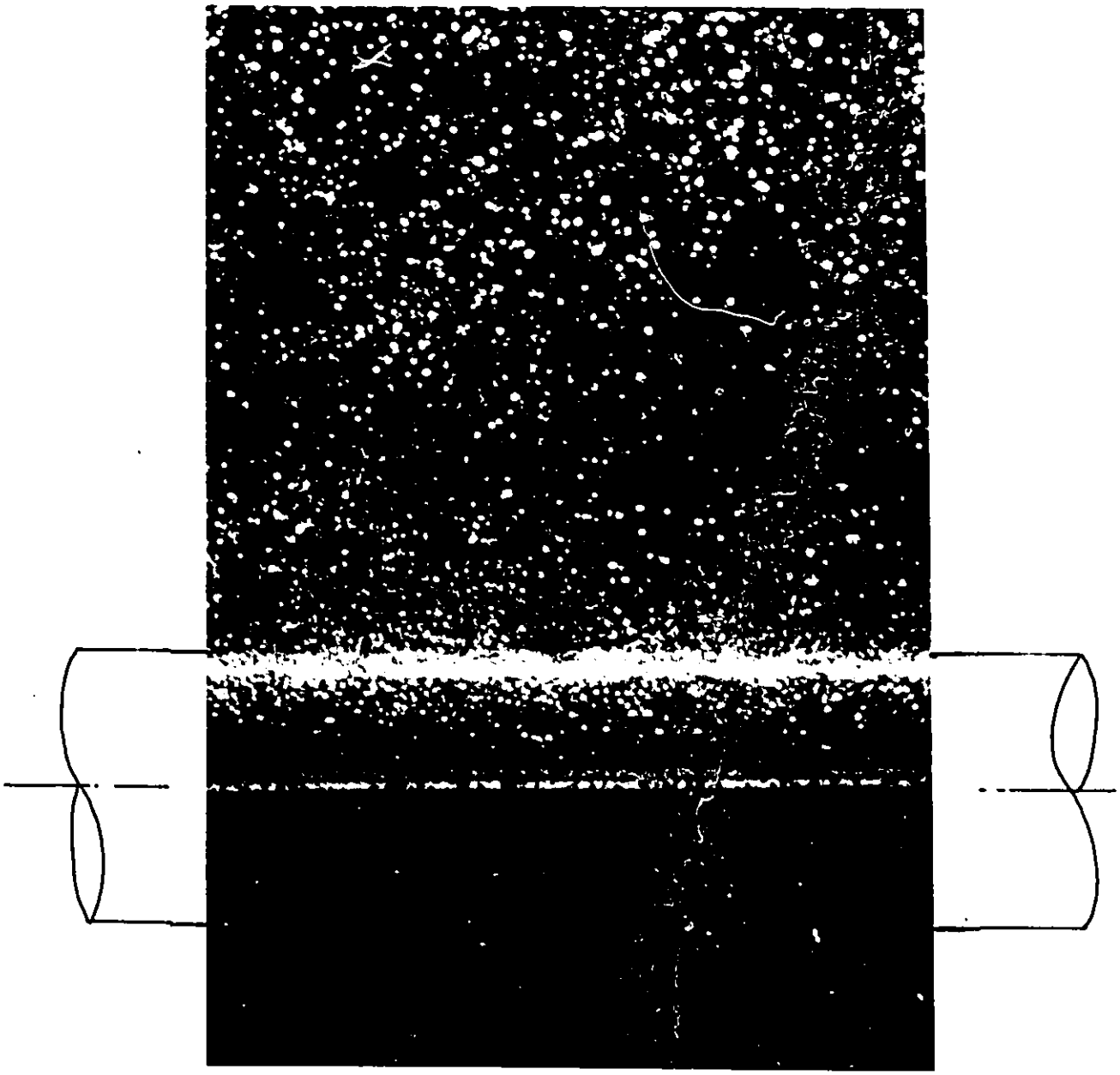

$K^* = 0.0212$
$\Delta T_{sub.} = 22.6°C$
$V = 0.3$ m/s
$P = 0.189$ Mpa
$\bar{q} = 49$ kw/m^2

Figure 5.2 Photograph of Forced Convection Nucleate Boiling

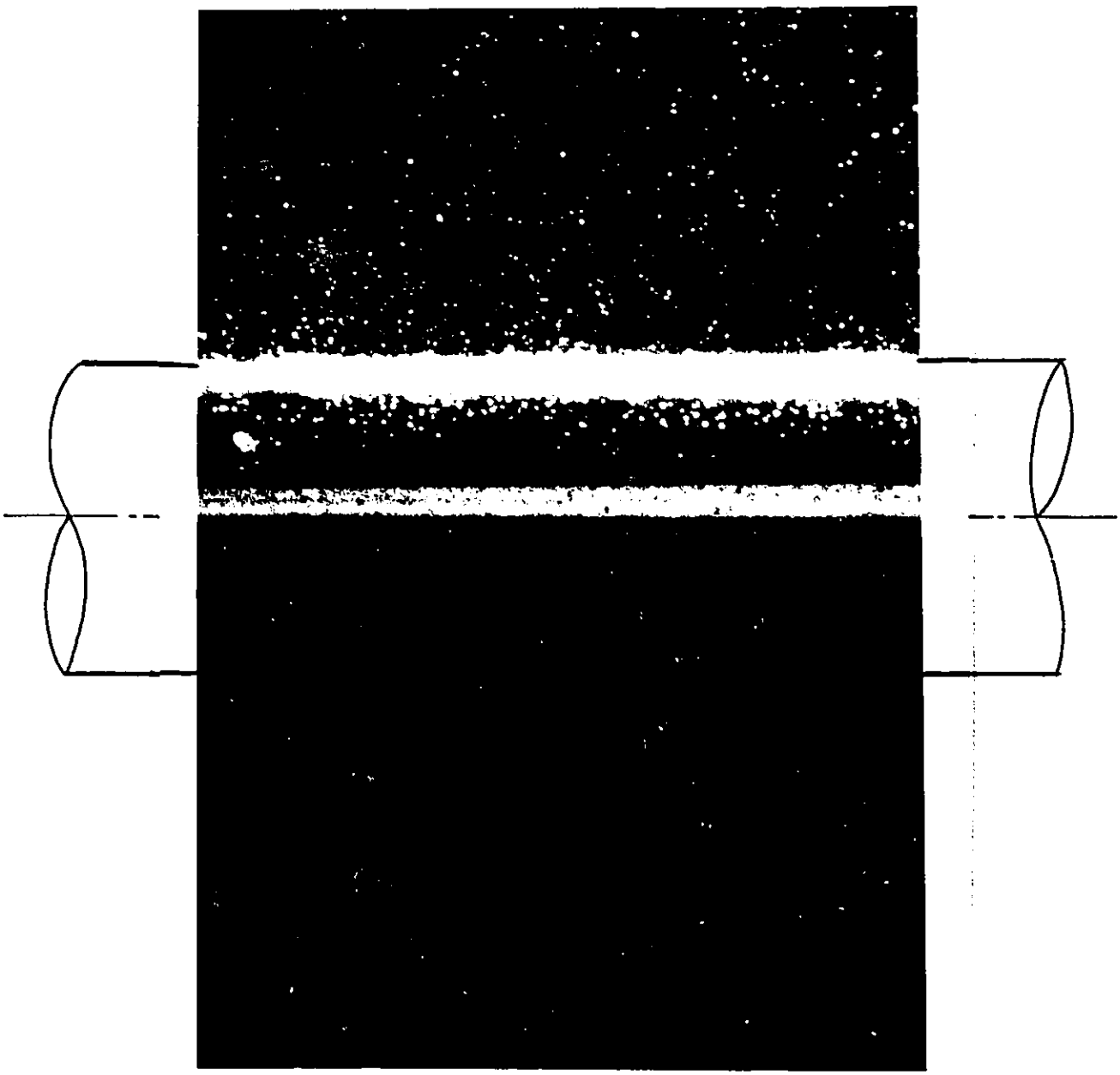

$K^* = 0.0212$
$\Delta T_{sub.} = 33.1°C$
$V = 0.3$ m/s
$P = 0.189$ Mpa
$\bar{q} = 49$ kw/m^2

Figure 5.3 Photograph of Forced Convection Nucleate Boiling

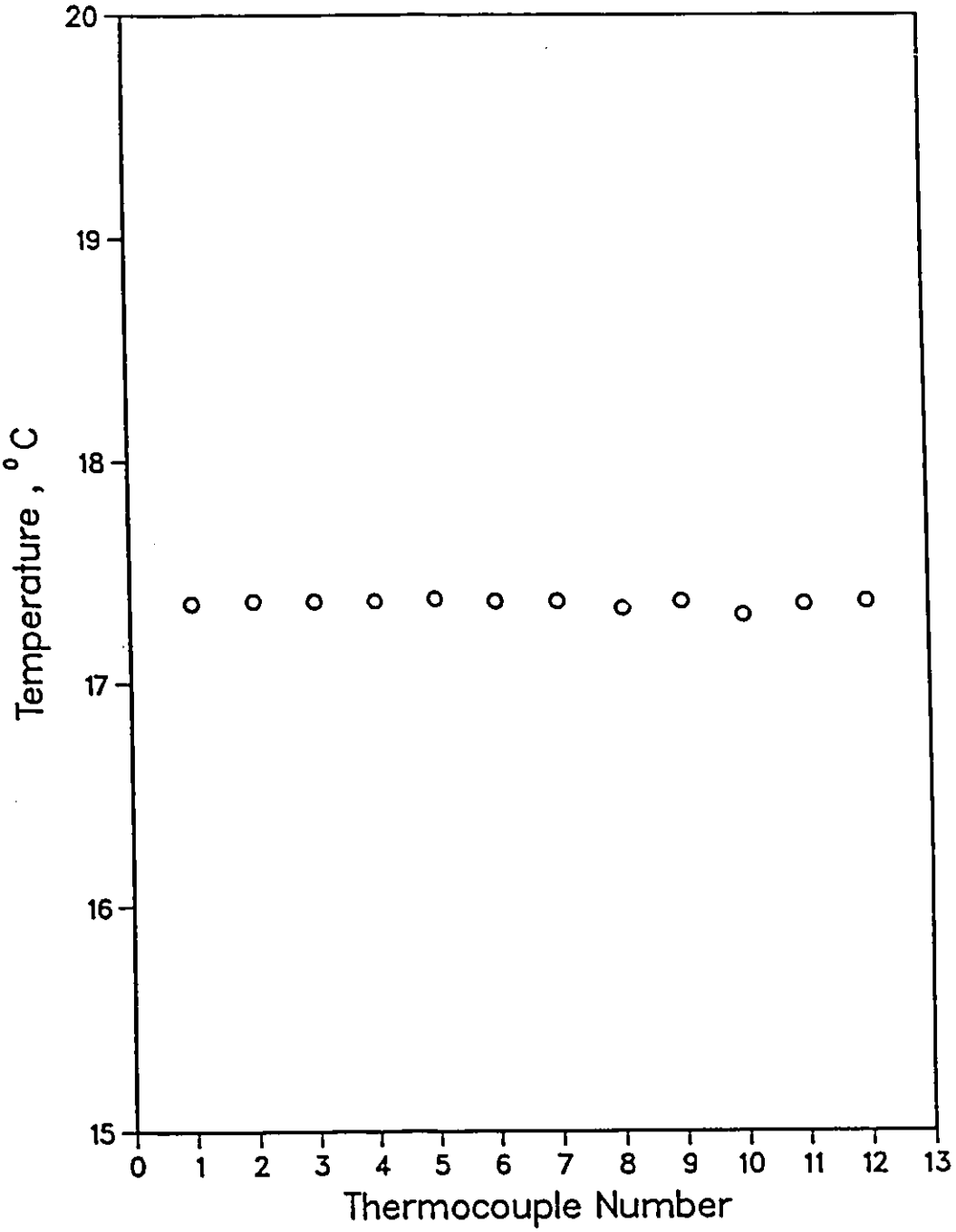

Figure 5.4 Typical Temperature Reading before Experiment

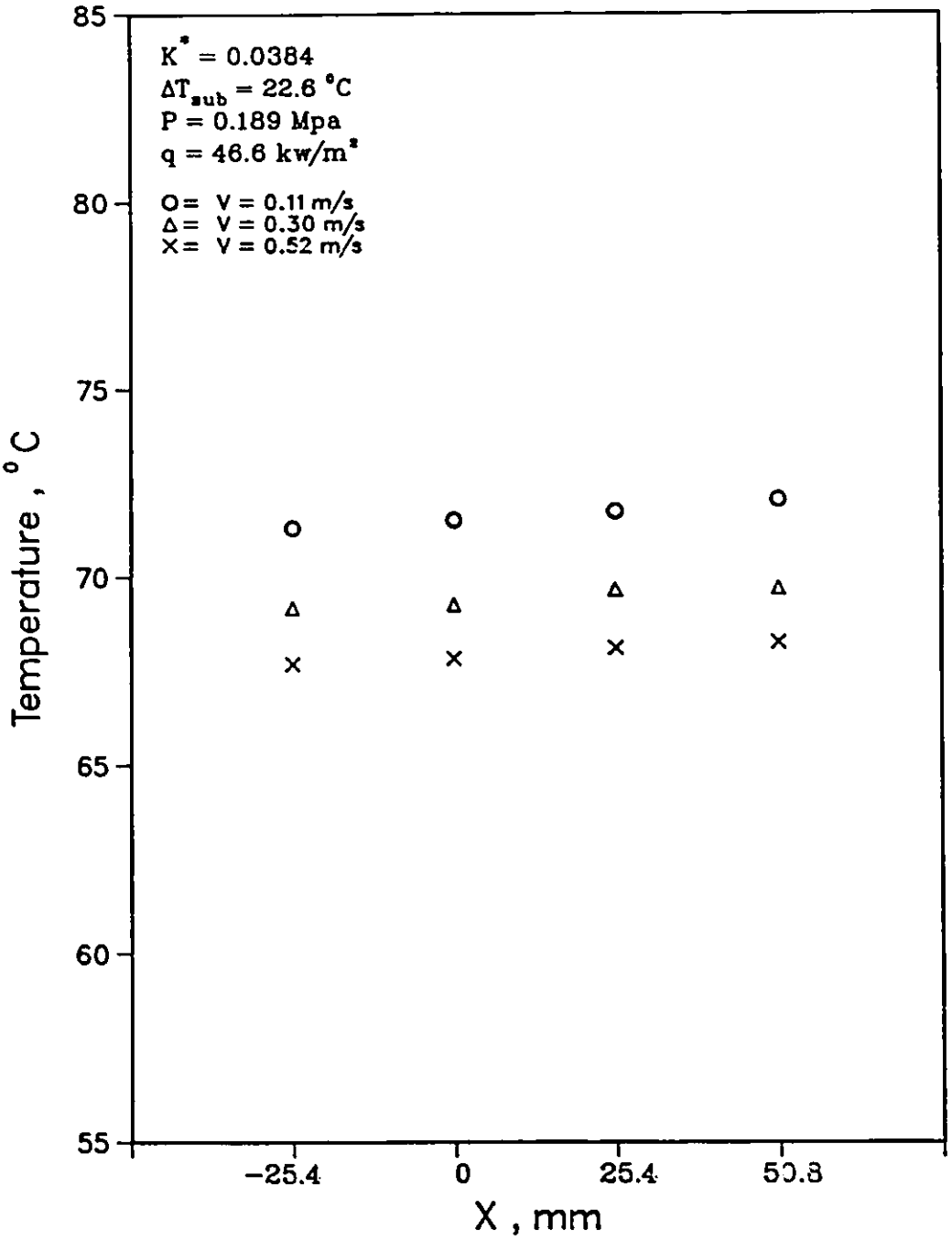

Figure 5.5 Typical Axial Temperature

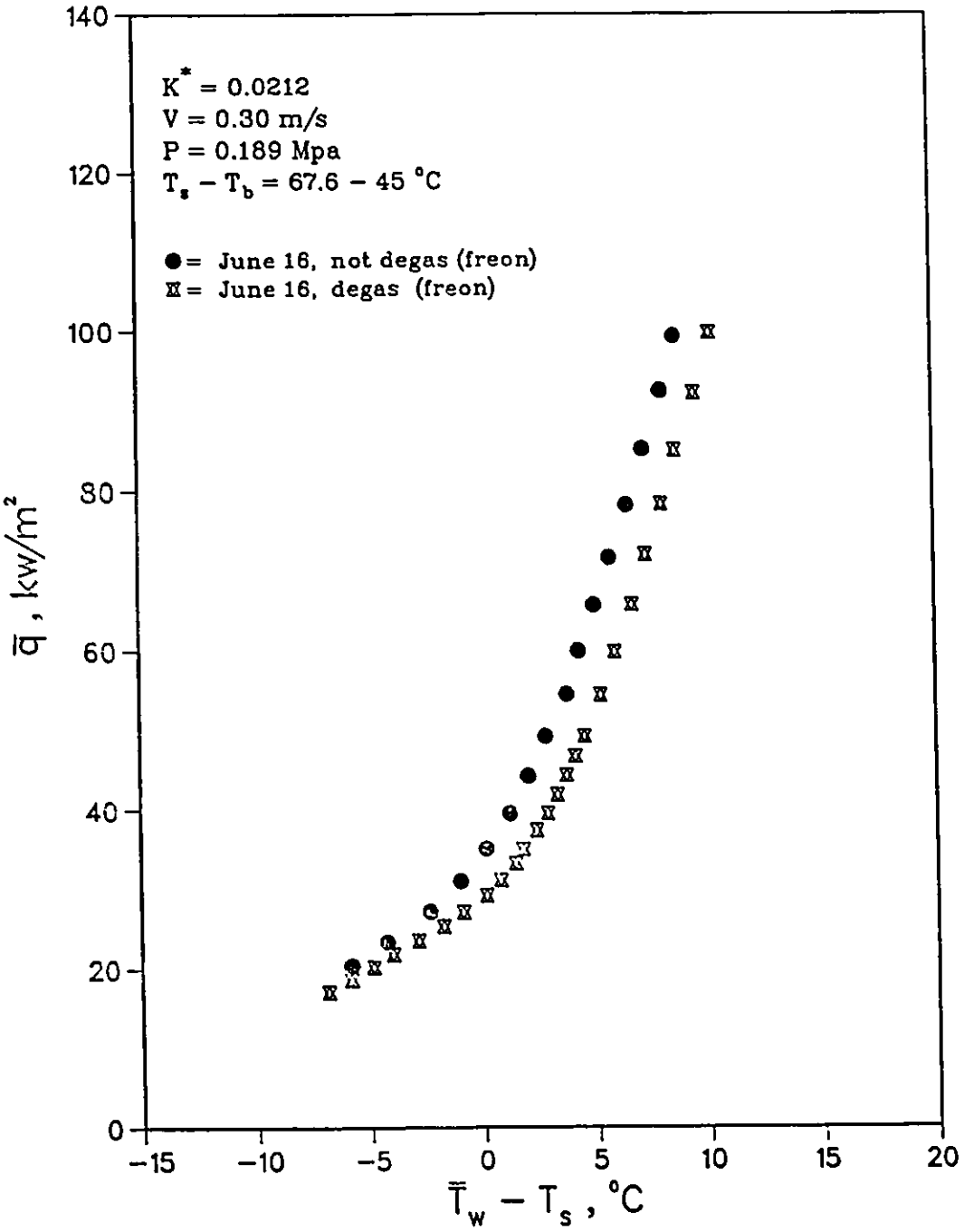

Figure 5.6 Effect of Degassing in Crossflow Nucleate Boiling

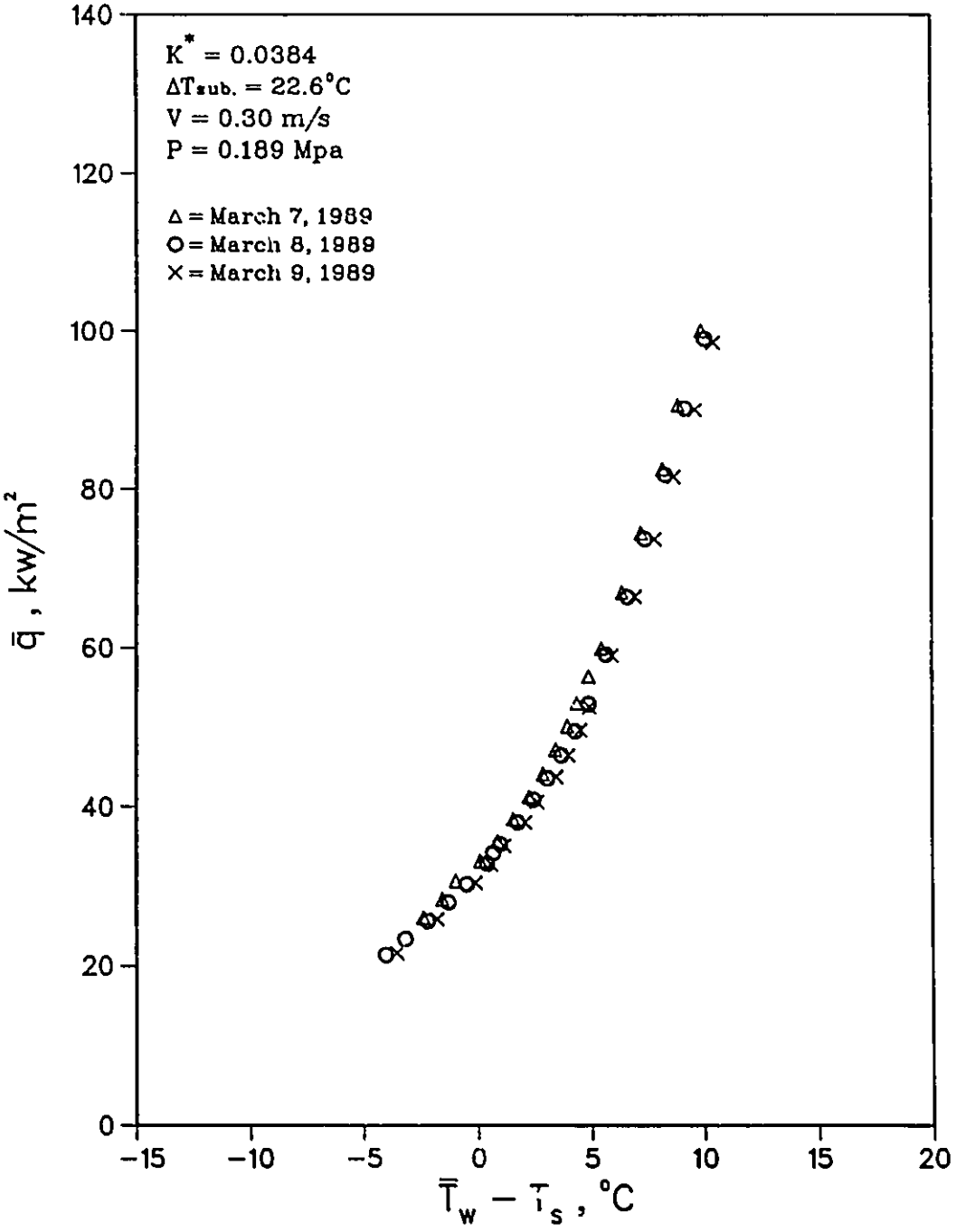

Figure 5.7 **Experimental Data Reproducibility in Crossflow Nucleate Boiling**

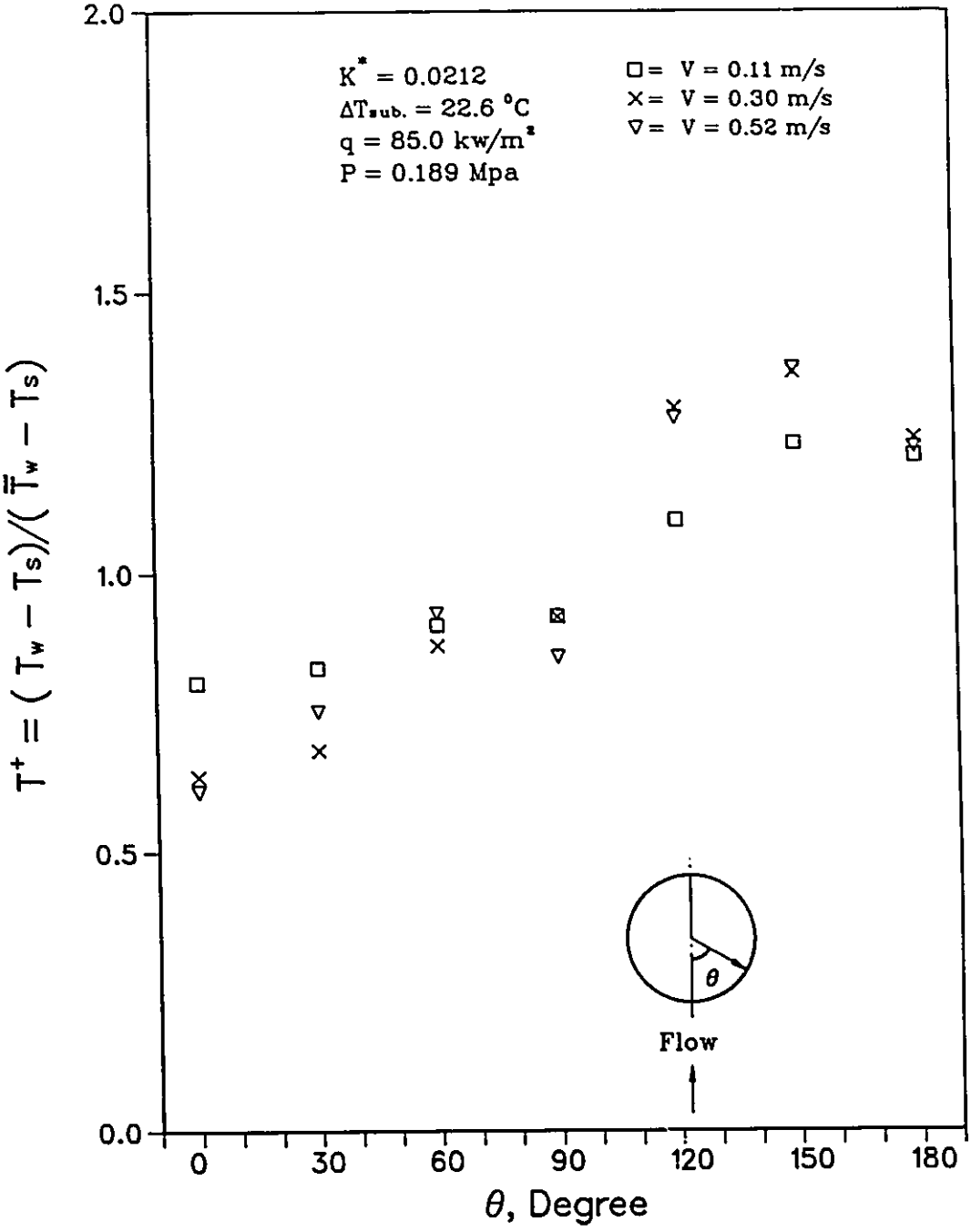

Figure 5.8 **Non-dimensional Temperature in Crossflow Nucleate Boiling for Different Flow Velocity**

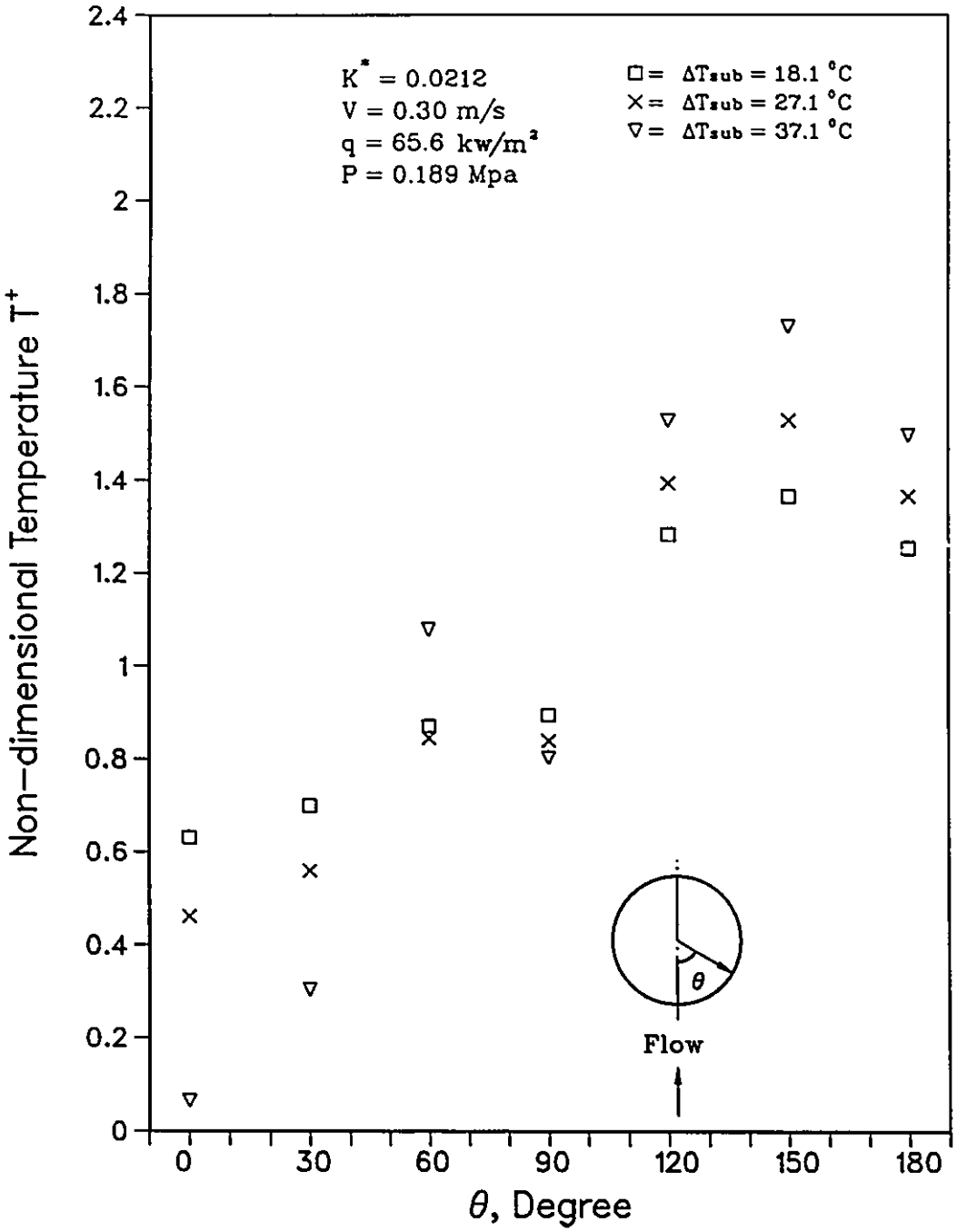

Figure 5.9 **Non-dimensional Temperature in Crossflow Nucleate Boiling for Different Degree of Subcooling**

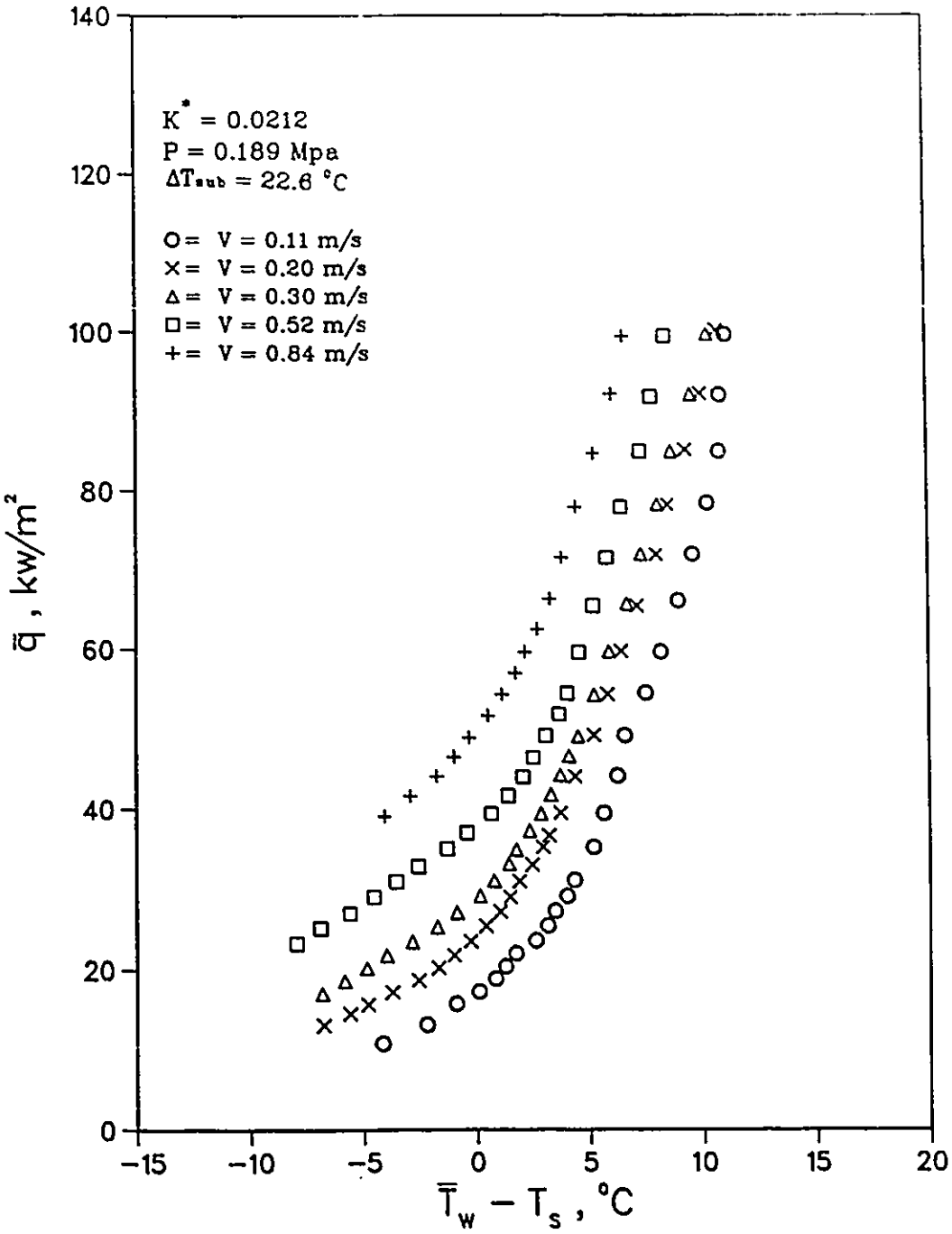

Figure 5.10 Effect of Flow Velocity in Crossflow Nucleate Boiling (a)

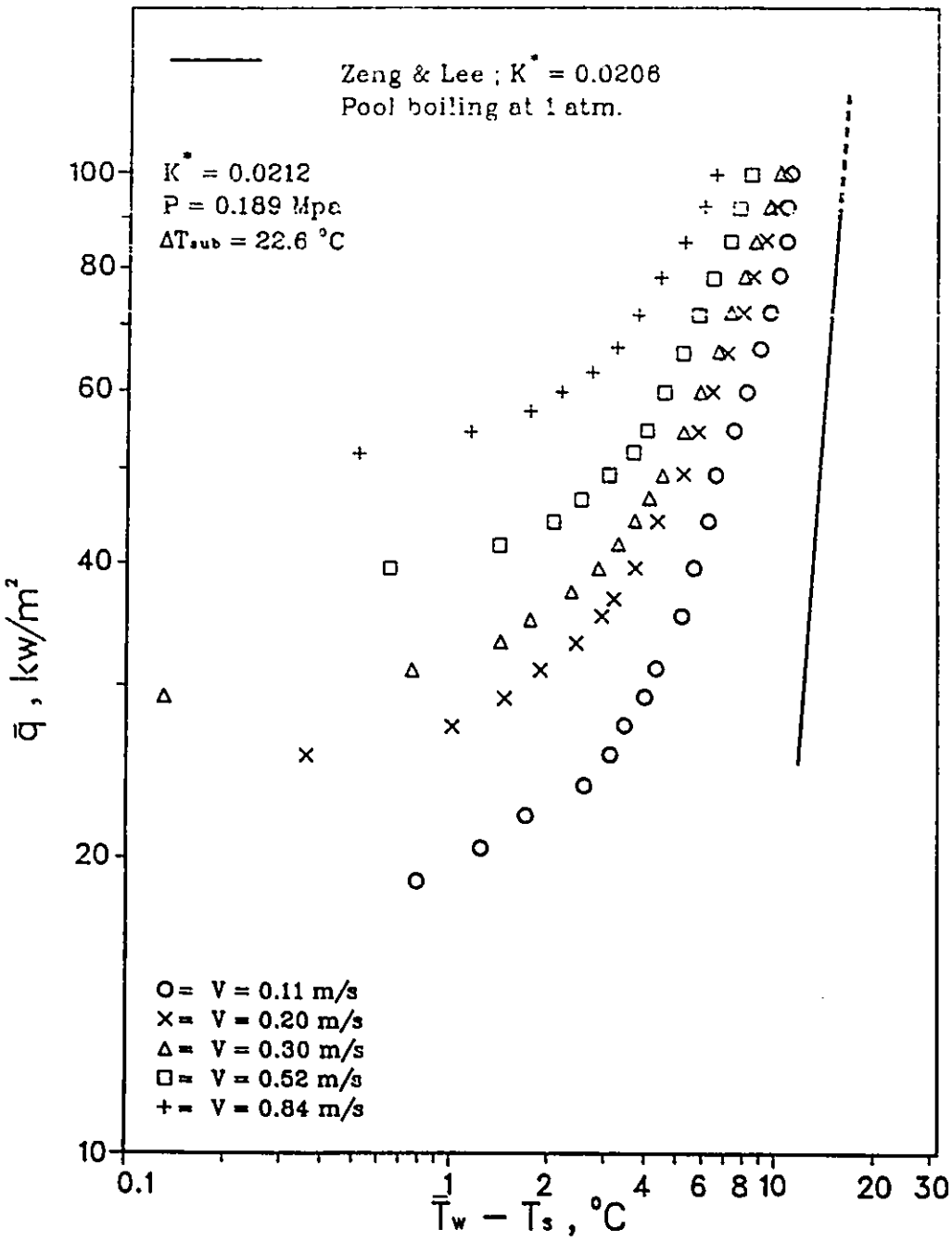

Figure 5.11 Effect of Flow Velocity in Crossflow Nucleate Boiling (b)

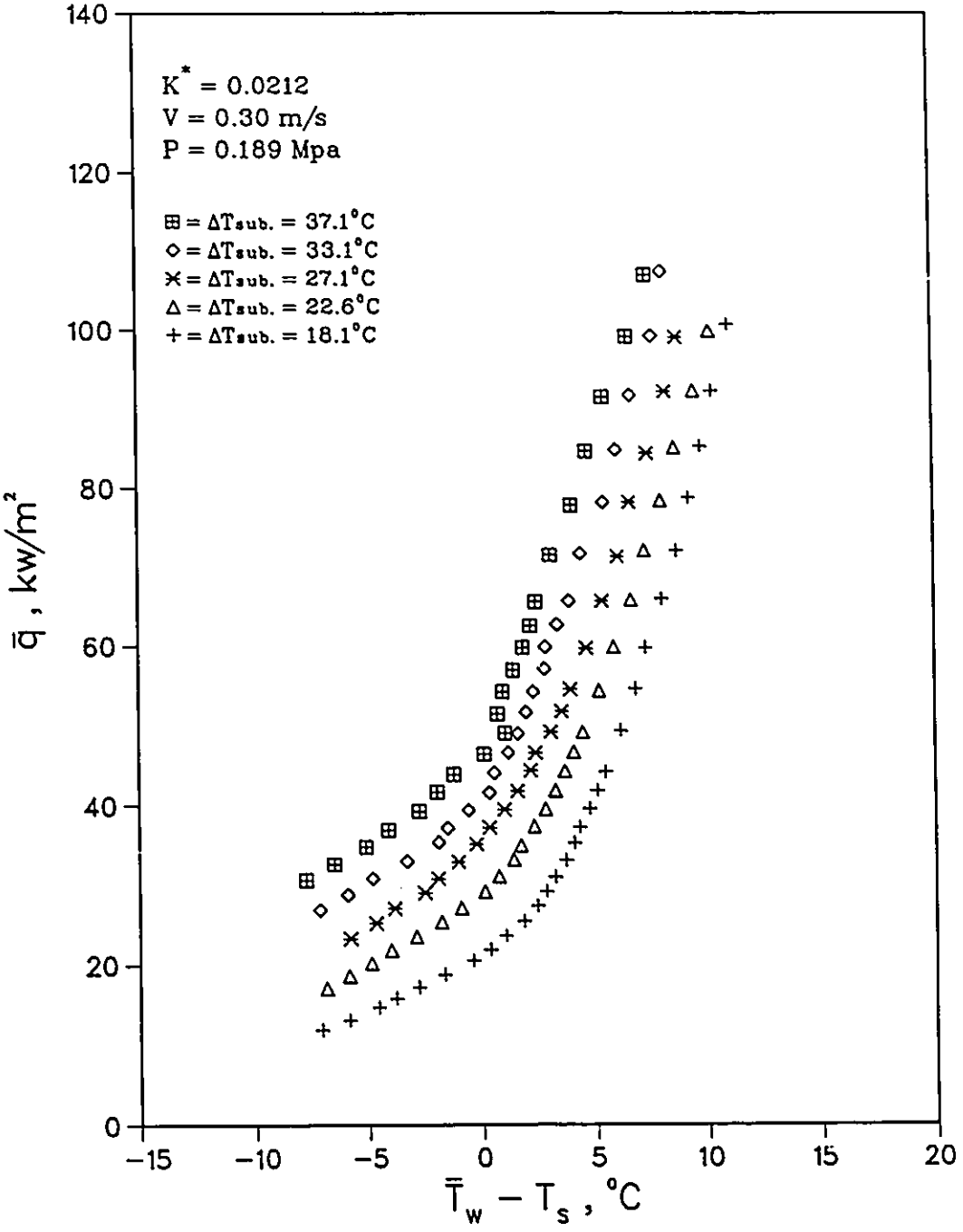

Figure 5.12 Effect of Degree of Subcooling in Crossflow Nucleate Boiling (a)

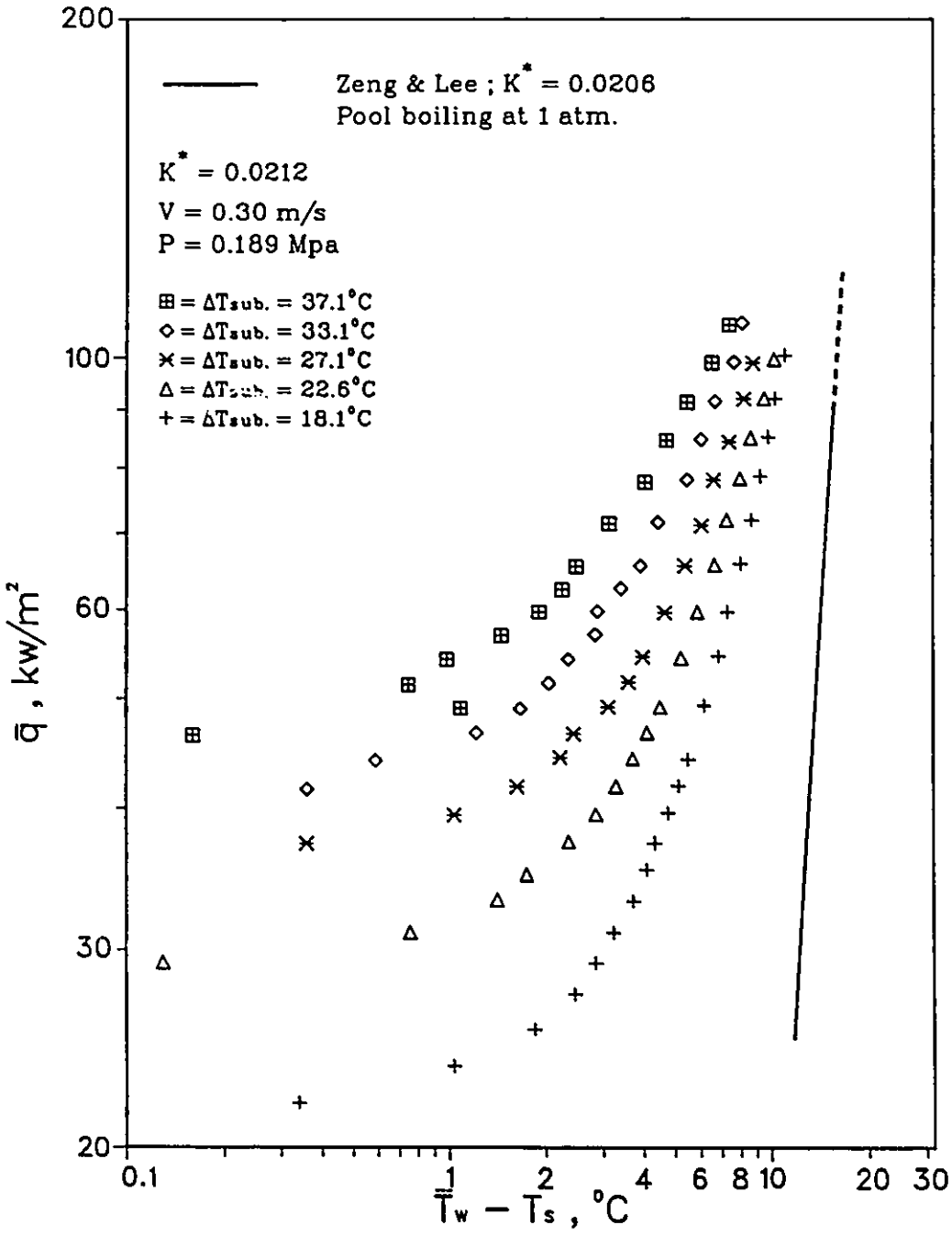

Figure 5.13 Effect of Degree of Subcooling in Crossflow Nucleate Boiling (b)

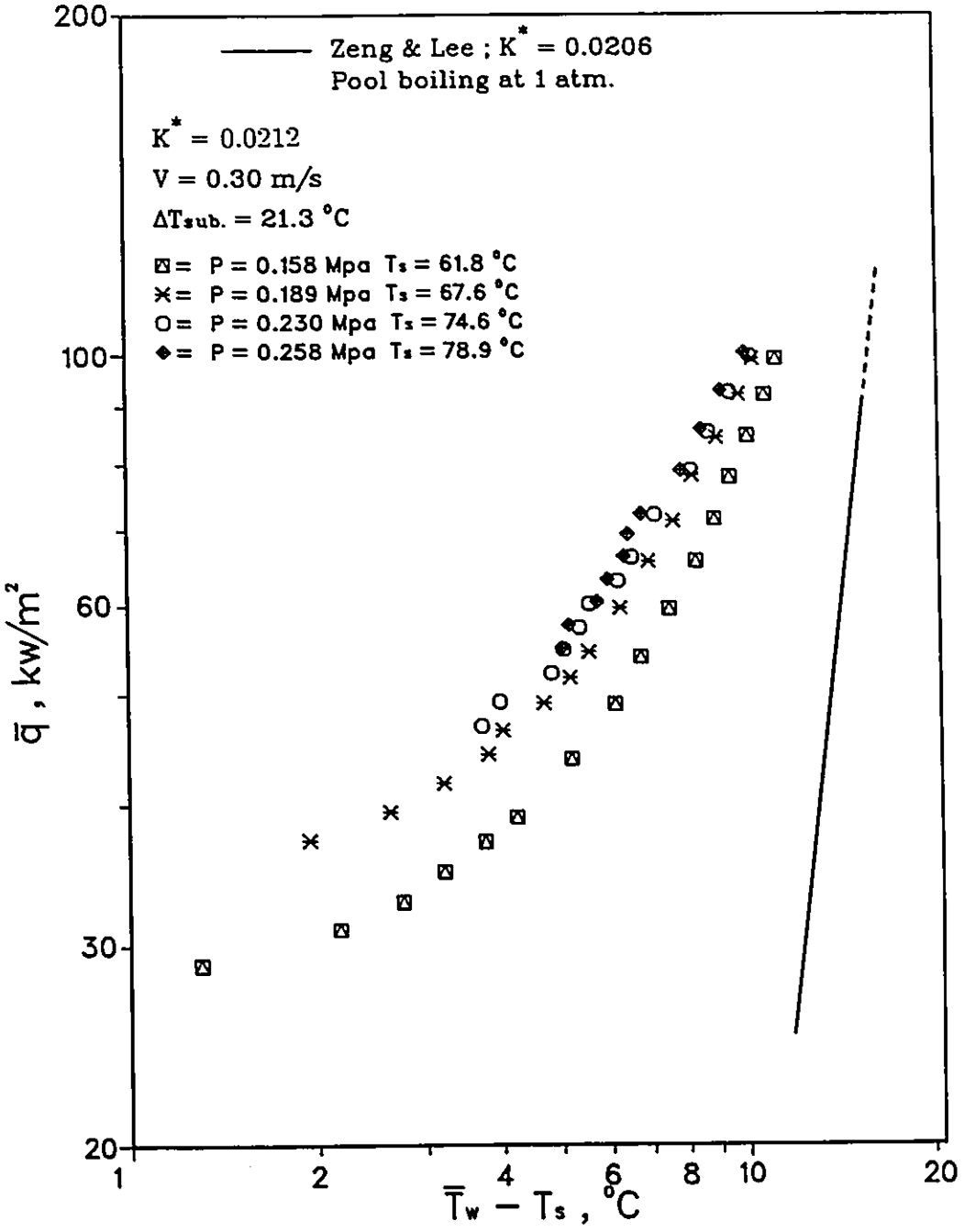

Figure 5.14 Effect of Pressure in Crossflow Nucleate Boiling

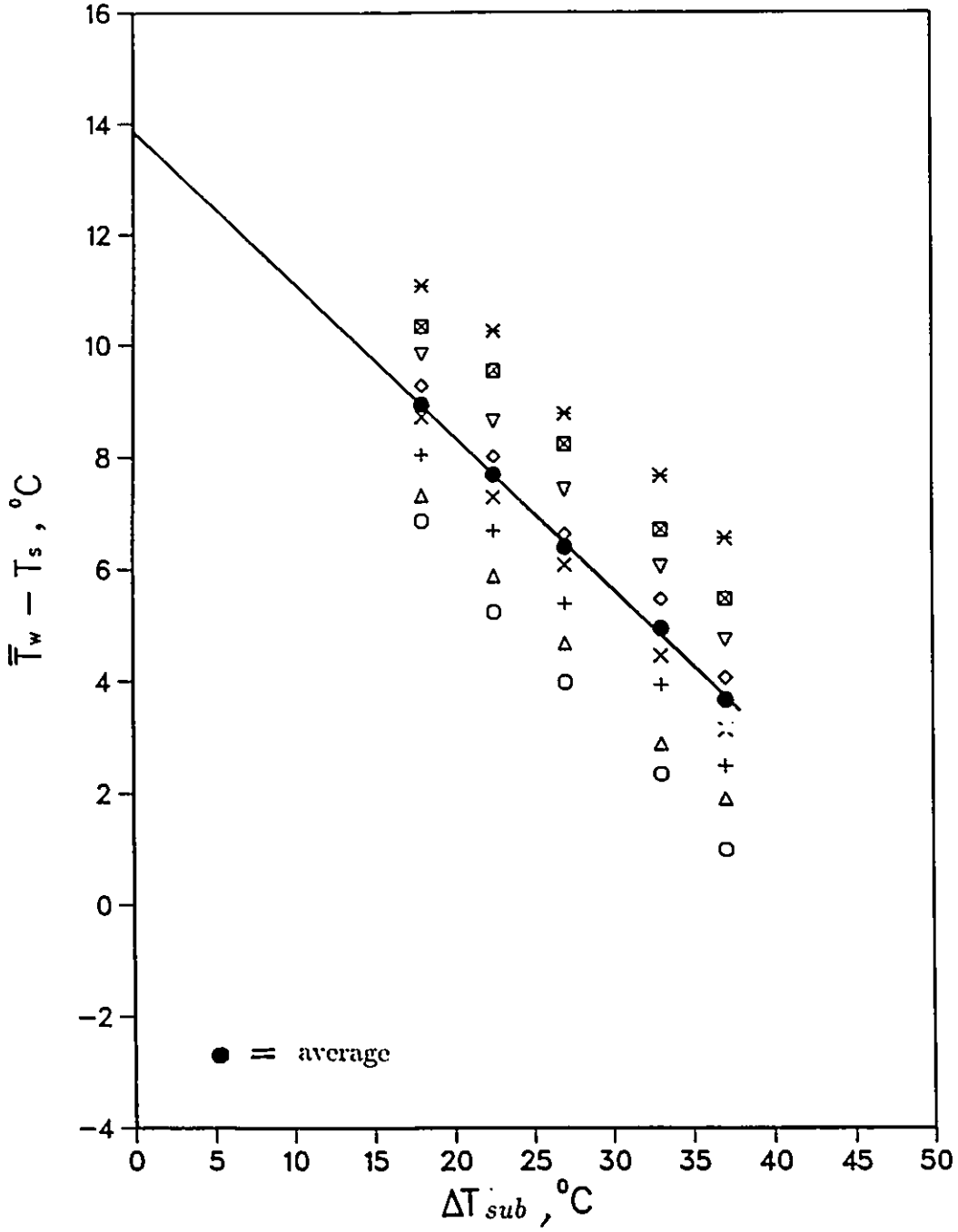

$\bar{T}_w - T_s = 13.861 - 0.273\Delta T$

Figure 5.15 Empirical Correlation for Liquid Subcooling in Crossflow Nucleate Boiling

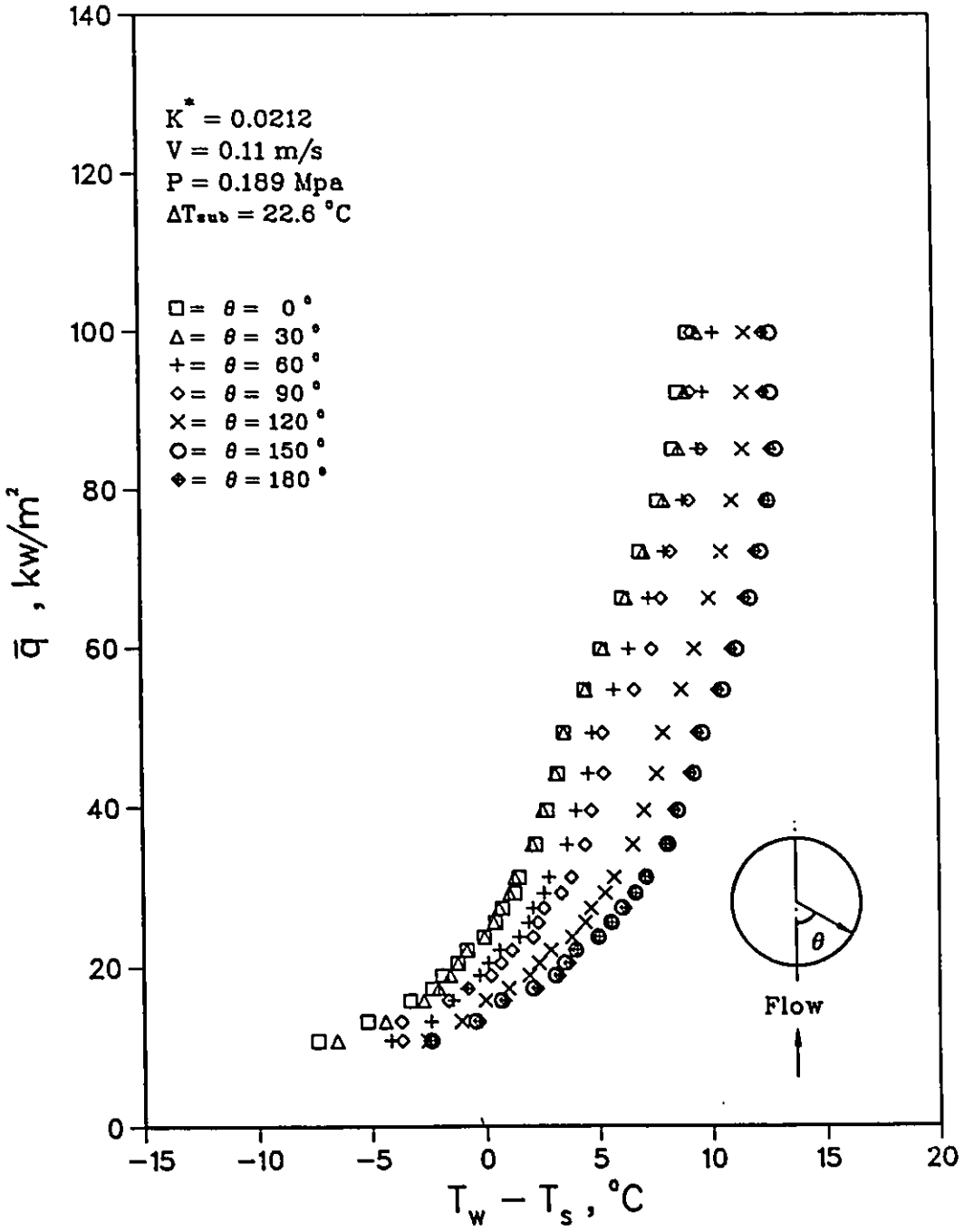

Figure 5.16 Local Crossflow Nucleate Boiling for $V = 0.11\ m/s$

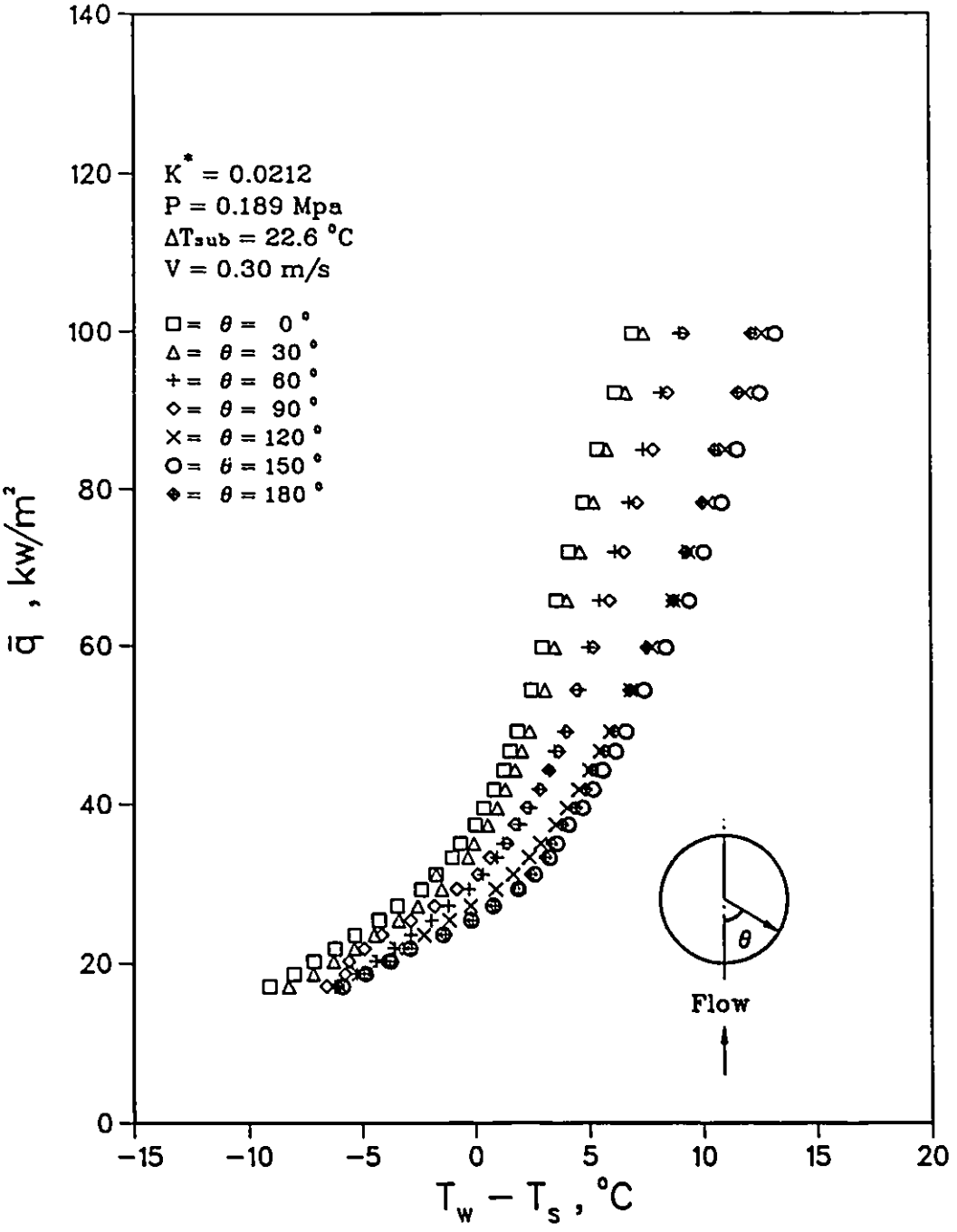

Figure 5.17 Local Crossflow Nucleate Boiling for $V = 0.30\ m/s$

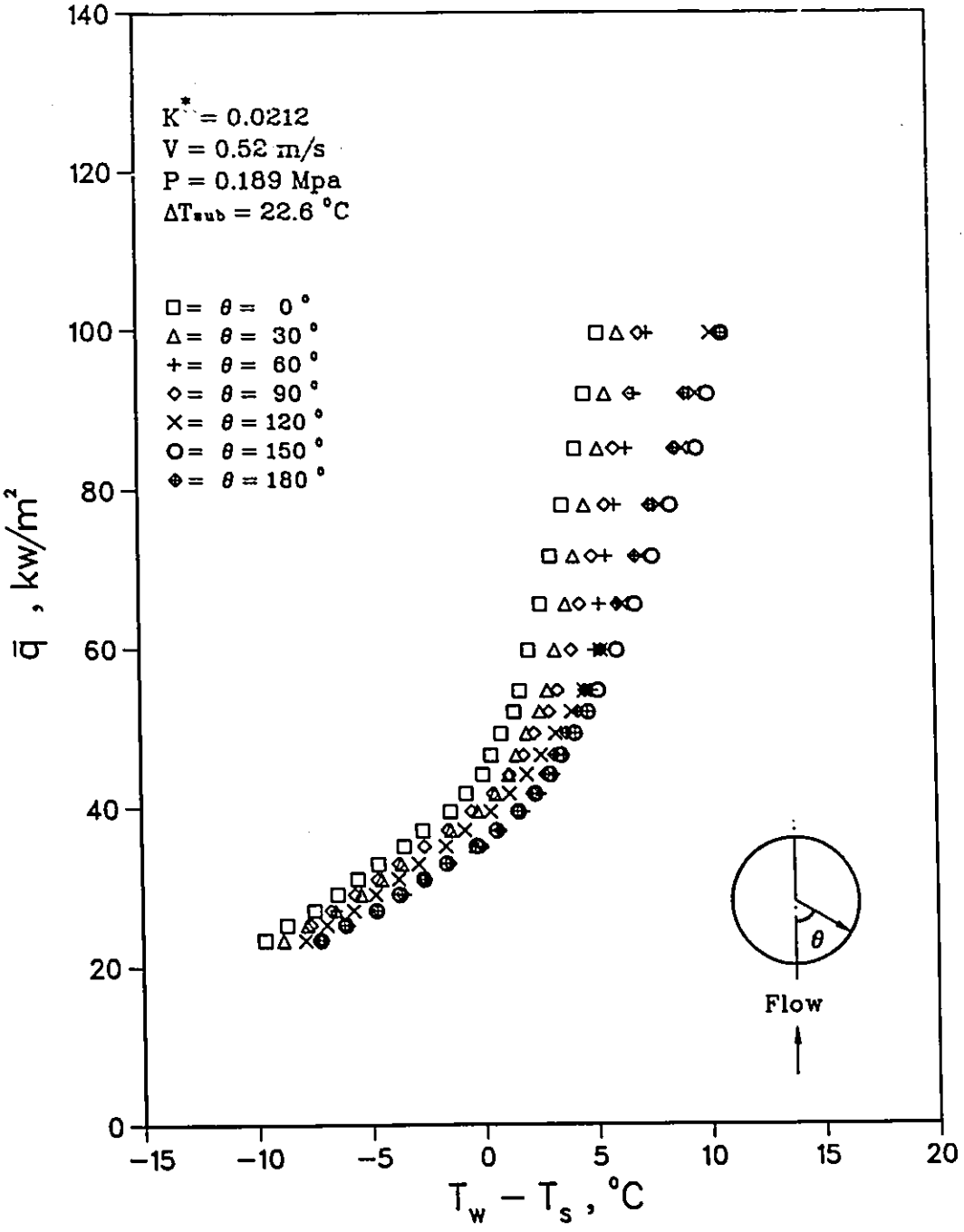

Figure 5.18 Local Crossflow Nucleate Boiling for $V = 0.52\ m/s$

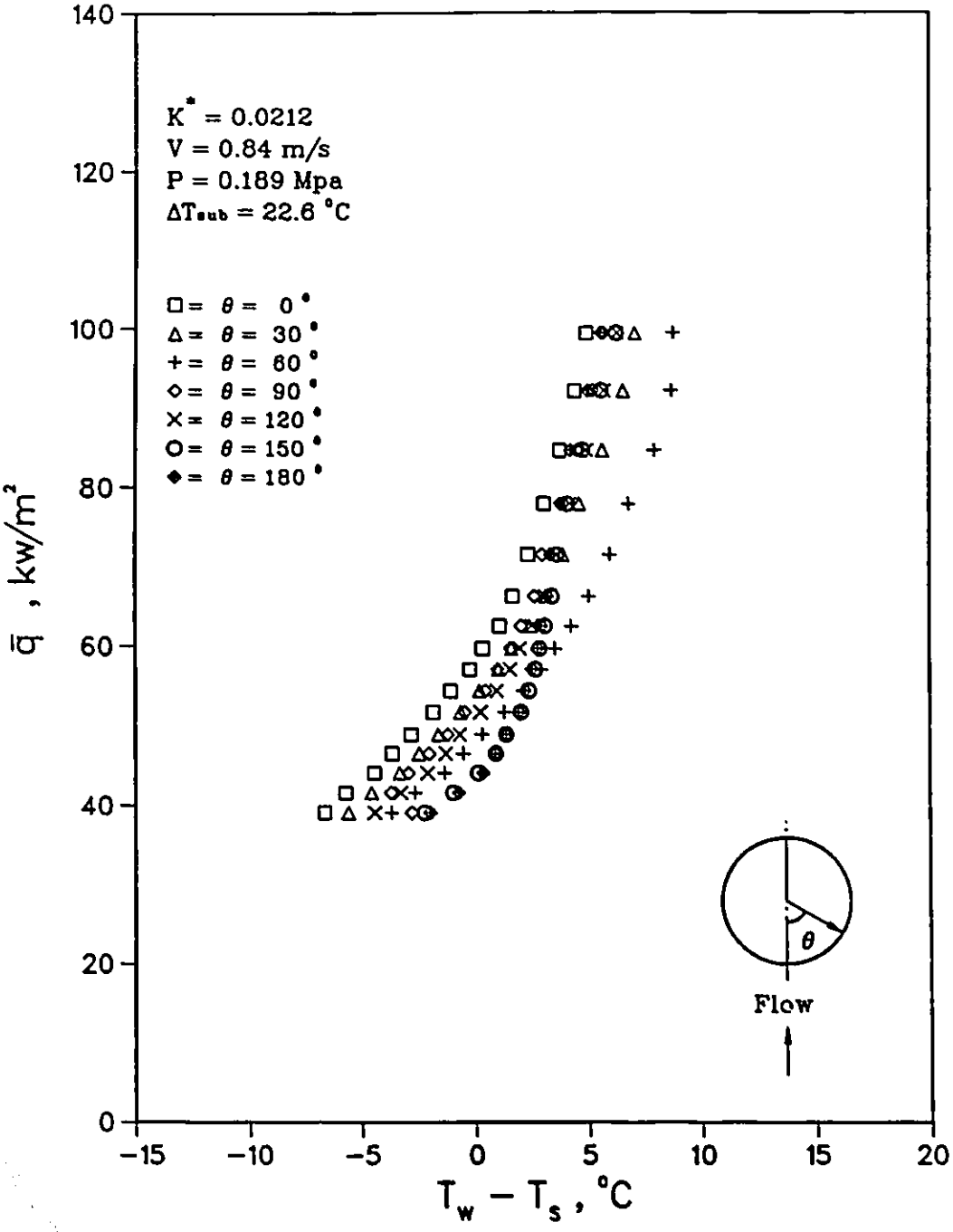

Figure 5.19 Local Crossflow Nucleate Boiling for $V = 0.84\ m/s$

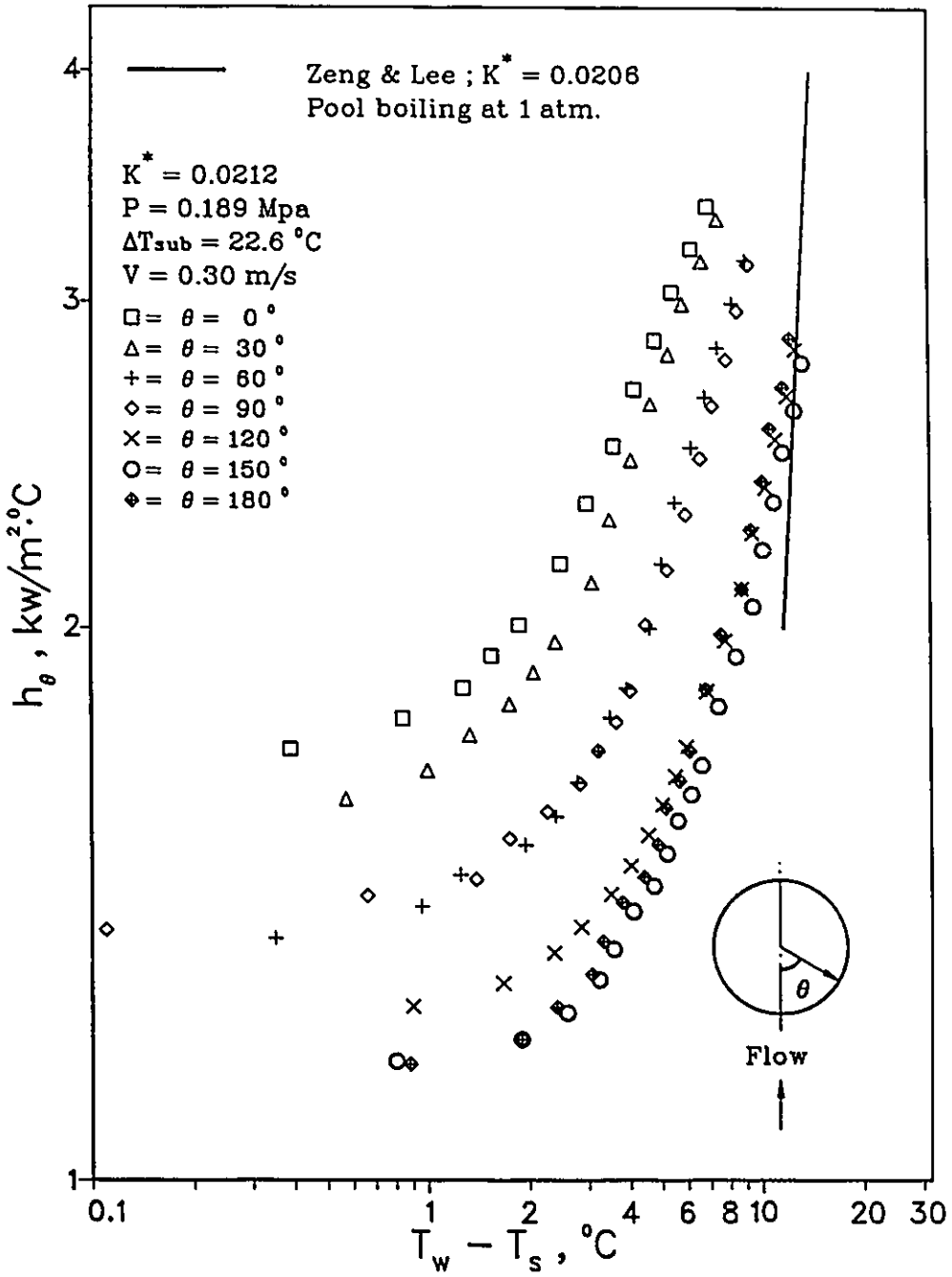

Figure 5.20 **Local Heat Transfer Coefficient h_θ for $V = 0.30\ m/s$ in Crossflow Nucleate Boiling**

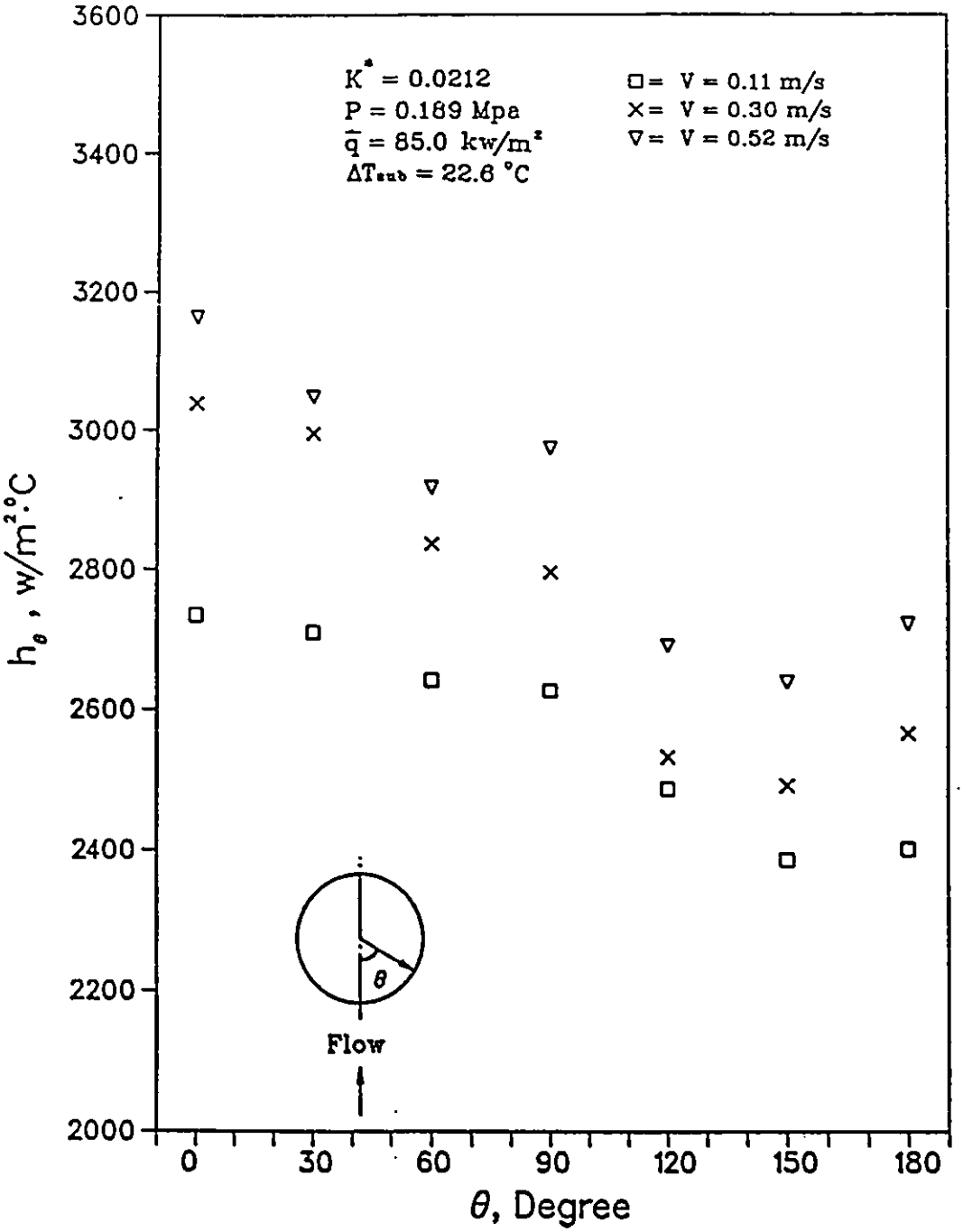

Figure 5.21 Effect of Flow Velocity in Distribution of Local h_θ in Crossflow Nucleate Boiling

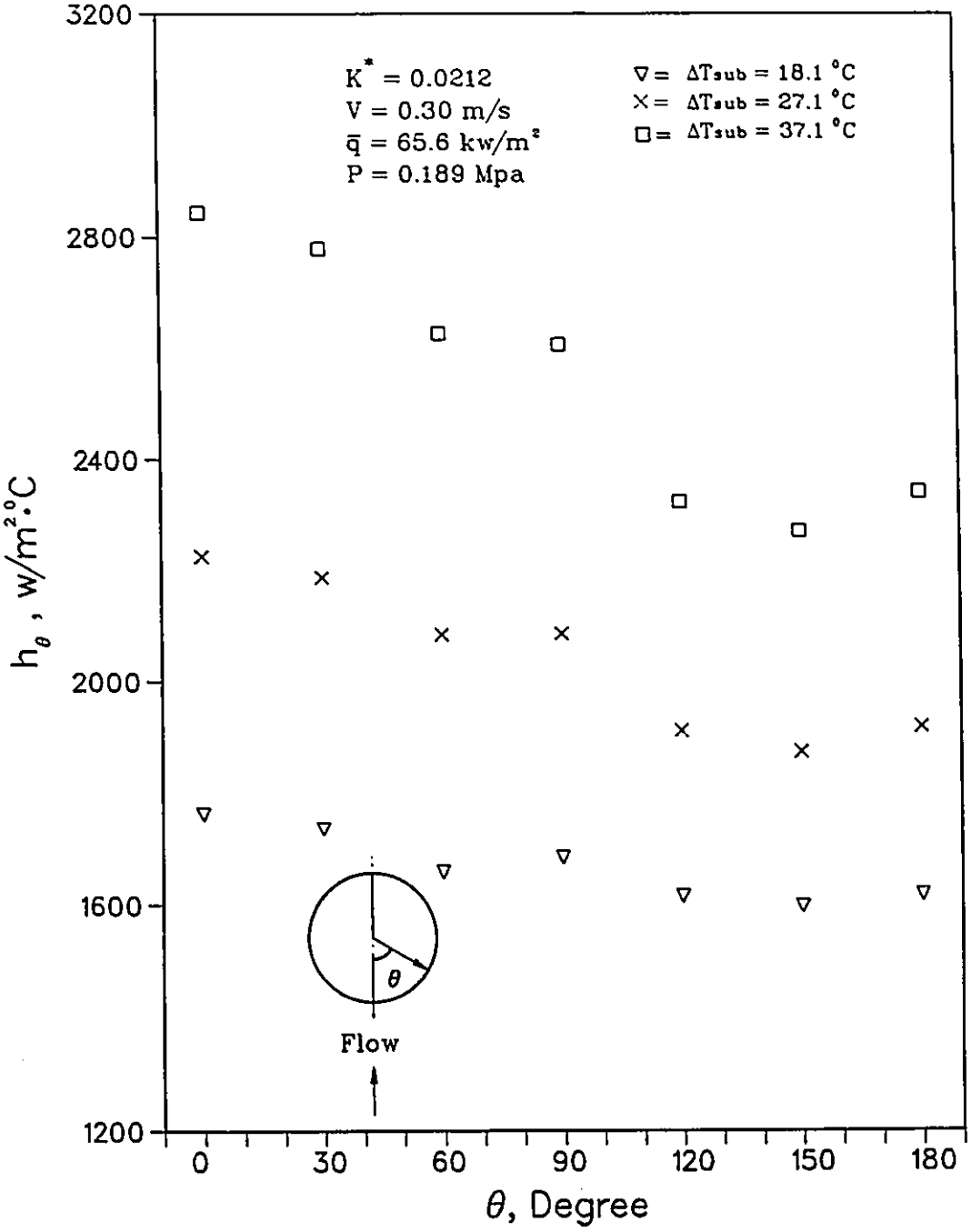

Figure 5.22 **Effect of Degree of Subcooling in Distribution of Local h_θ in Crossflow Nucleate Boiling**

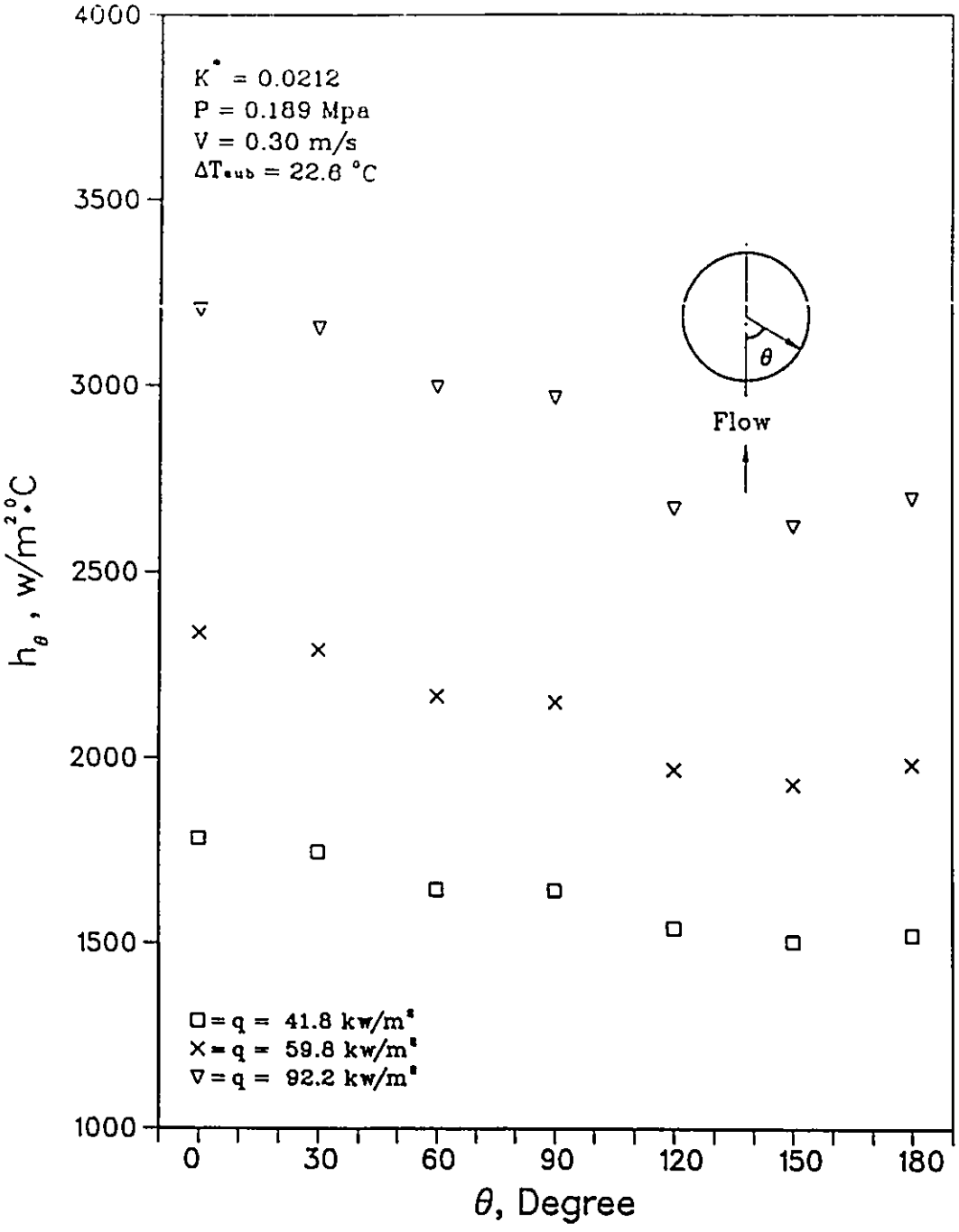

Figure 5.23 Effect of Heat Flux in Distribution of Local h_θ in Crossflow Nucleate Boiling

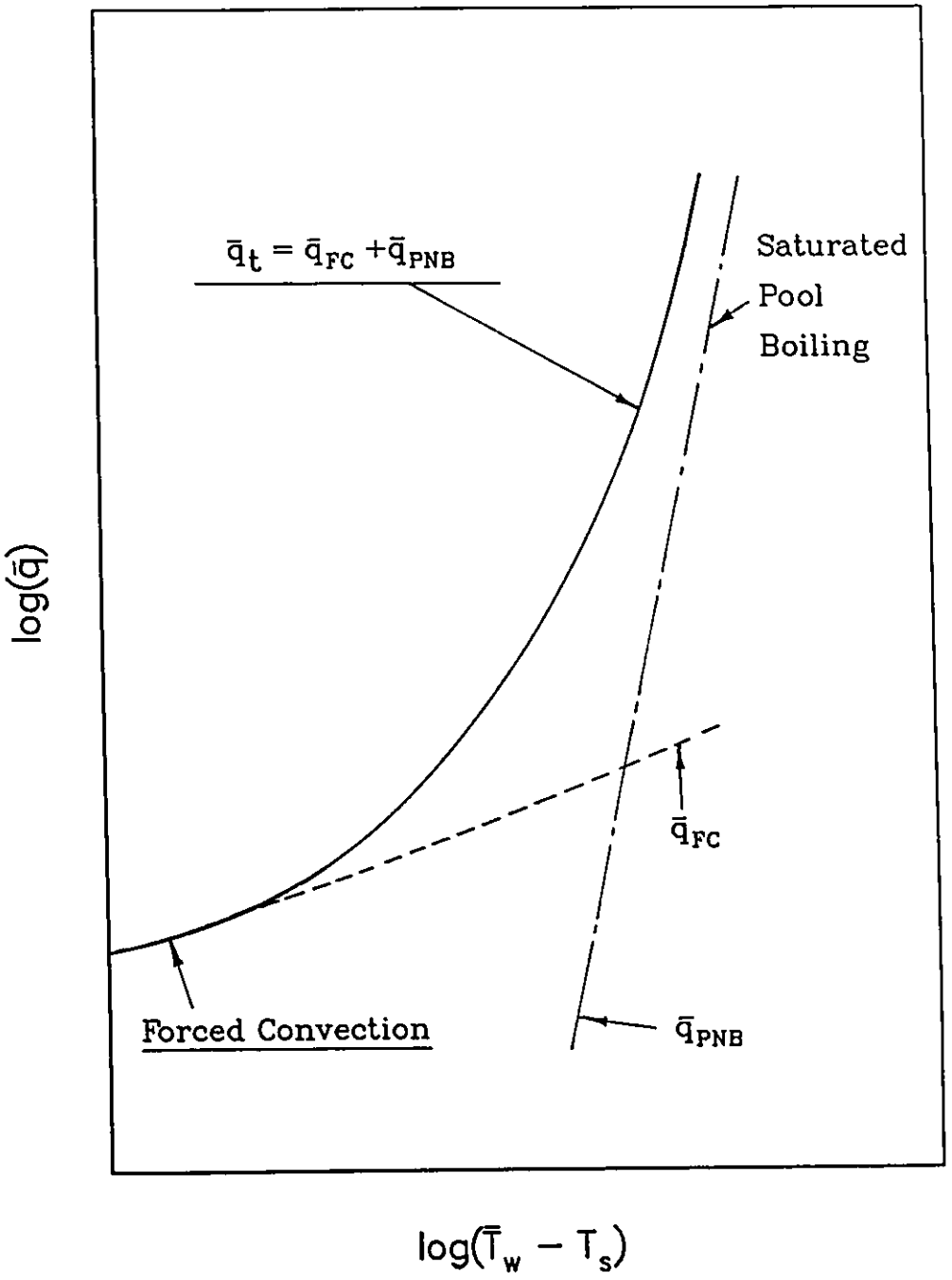

Figure 5.24 Superposition Procedure of Rohsenow

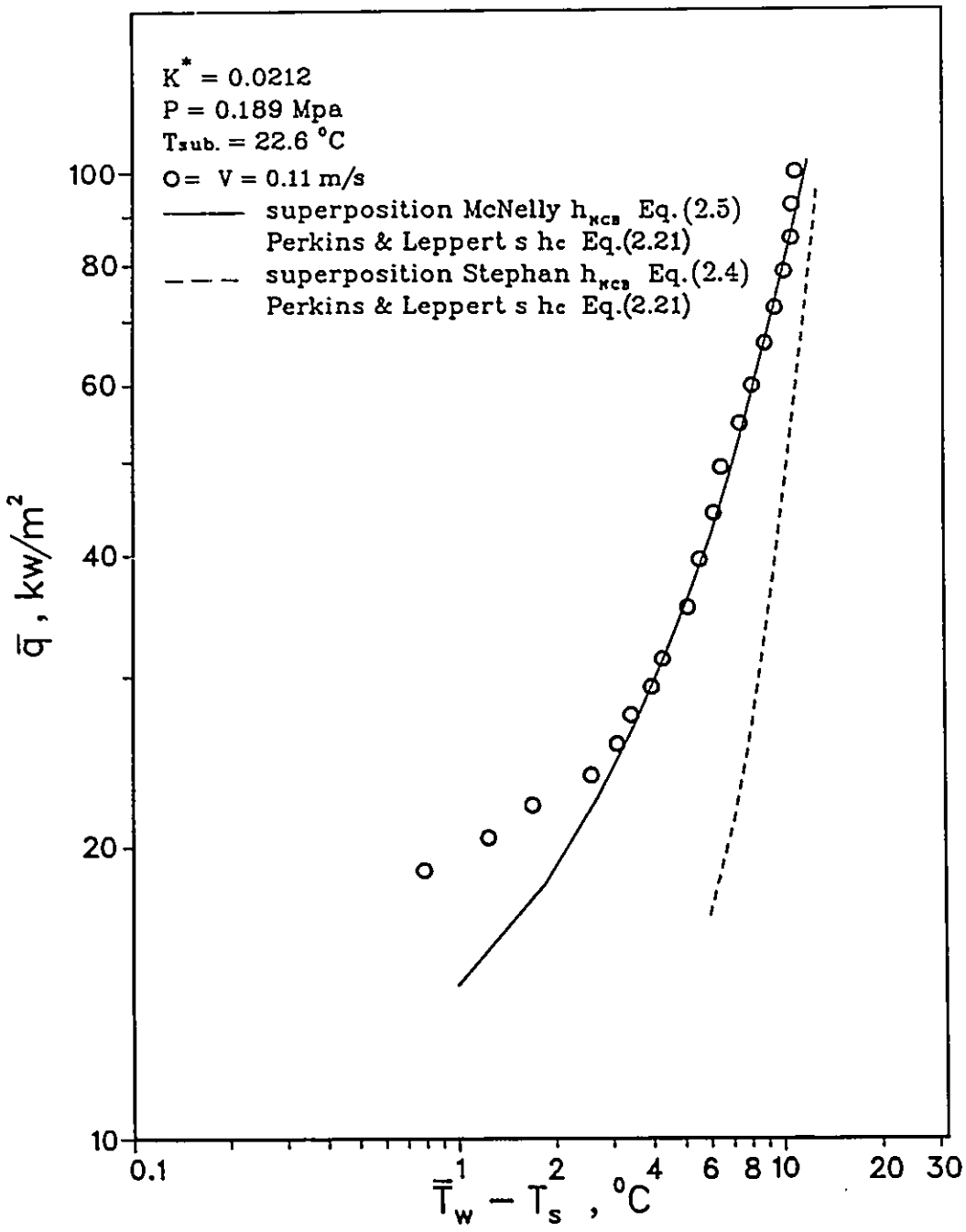

Figure 5.25 Comparison of Experimental Nucleate Boiling Curve ($V = 0.11\ m/s$) with Rohsenow's Prediction

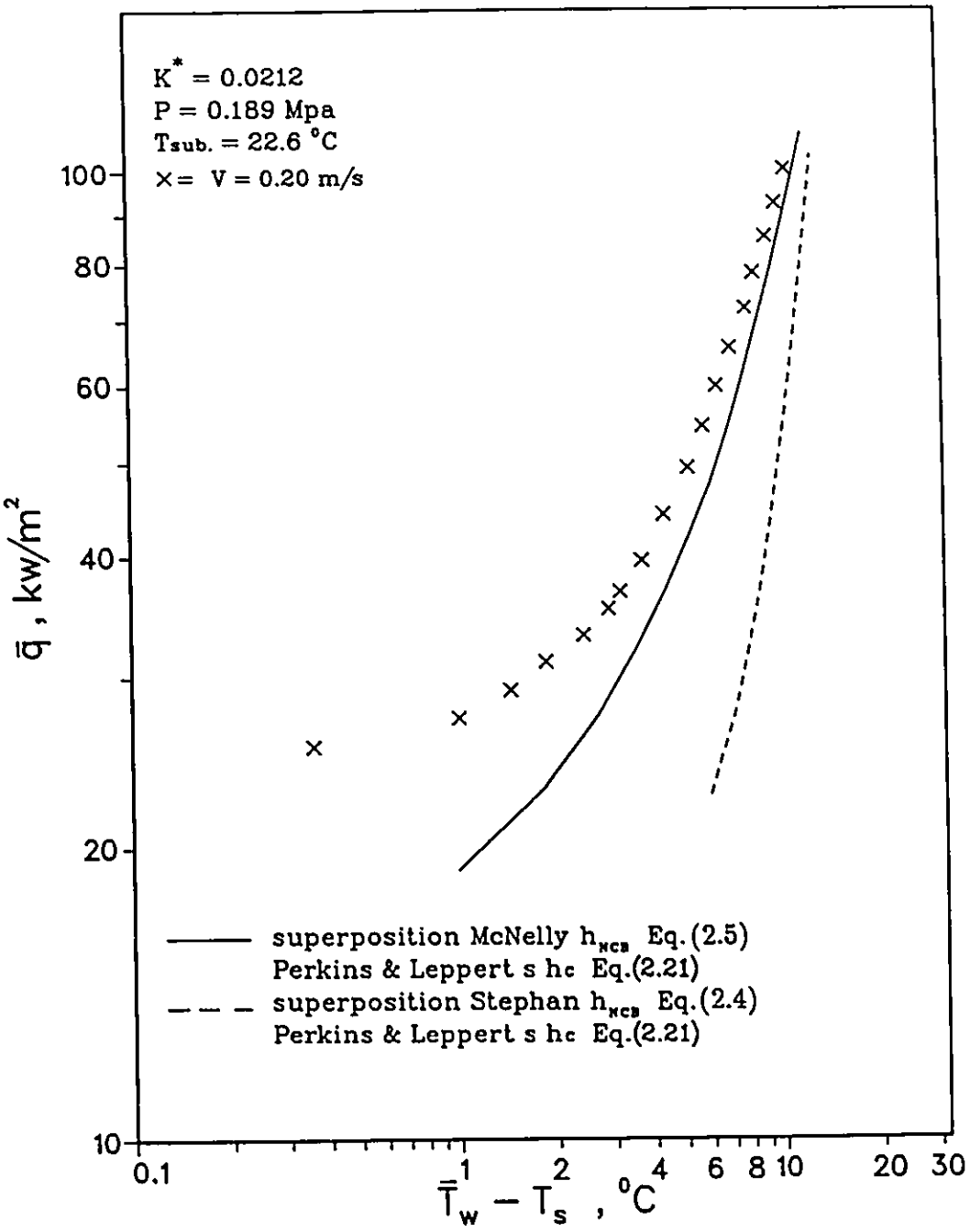

Figure 5.26 **Comparison of Experimental Nucleate Boiling Curve ($V = 0.20\ m/s$) with Rohsenow's Prediction**

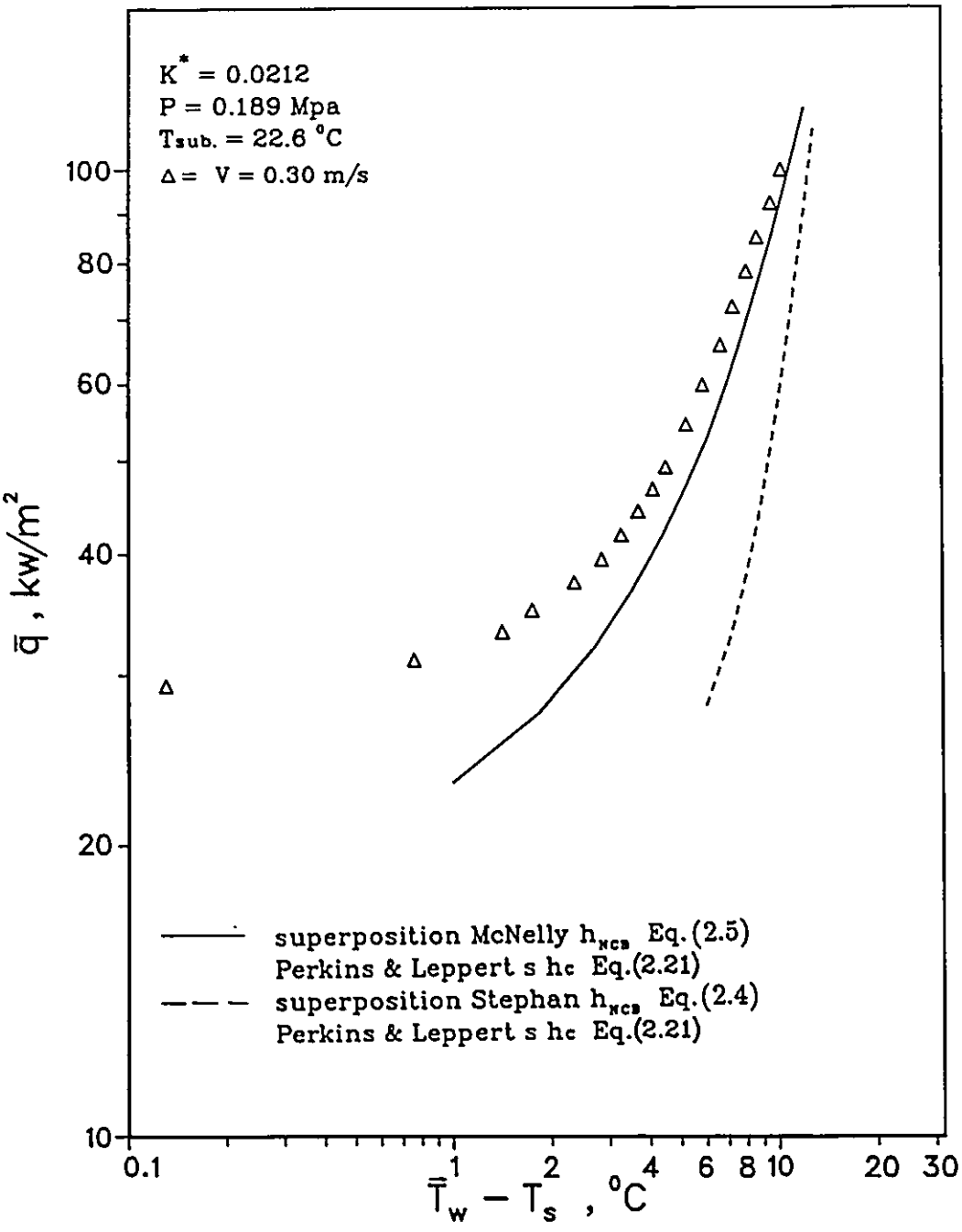

Figure 5.27 Comparison of Experimental Nucleate Boiling Curve ($V = 0.30\ m/s$) with Rohsenow's Prediction

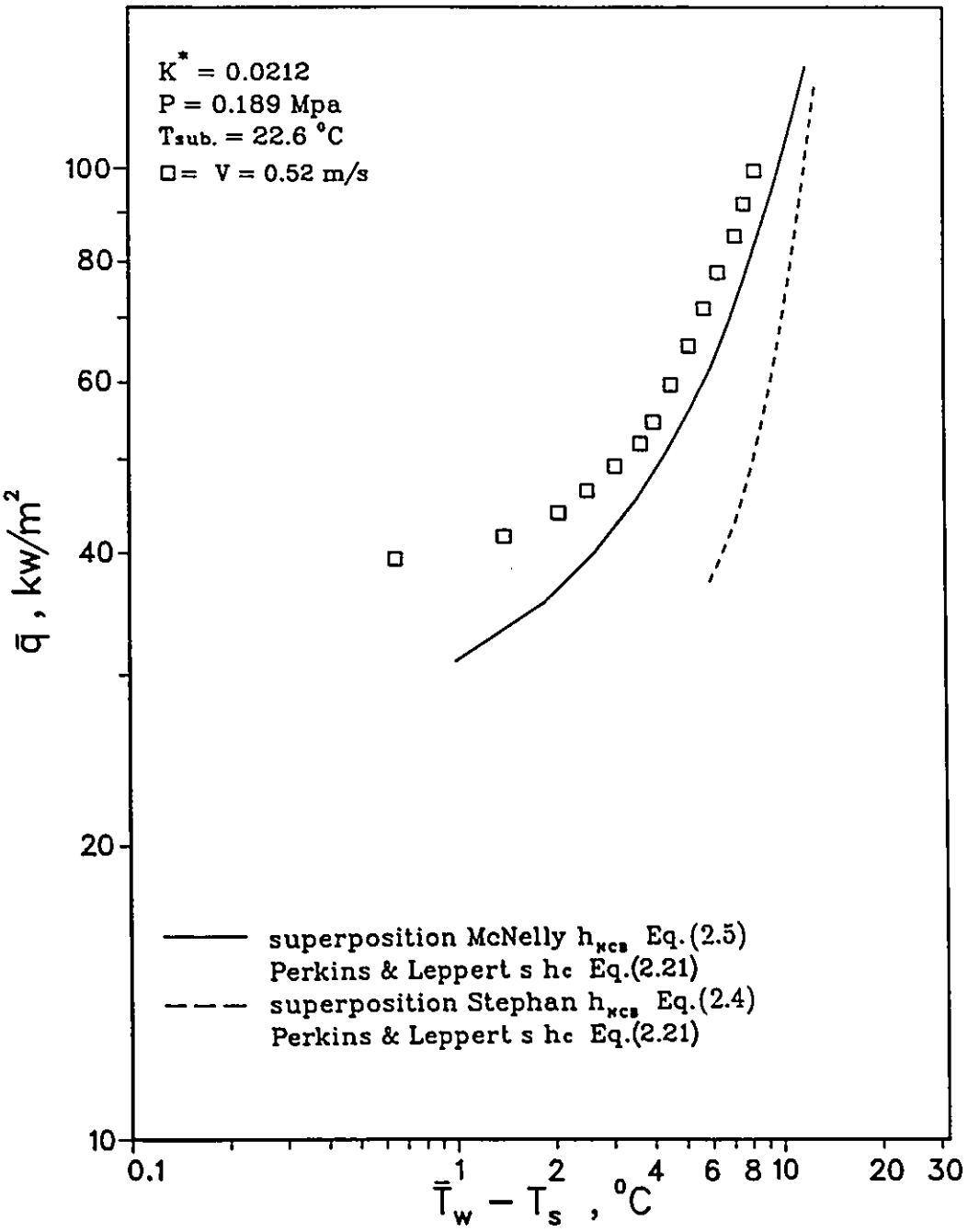

Figure 5.28 Comparison of Experimental Nucleate Boiling Curve ($V = 0.52\ m/s$) with Rohsenow's Prediction

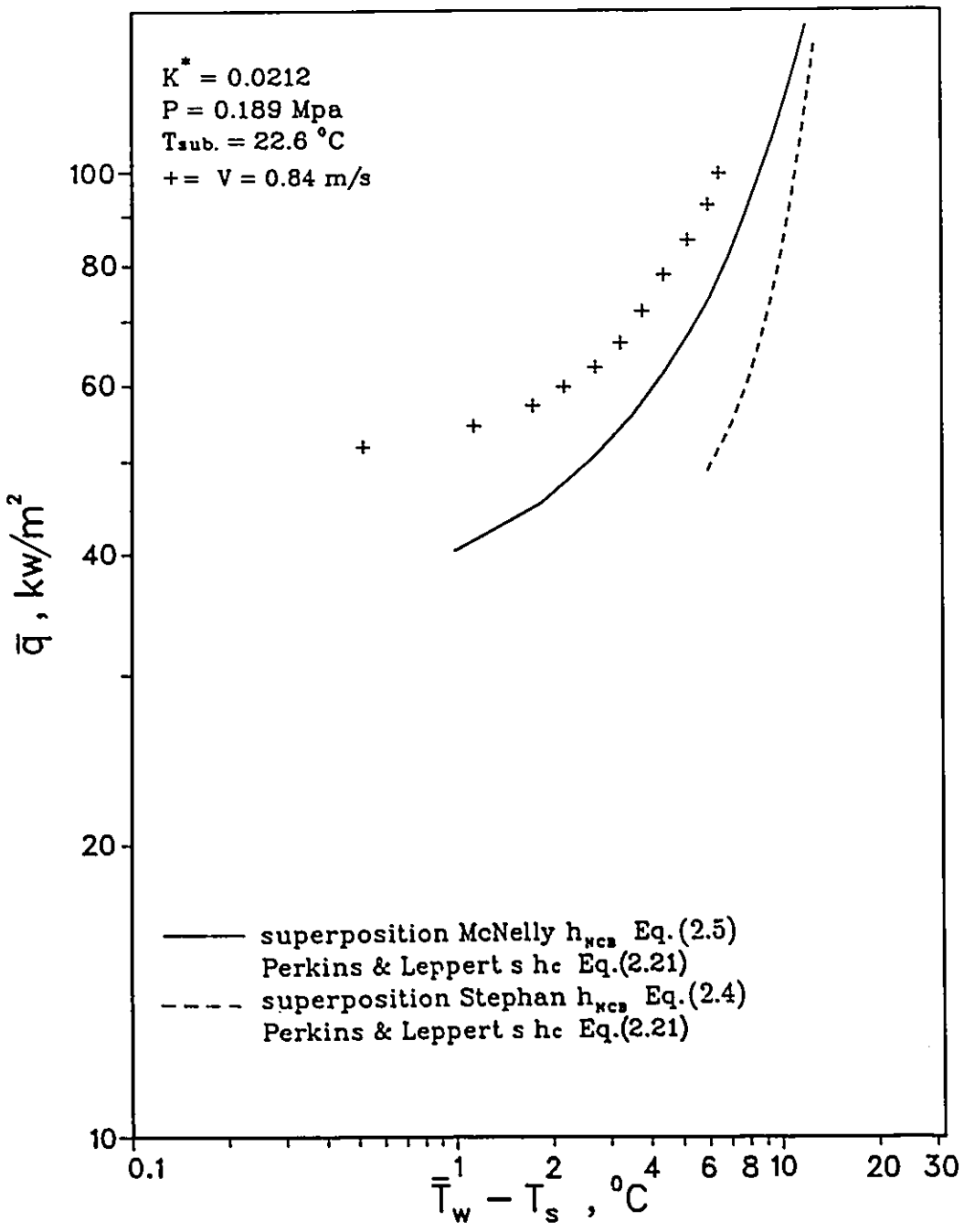

Figure 5.29 Comparison of Experimental Nucleate Boiling Curve ($V = 0.84\ m/s$) with Rohsenow's Prediction

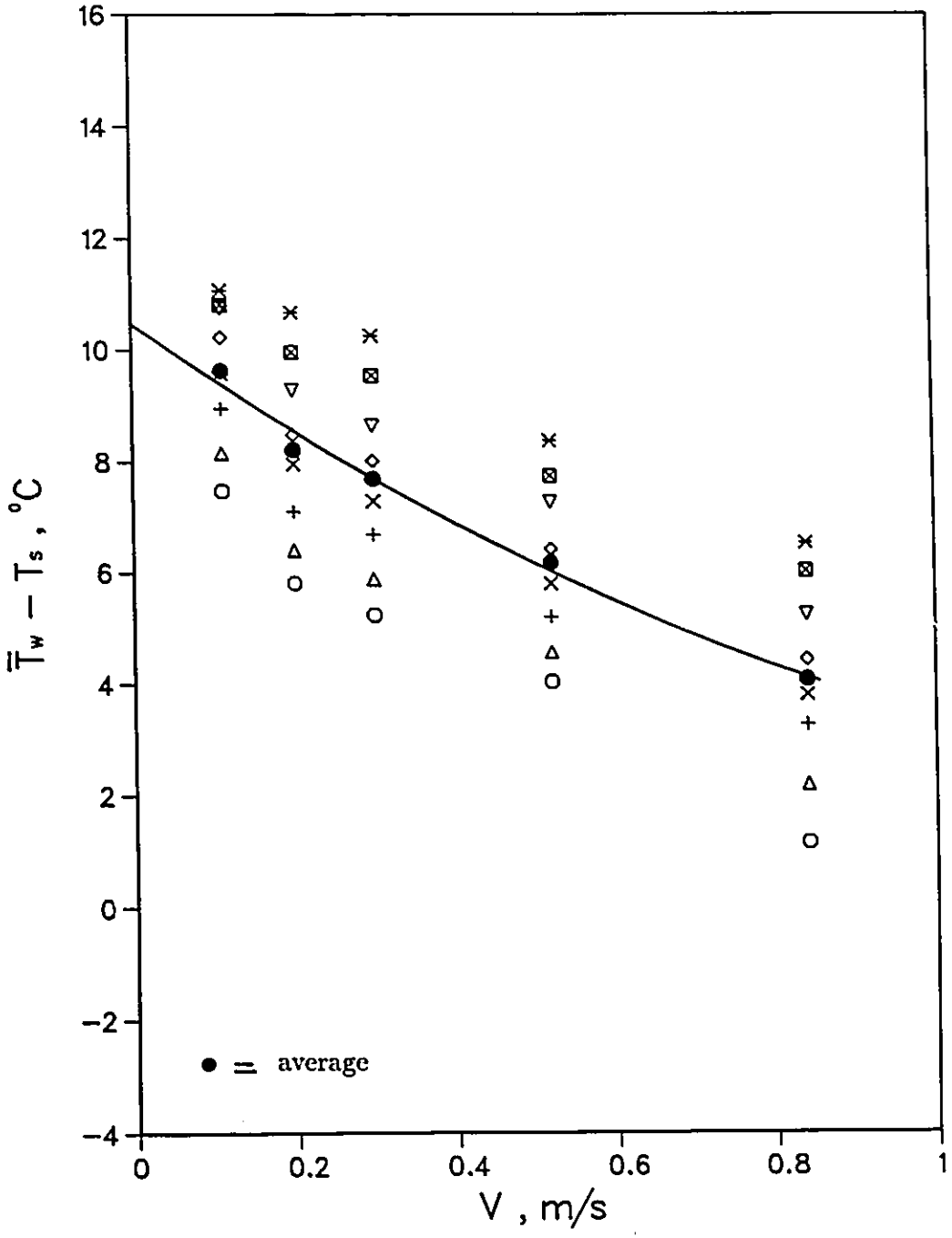

$$\bar{T}_w - T_s = 10.474 - 10.204V + 3.143V^2$$

Figure 5.30 Empirical Correlation for Flow Velocity in Crossflow Nucleate Boiling

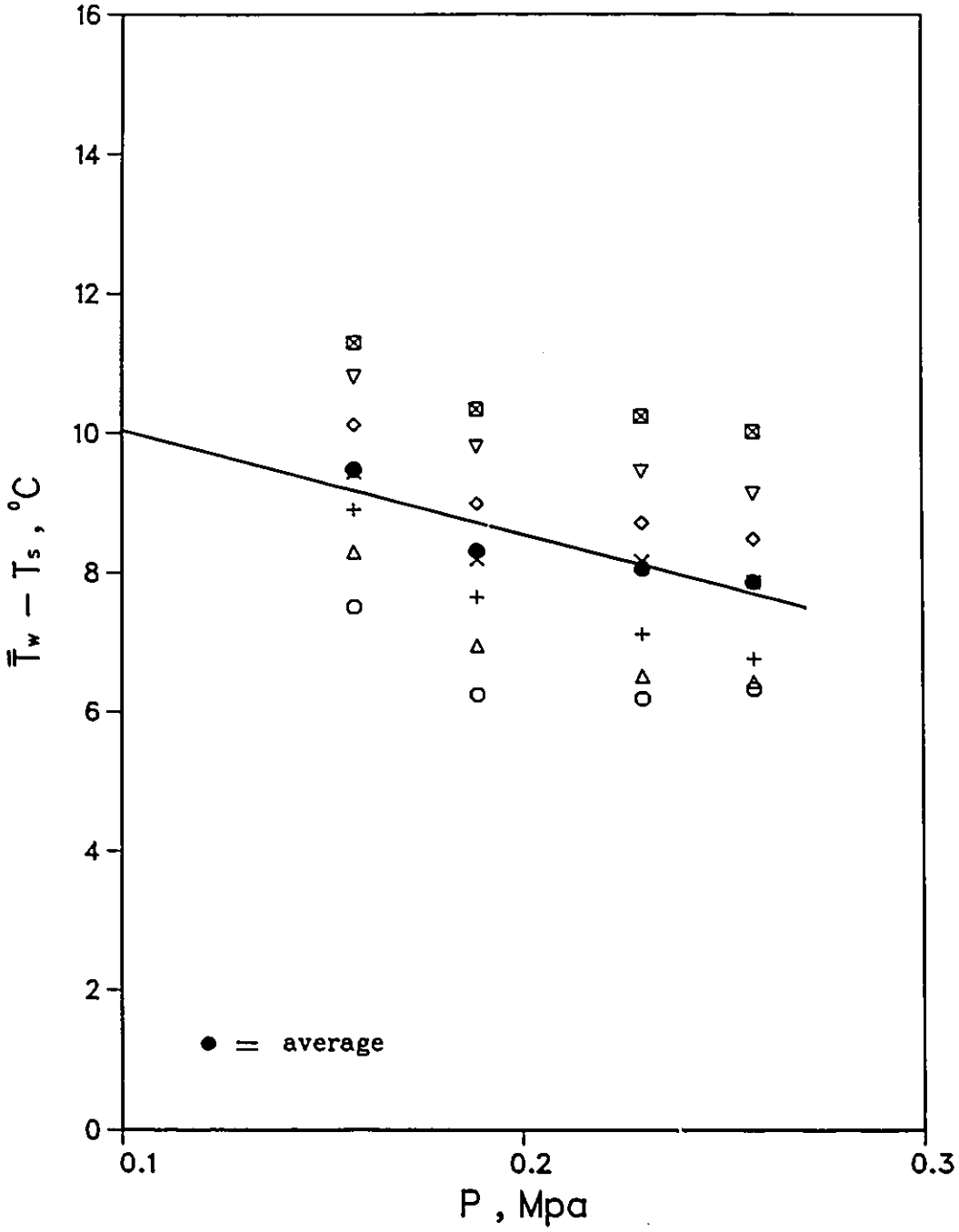

$\bar{T}_w - T_s = 11.515 - 14.7395P$

Figure 5.31 Empirical Correlation for System Pressure in Crossflow Nucleate Boiling

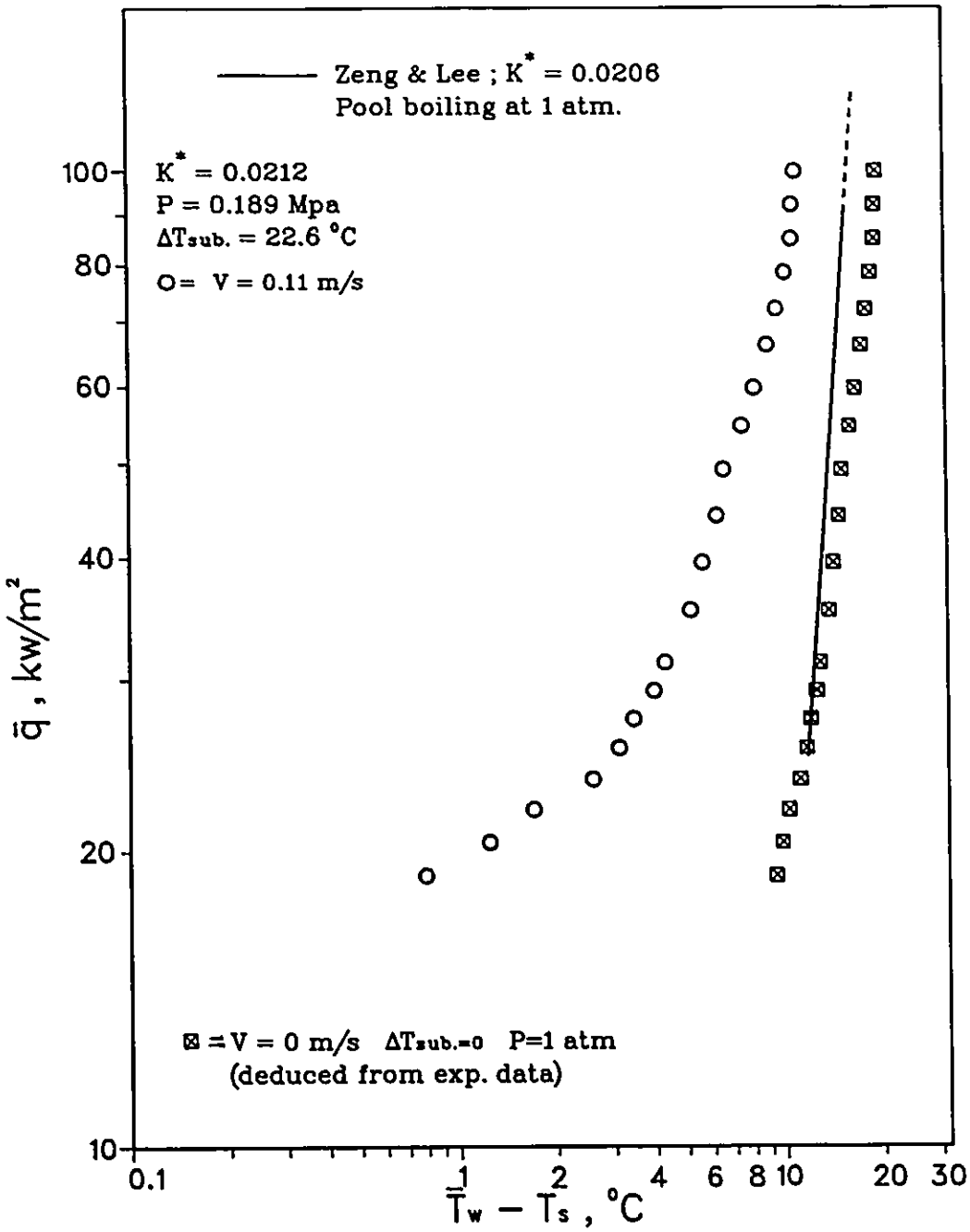

Figure 5.32 Comparison of Results in Nucleate Boiling ($V = 0.11\ m/s$)

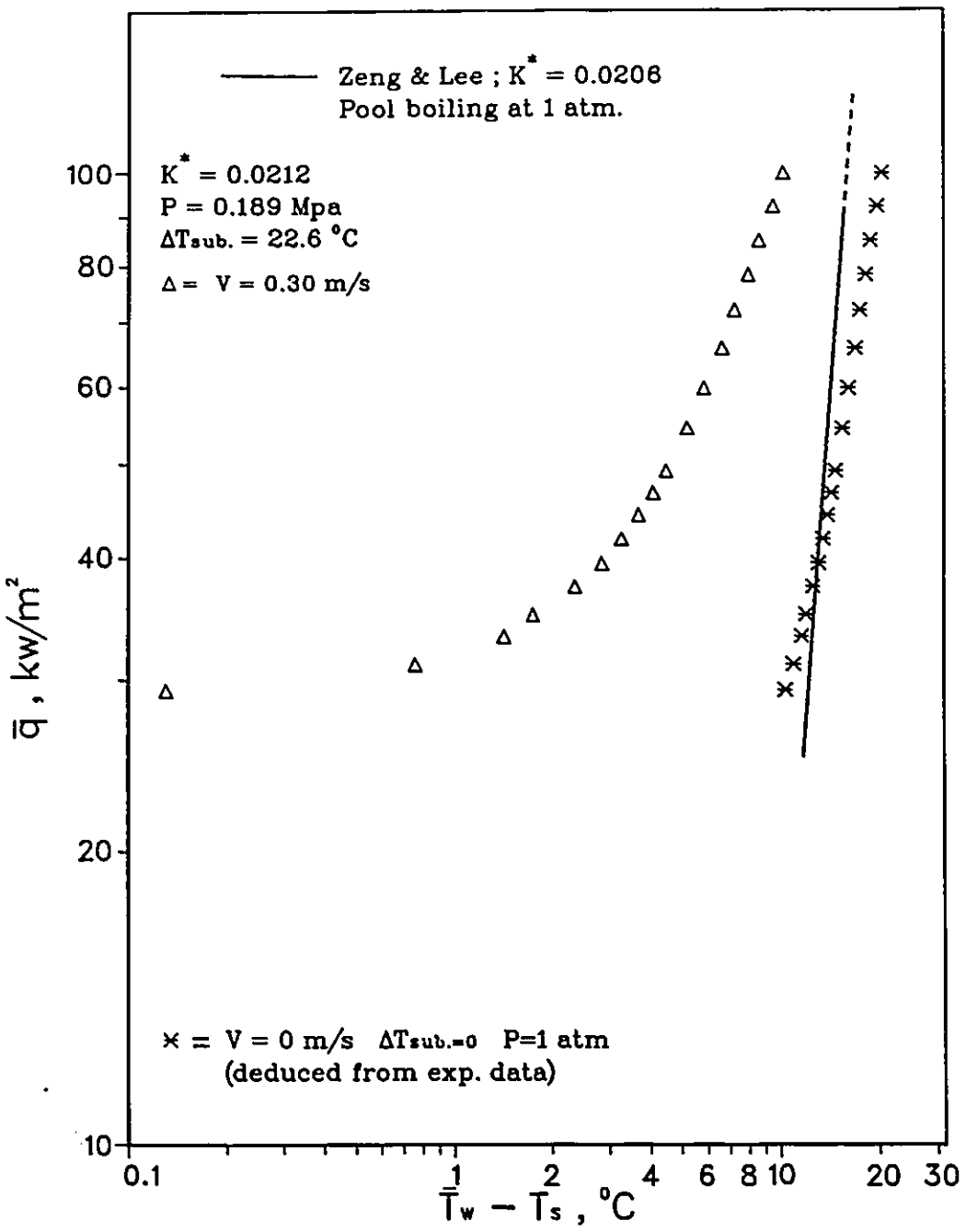

Figure 5.33 Comparison of Results in Nucleate Boiling ($V = 0.30\,m/s$)

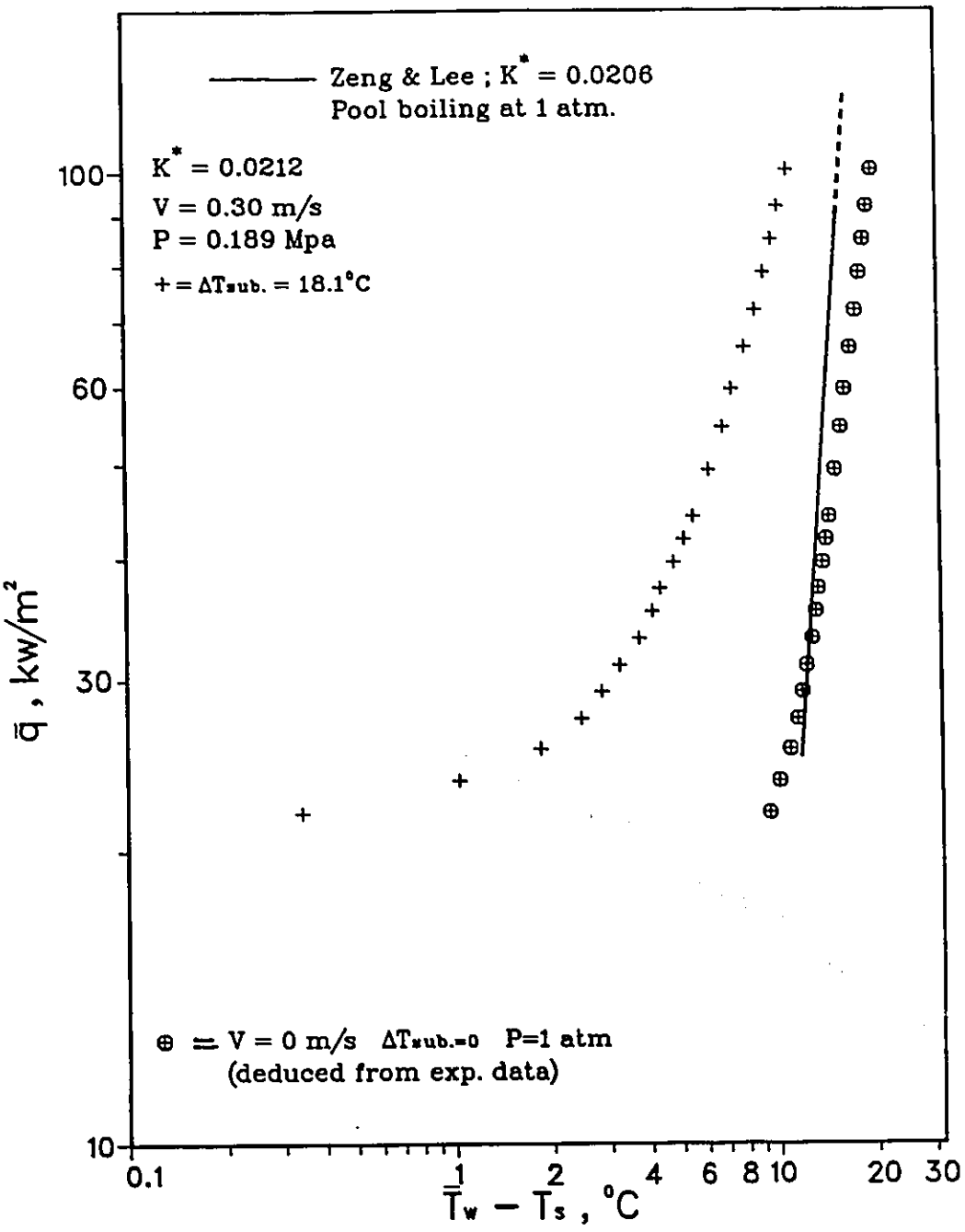

Figure 5.34 Comparison of Results in Nucleate Boiling ($\Delta T_{sub.} = 18.1\,°C$)

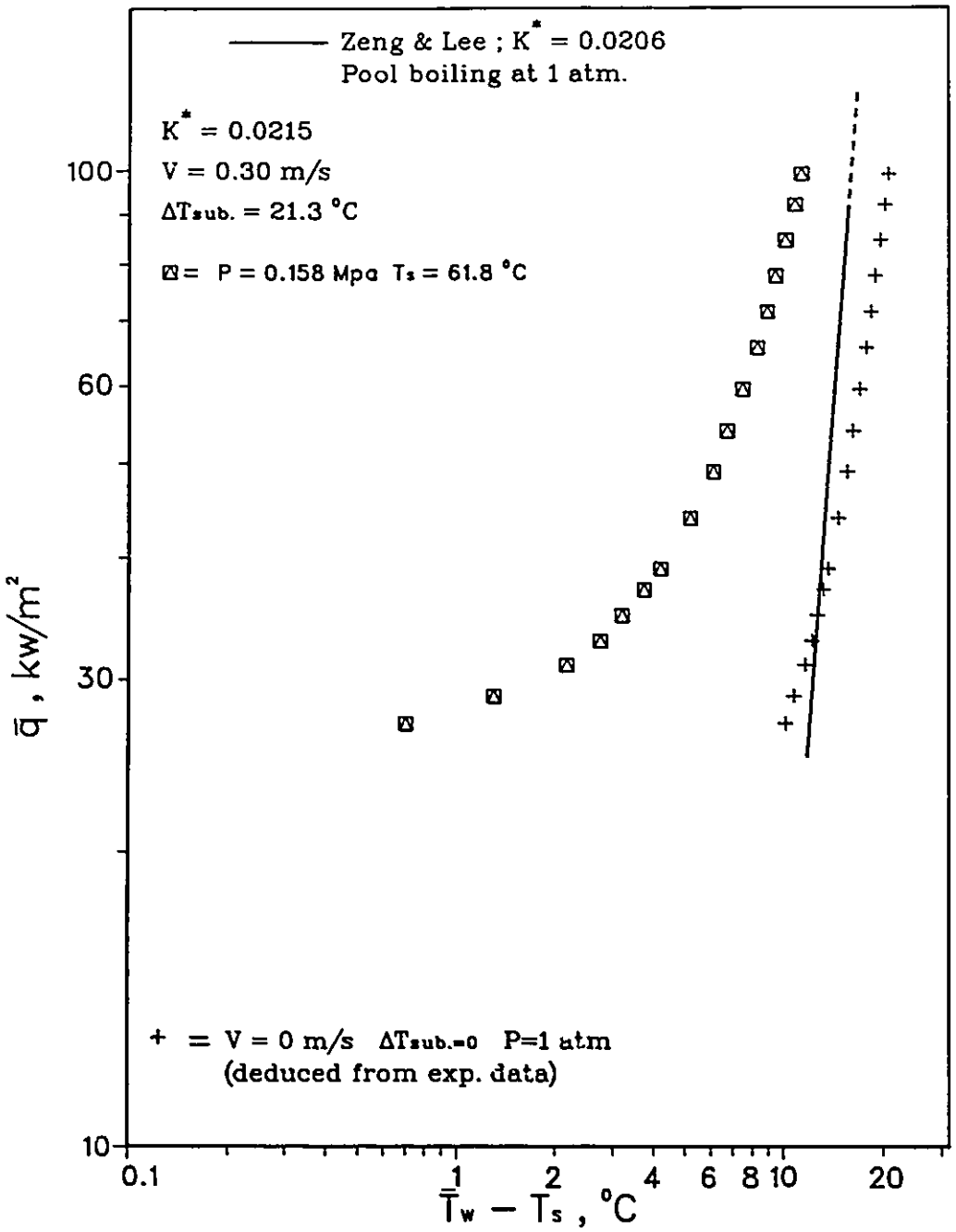

Figure 5.35 Comparison of Results in Nucleate Boiling ($P = 0.158\ Mpa$)

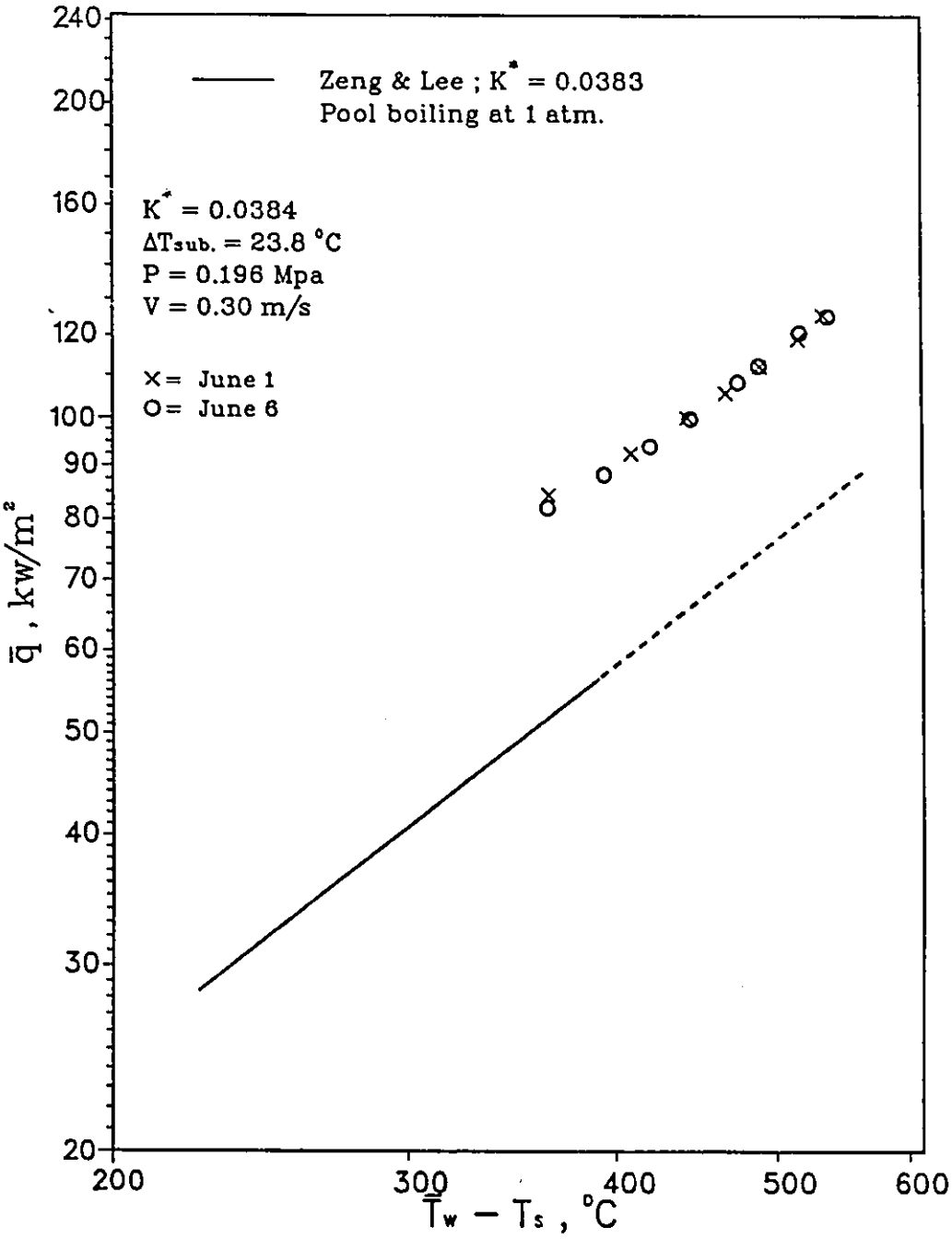

Figure 5.36 Experimental Data Reproducibility in Crossflow Film Boiling

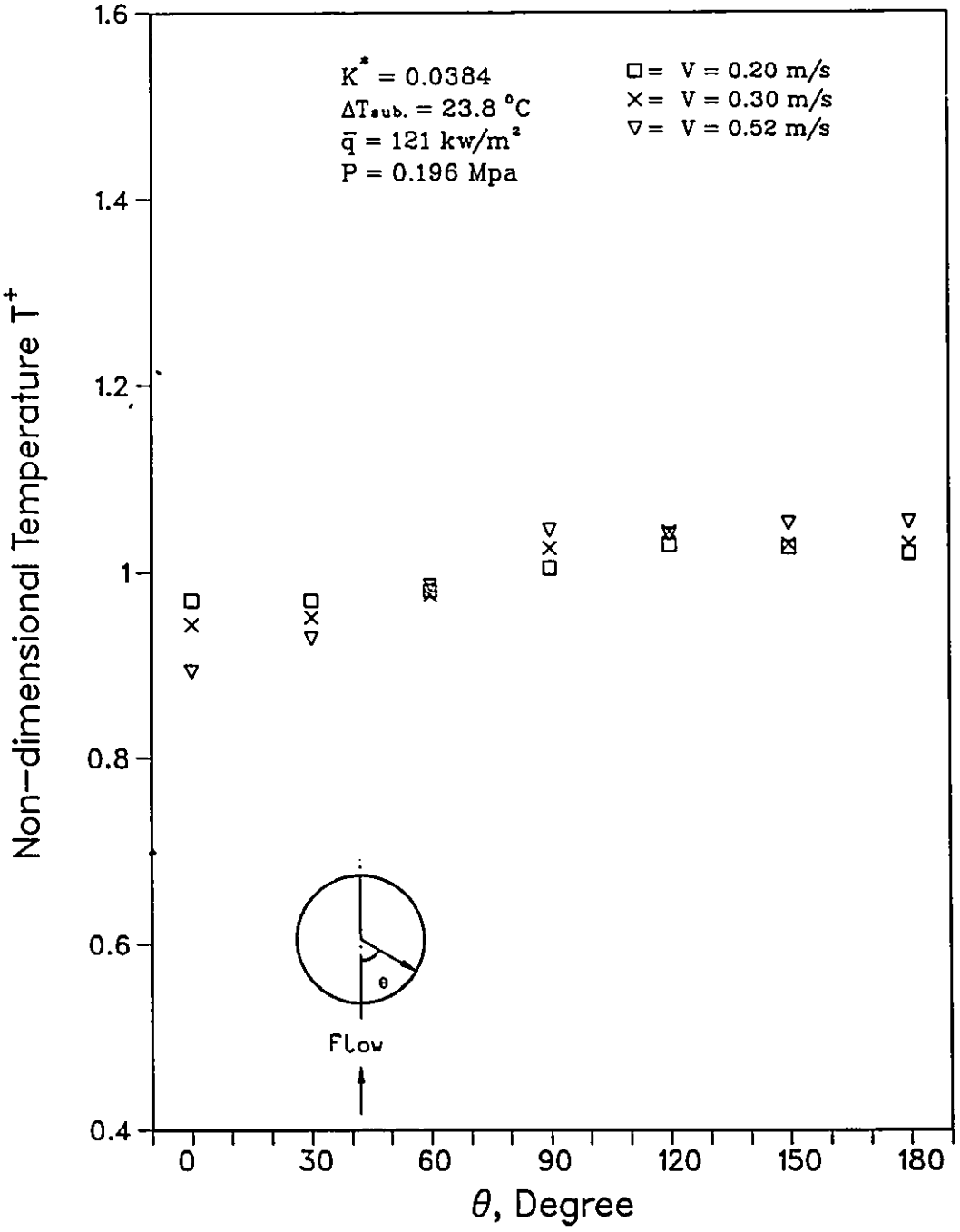

Figure 5.37 Non-dimensional Temperature in Crossflow Film boiling for Different Flow Velocity

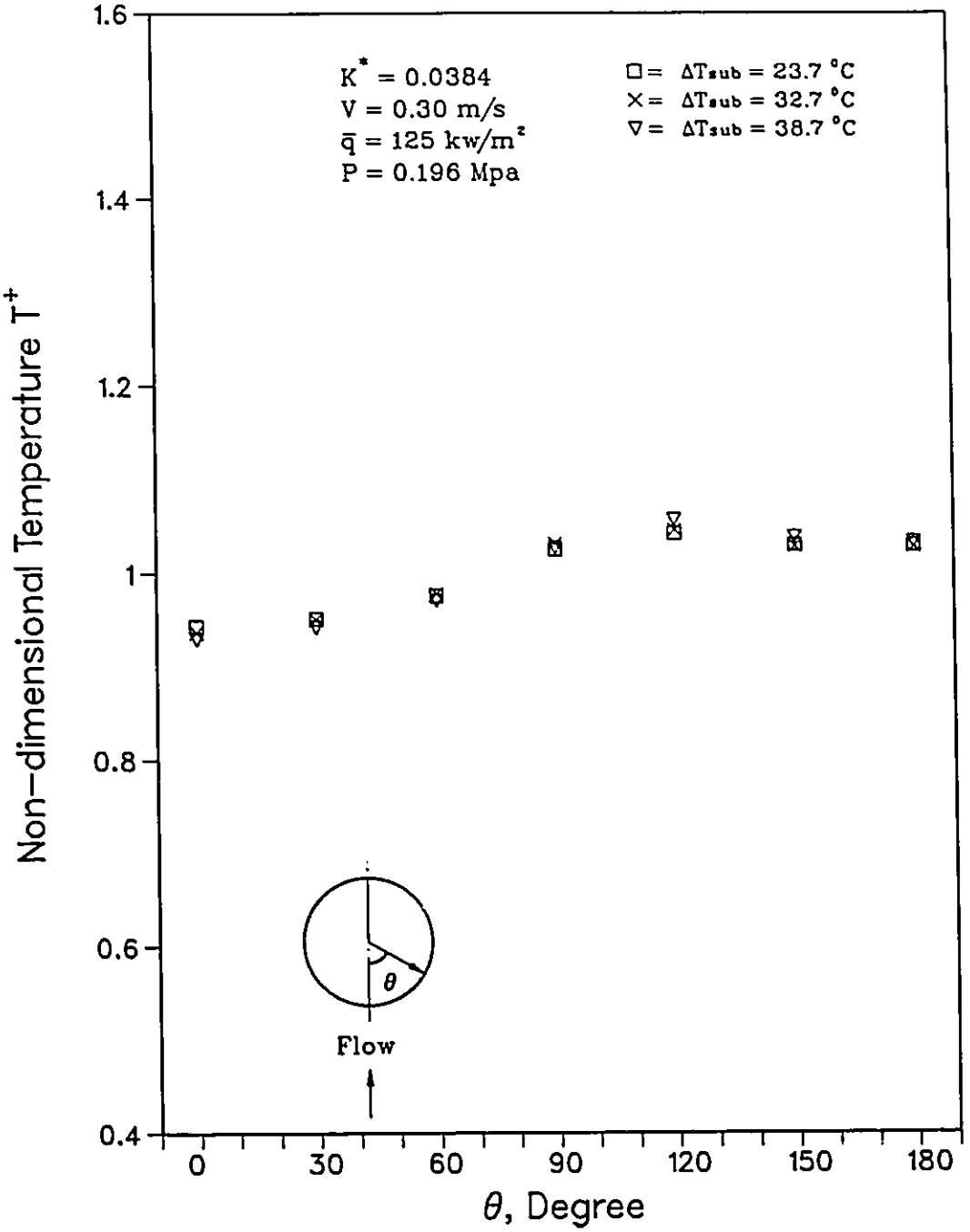

Figure 5.38 Non-dimensional Temperature in Crossflow Film boiling for Different Degree of Subcooling

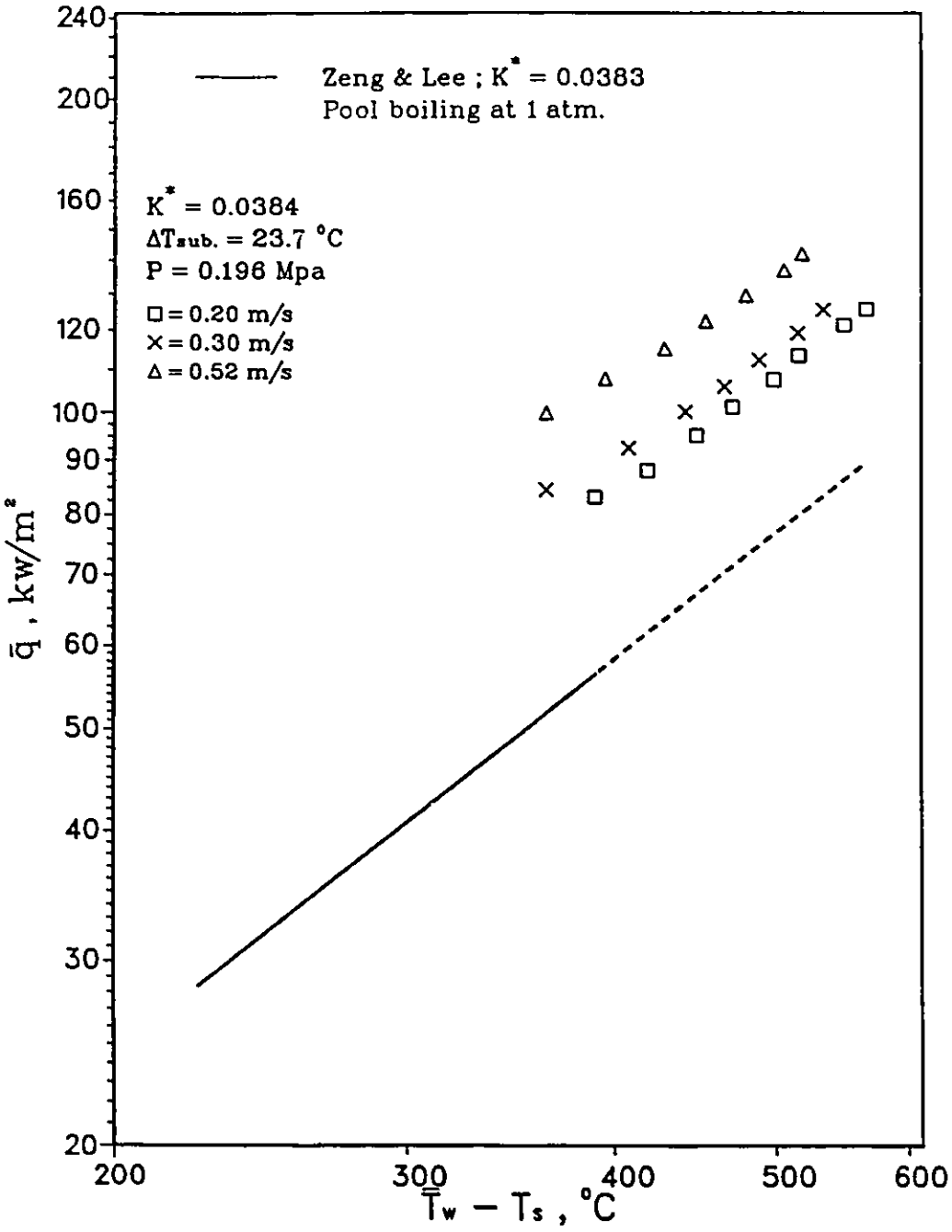

Figure 5.39 Effect of Velocity in Crossflow Film Boiling

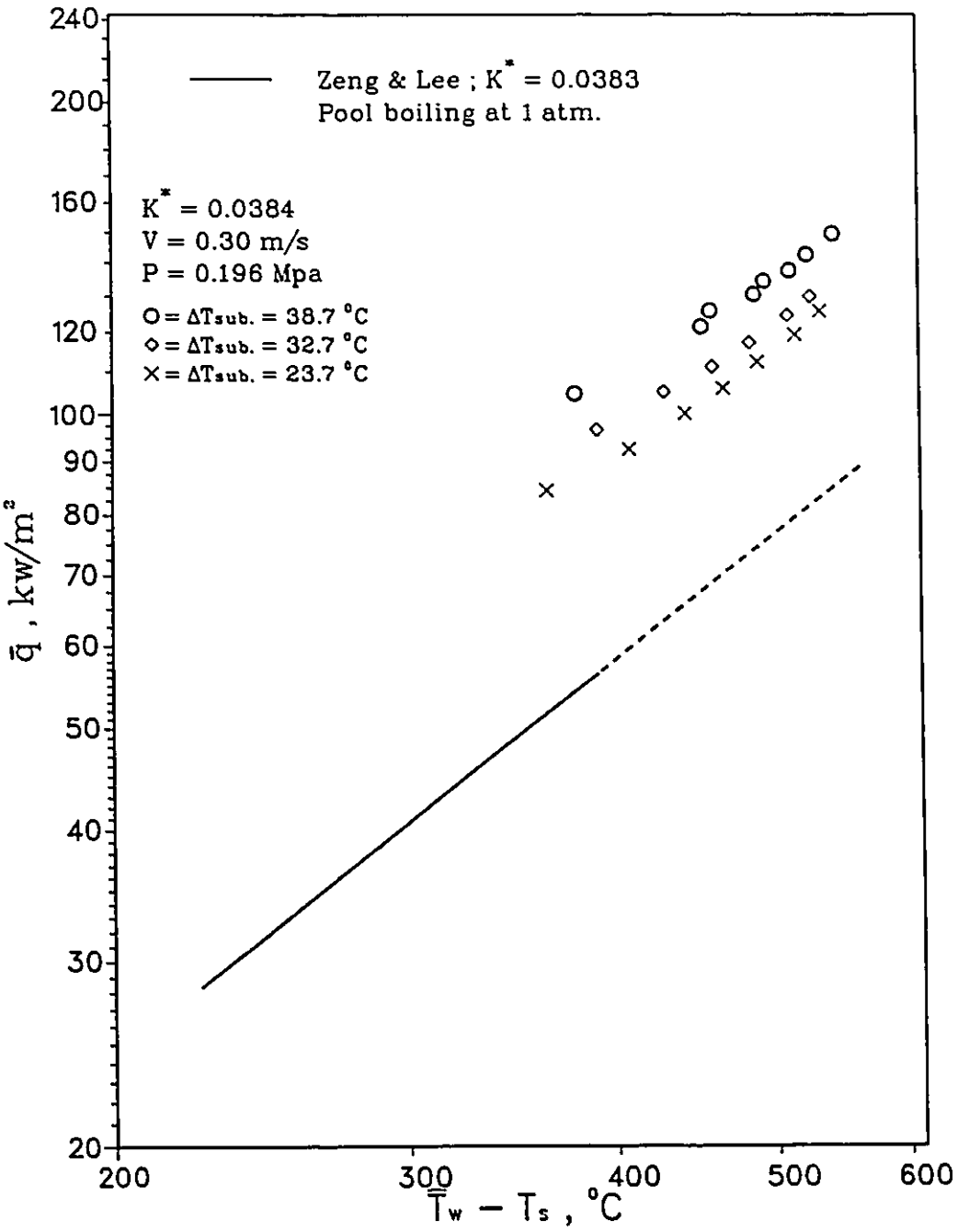

Figure 5.40 Effect of Degree of Subcooling in Crossflow Film Boiling

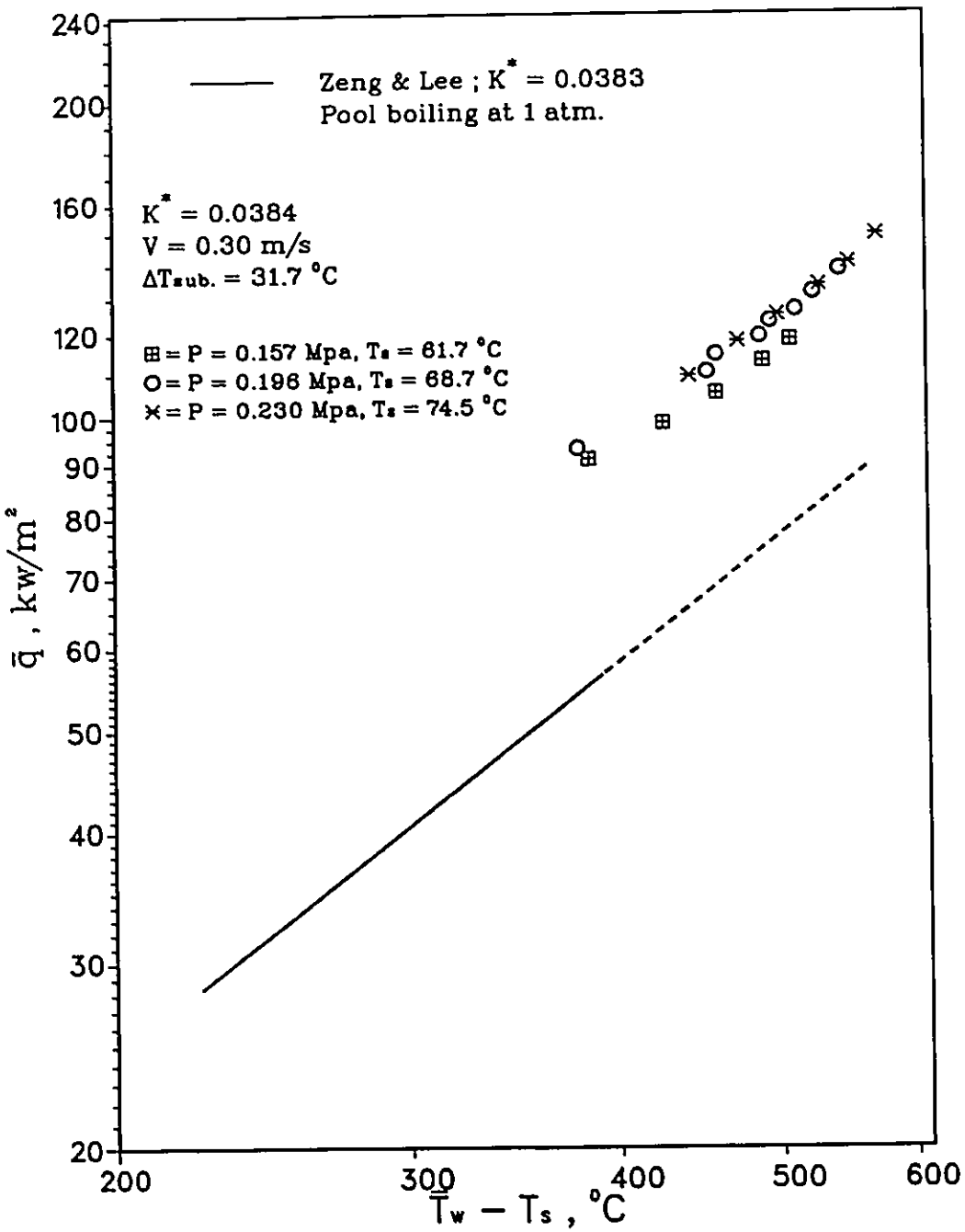

Figure 5.41 Effect of Pressure in Crossflow Film Boiling

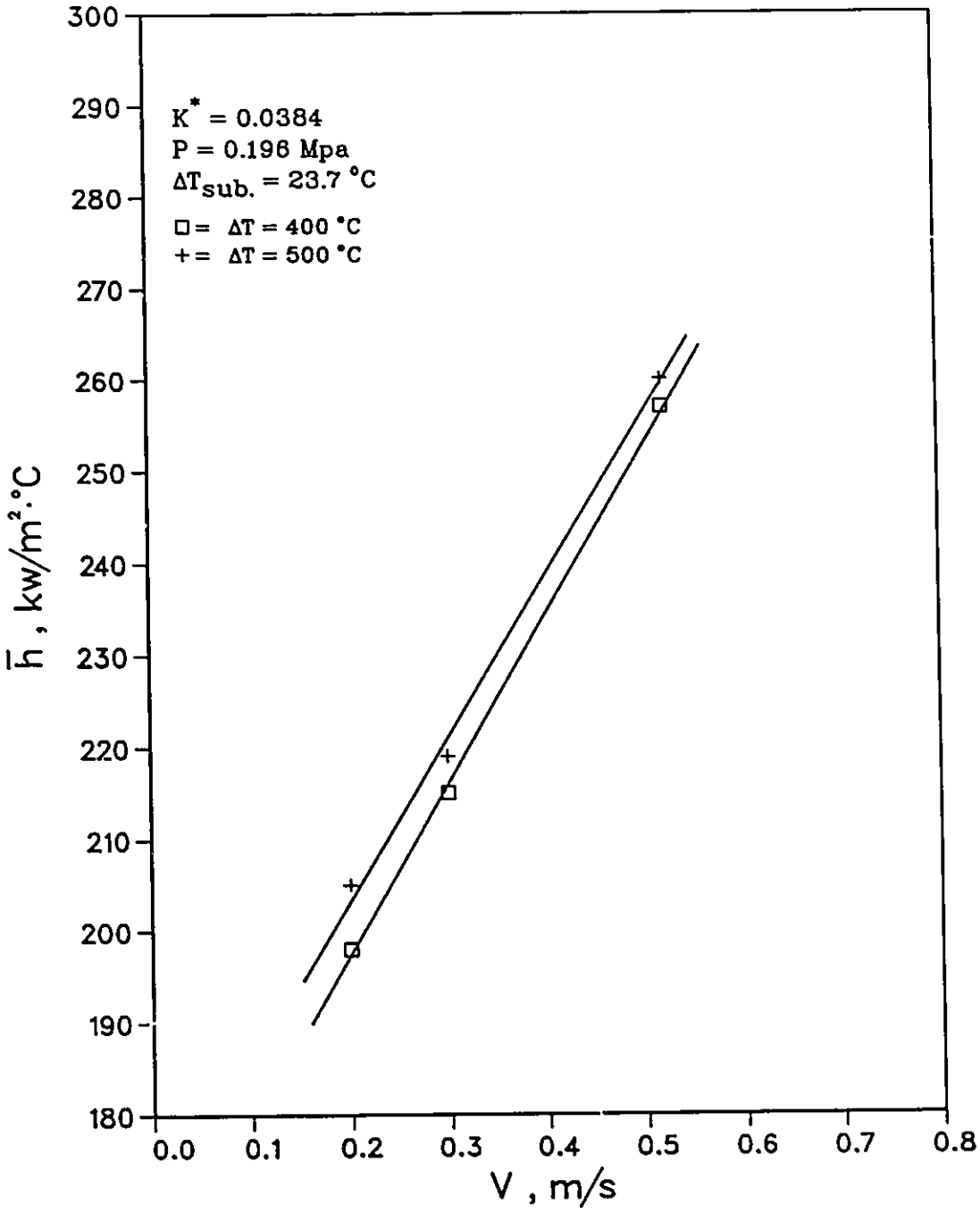

Figure 5.42 Crossflow Film Boiling Heat Transfer Coefficient versus Flow Velocity

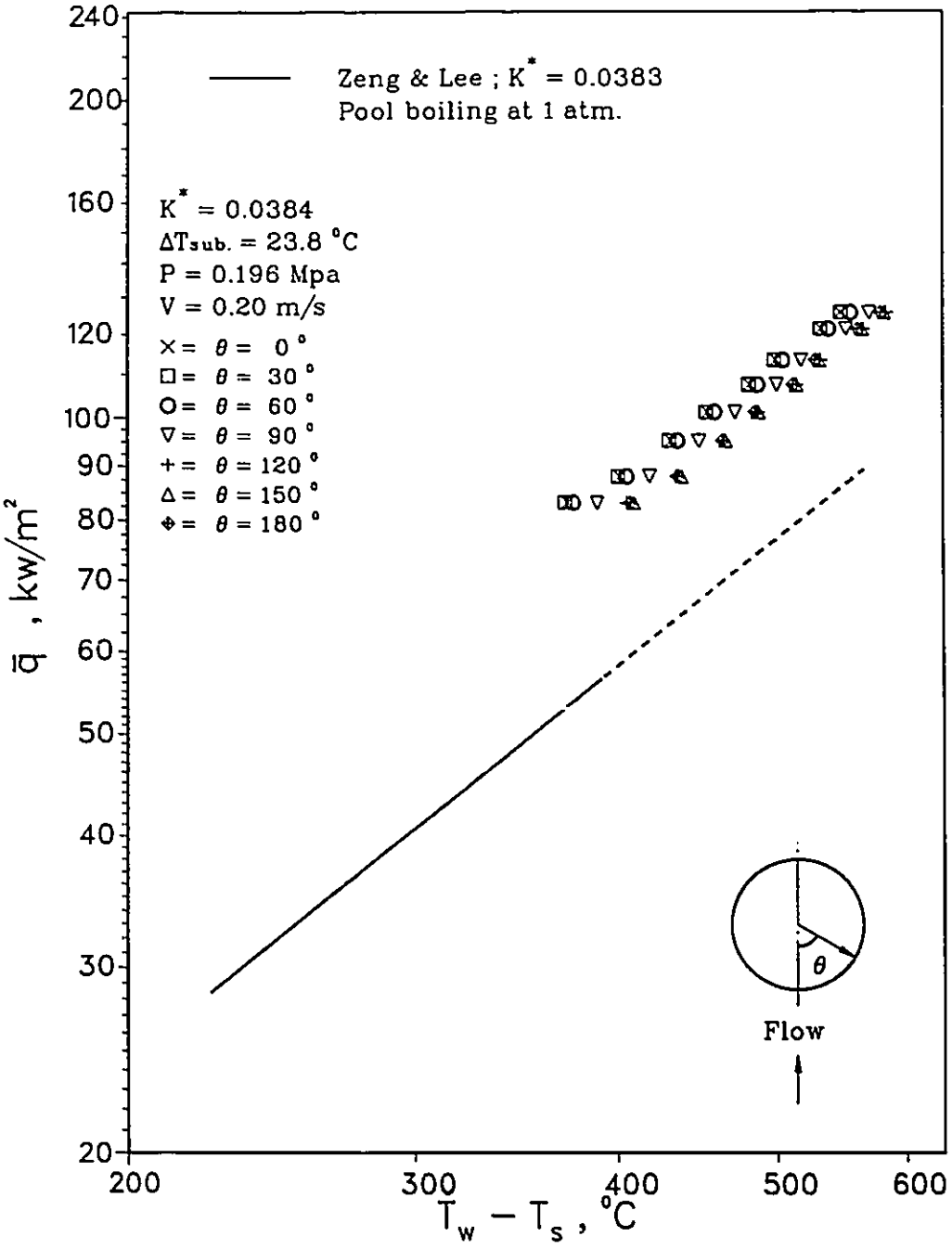

Figure 5.43 Local Crossflow Film Boiling for $V = 0.20\ m/s$

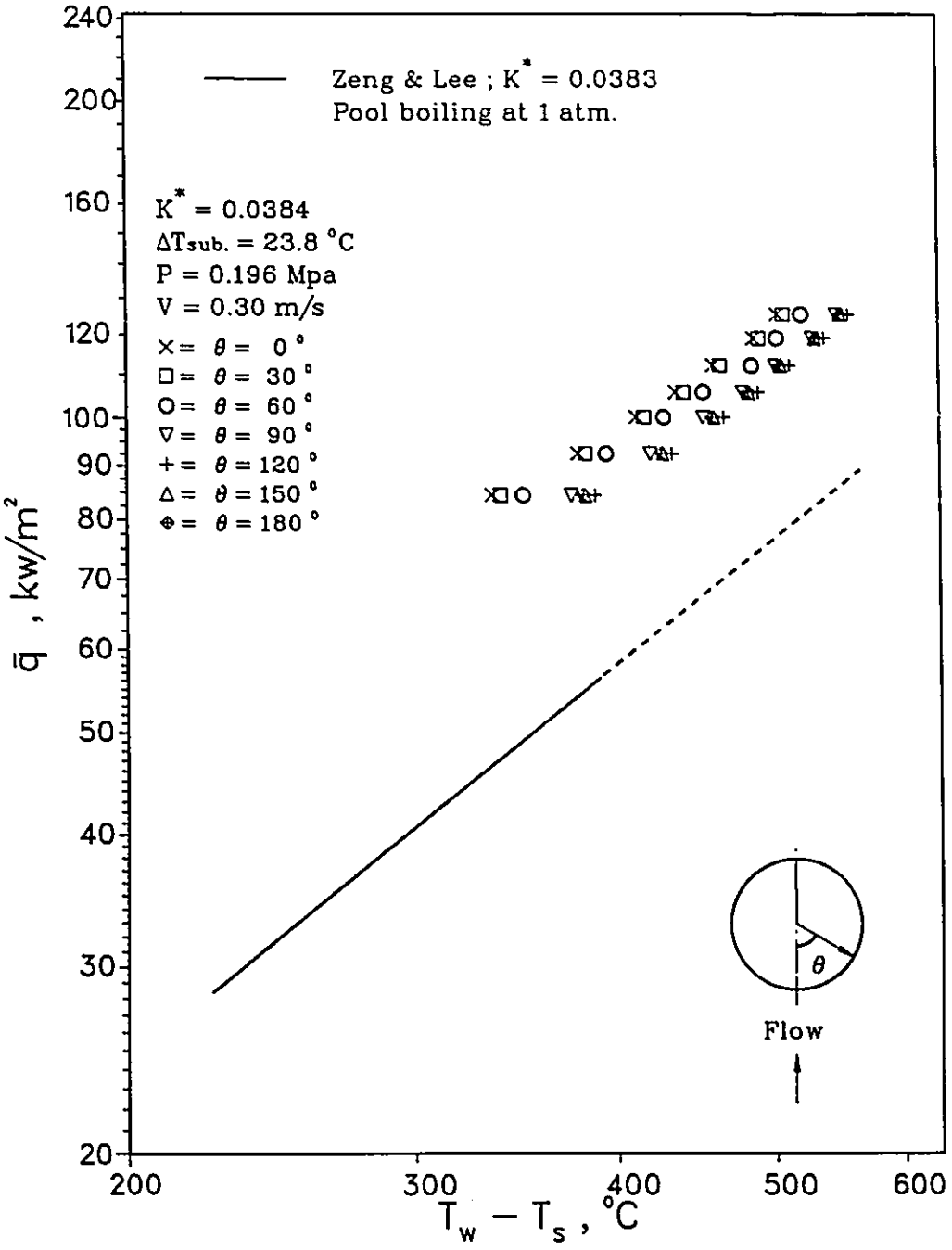

Figure 5.44 **Local Crossflow Film Boiling for $V = 0.30\ m/s$**

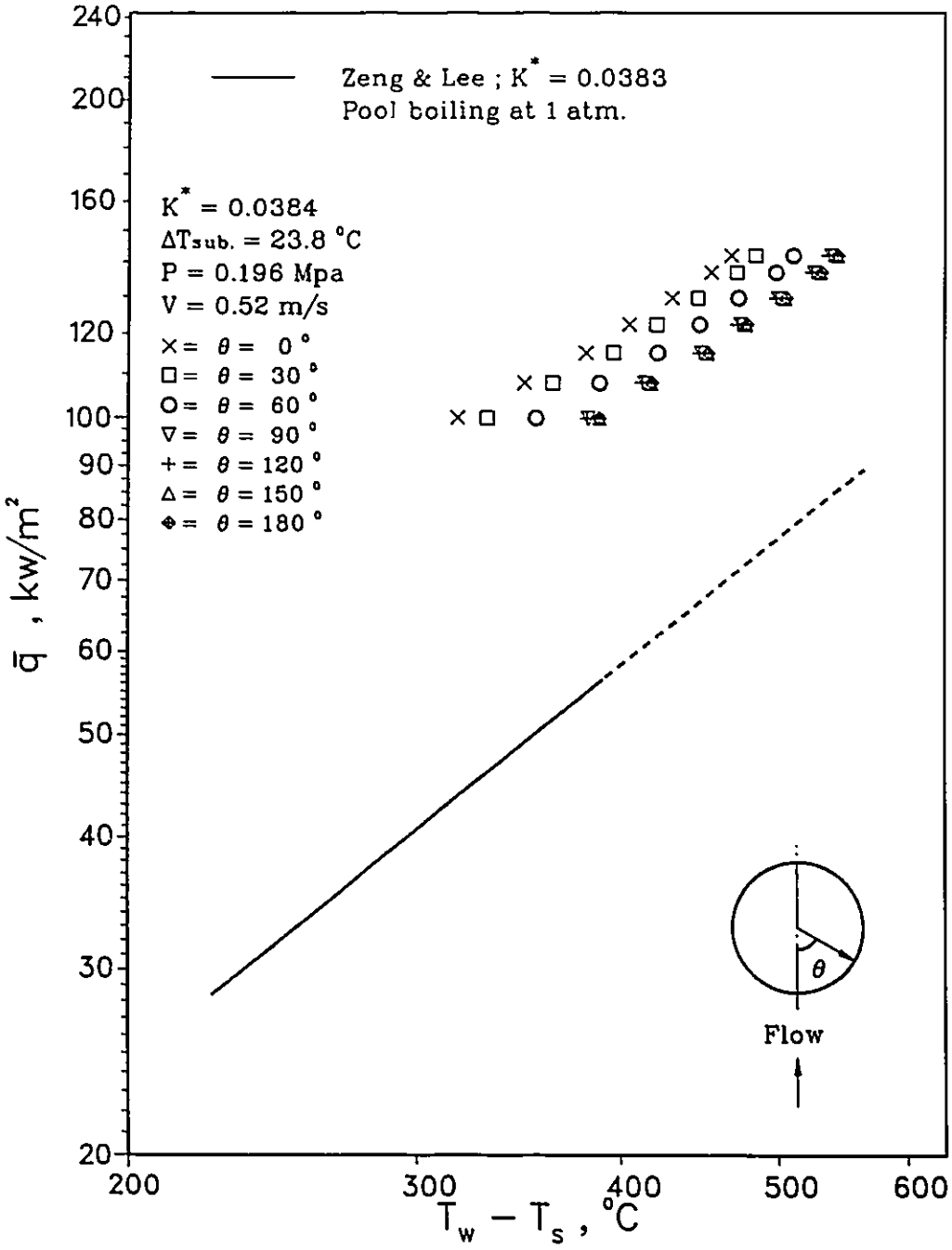

Figure 5.45 Local Crossflow Film Boiling for $V = 0.52\ m/s$

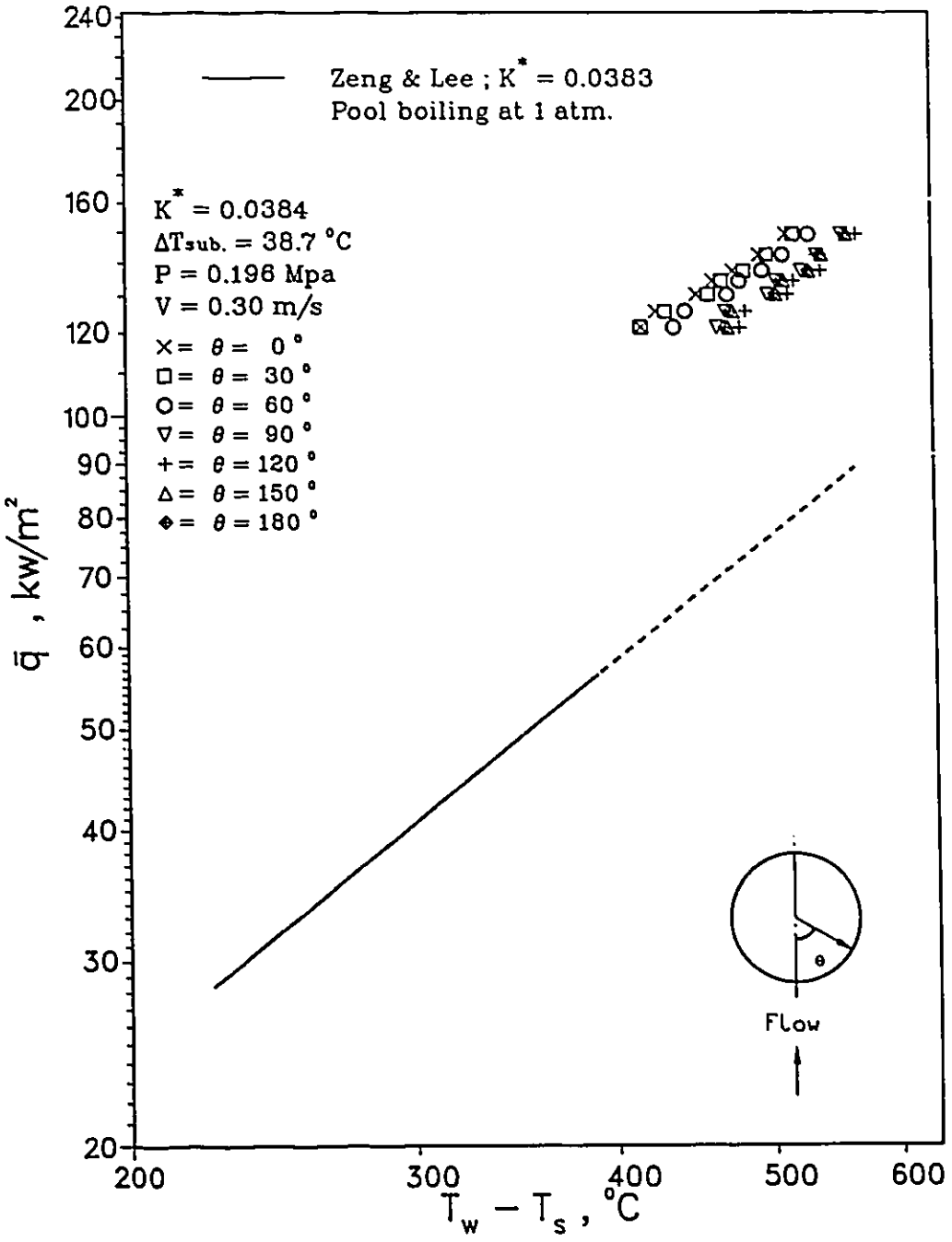

Figure 5.46 Local Crossflow Film Boiling for $\Delta T_{sub.} = 38.7\,^{o}C$

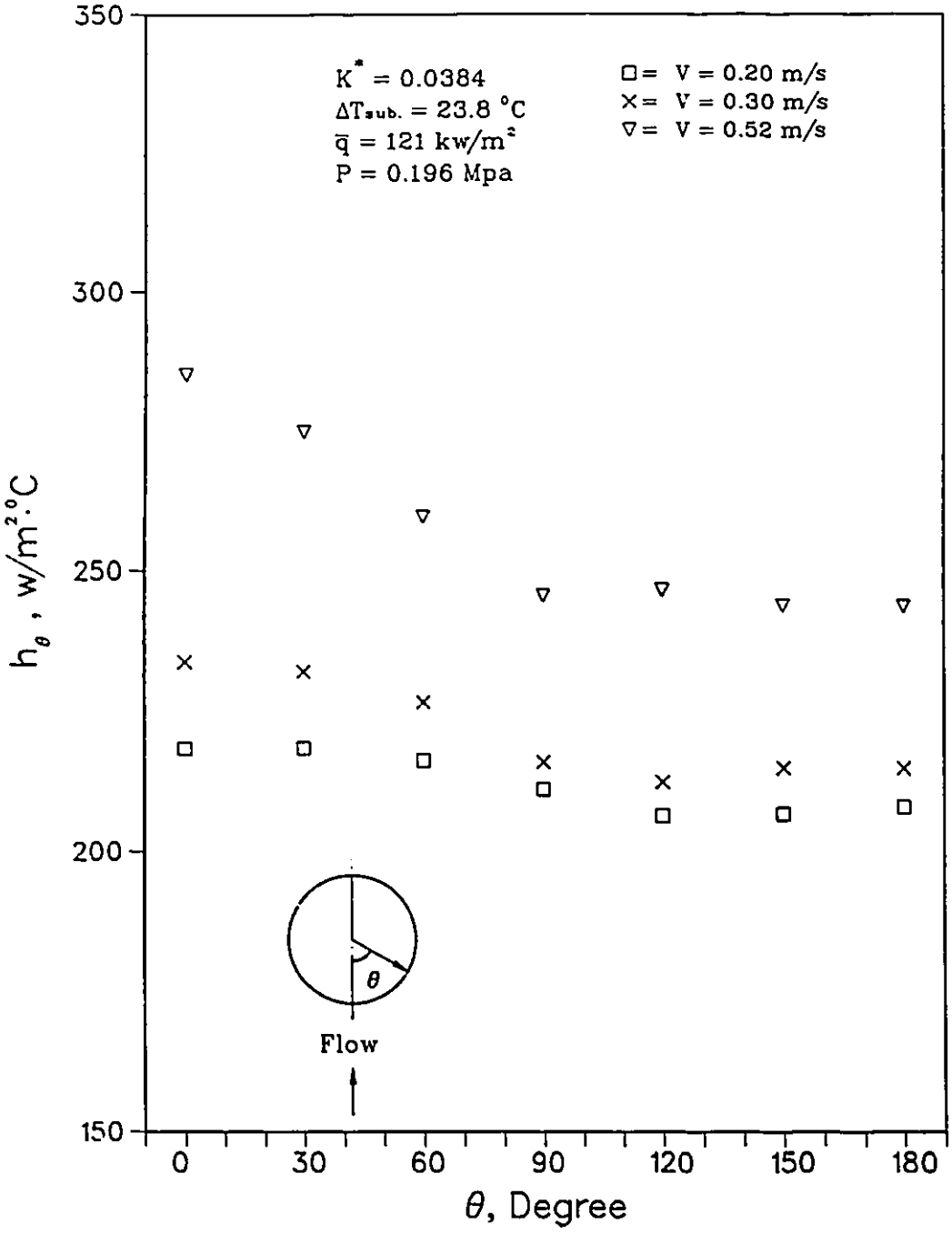

Figure 5.47 Effect of Flow Velocity in Distribution of Local h_θ in Crossflow Film Boiling

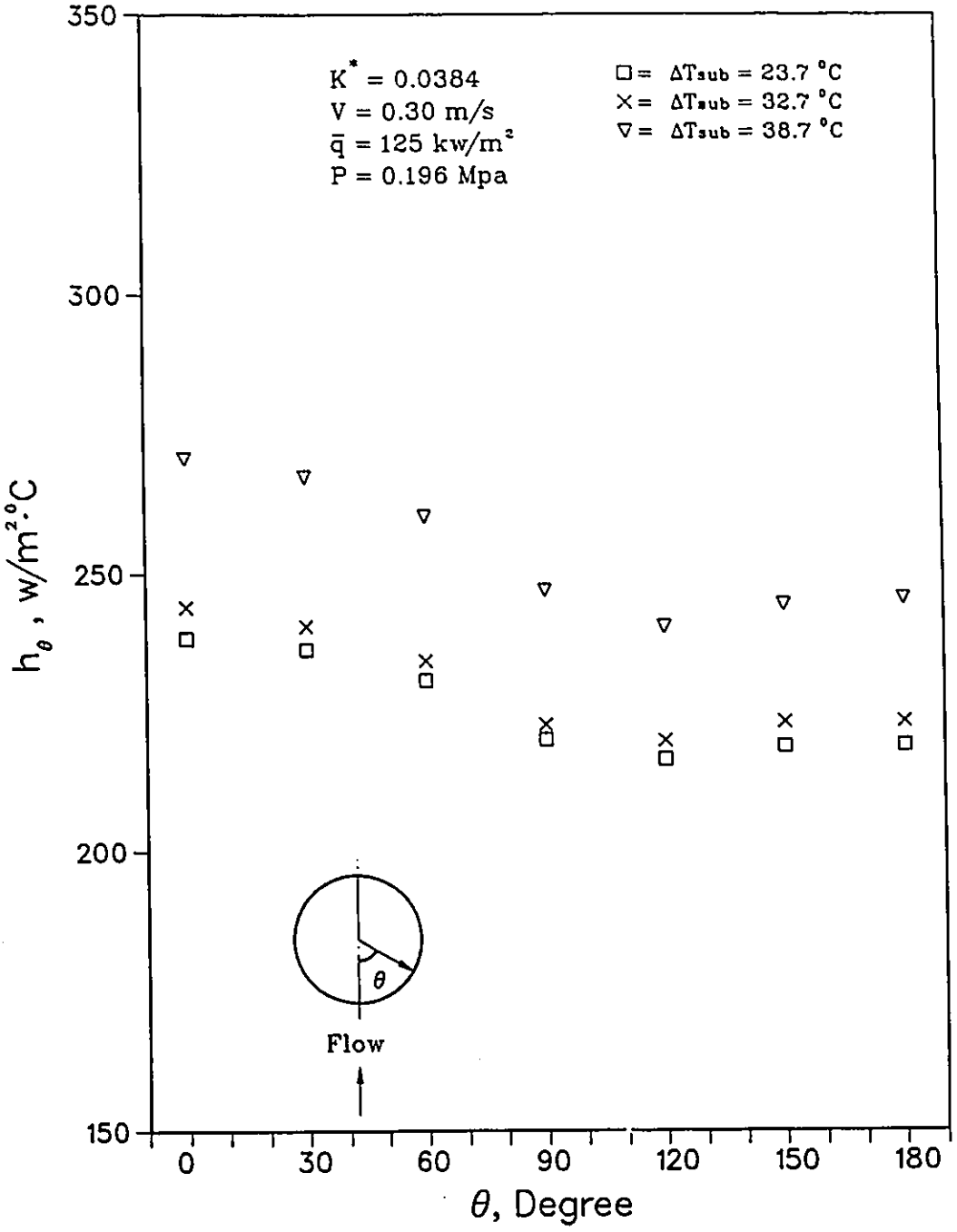

Figure 5.48 **Effect of Degree of Subcooling in Distribution of Local h_θ in Crossflow Film Boiling**

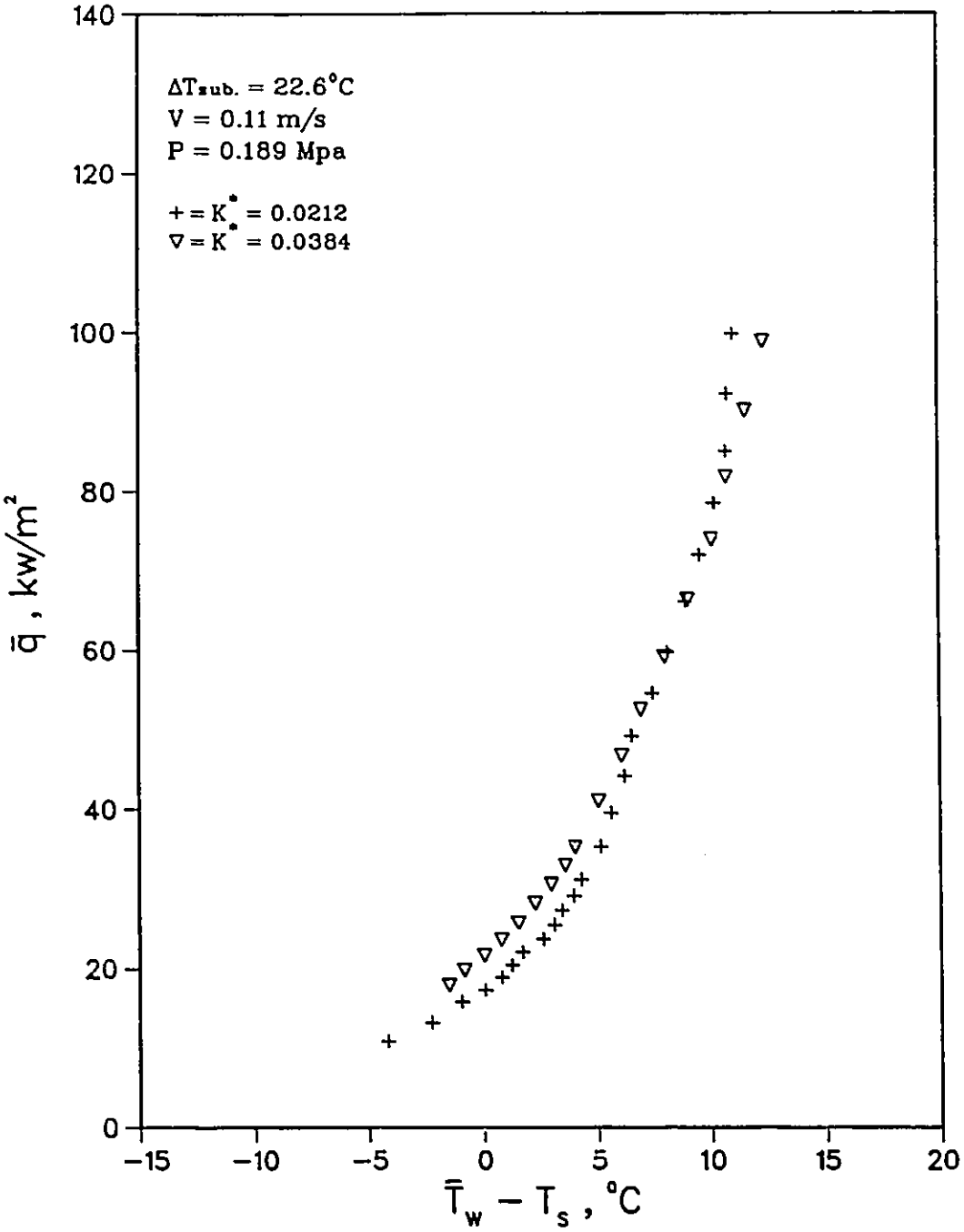

Figure 5.49 Effect of K^* on Crossflow Nucleate Boiling ($V = 0.11\ m/s$)

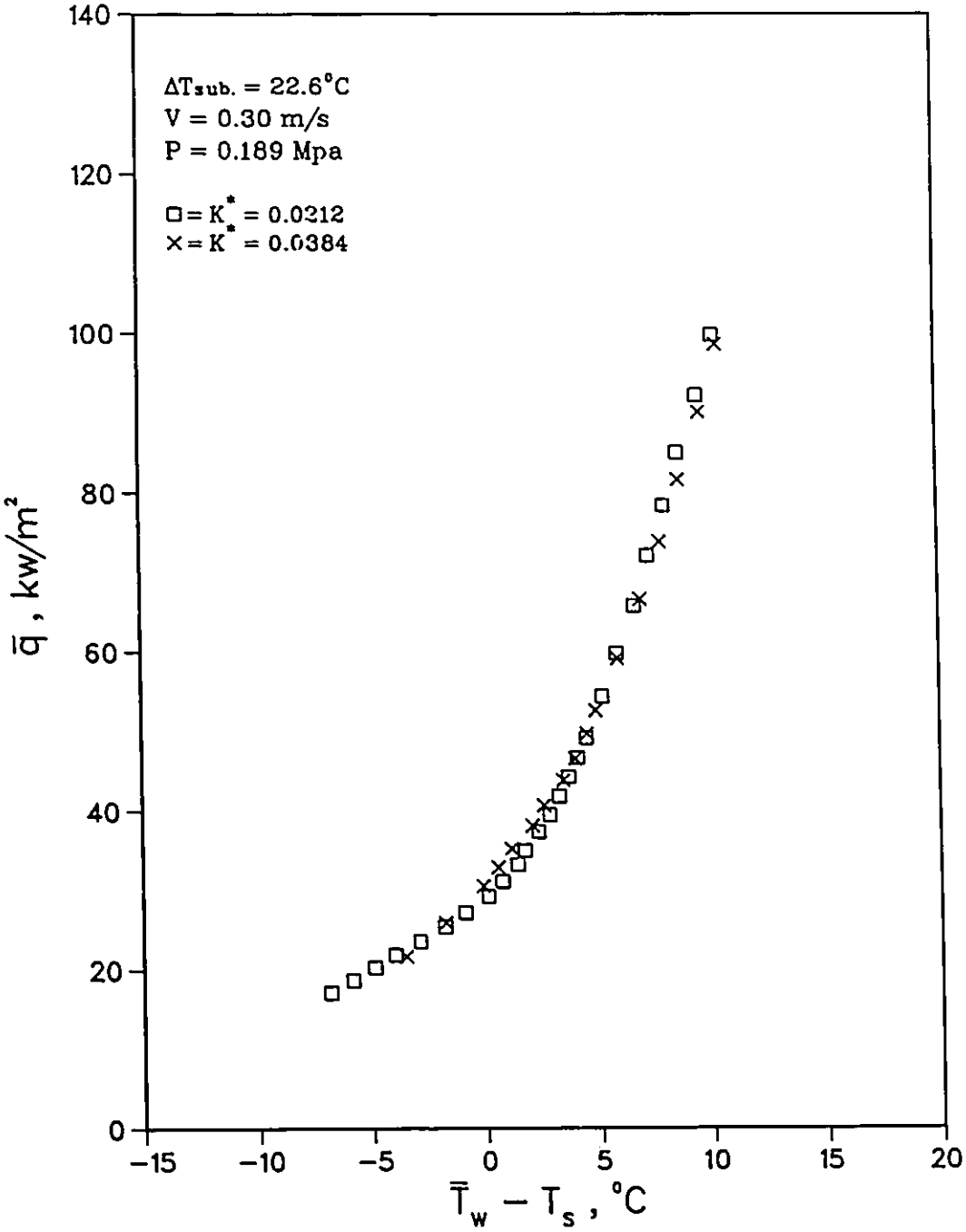

Figure 5.50 Effect of K^* on Crossflow Nucleate Boiling ($V = 0.30\ m/s$)

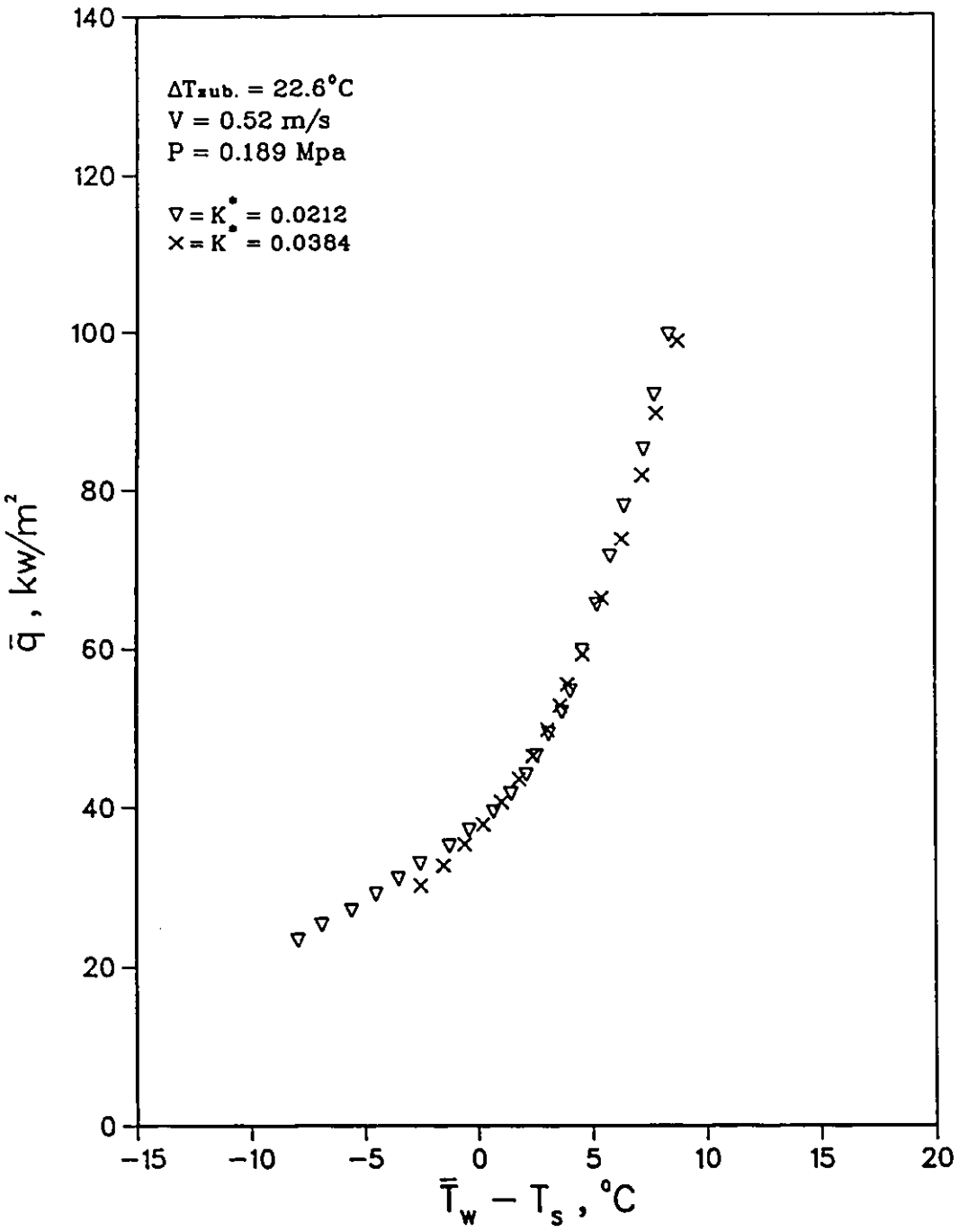

Figure 5.51 Effect of K^* on Crossflow Nucleate Boiling ($V = 0.52\ m/s$)

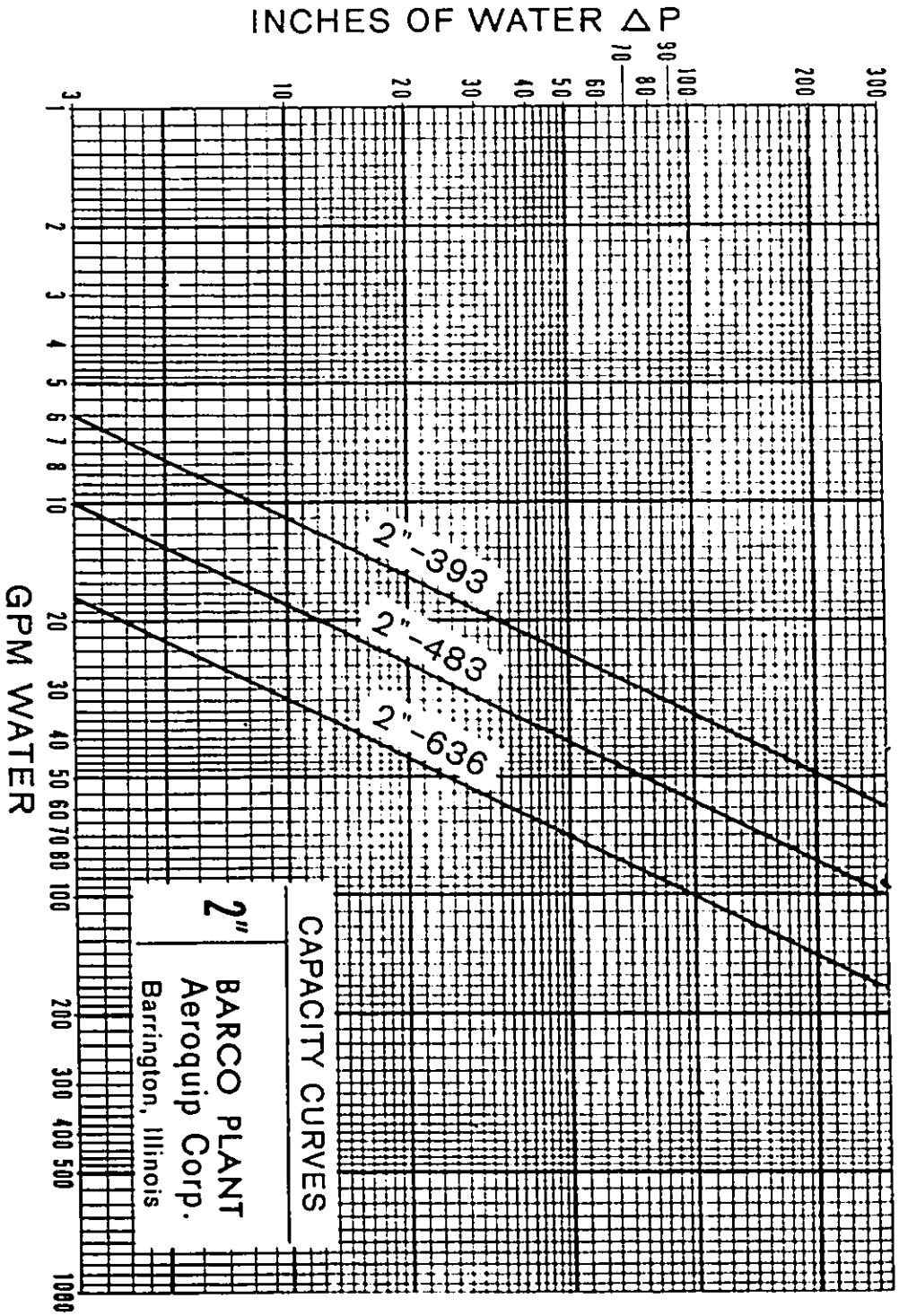

Figure A.1 Venturi Flow Rate Chart (2" Venturi)

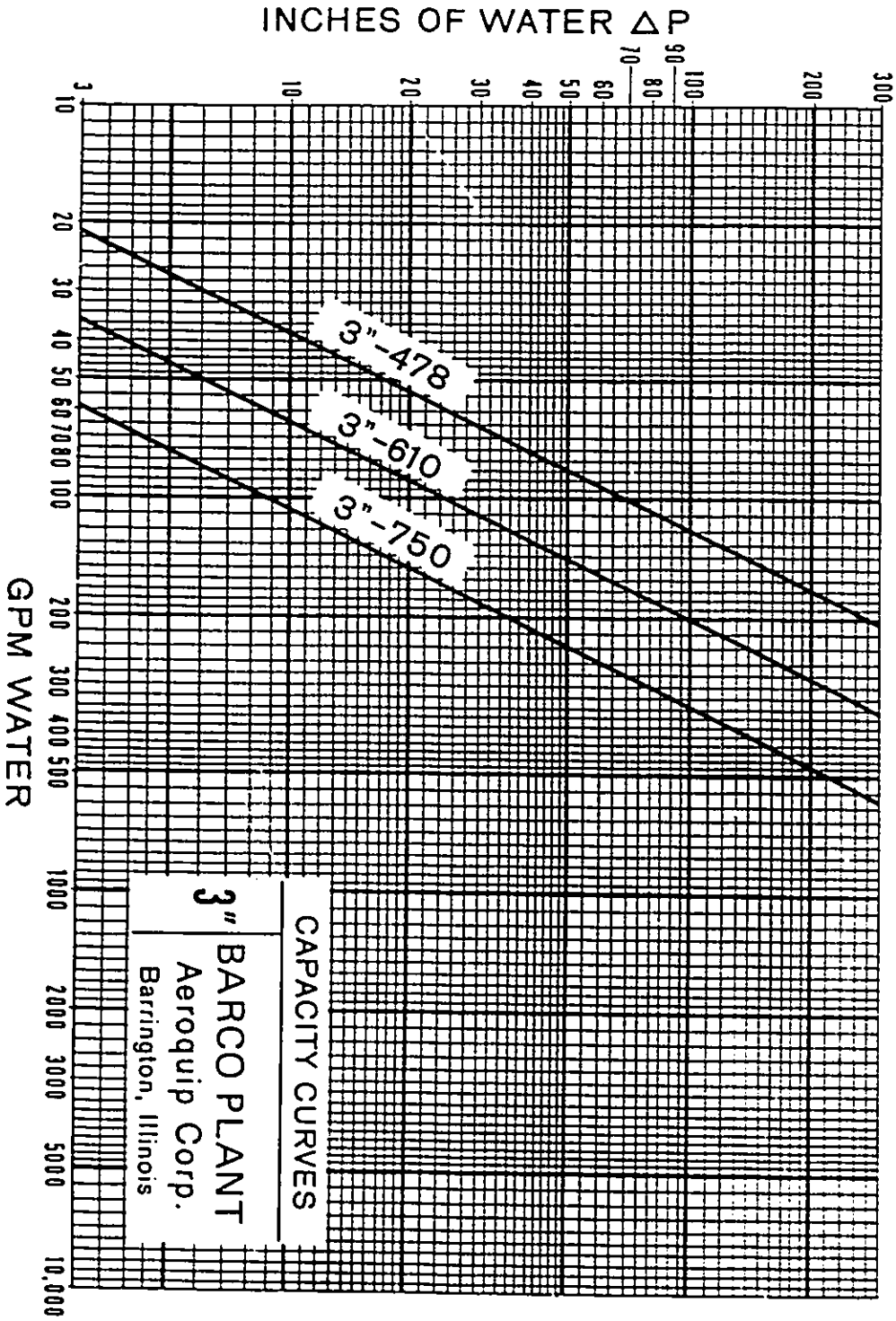

Figure A.2 Venturi Flow Rate Chart (3" Venturi)